0959

PB 208 237

Final Report

COMPACT CONDENSER FOR RANKINE CYCLE ENGINE

71-7464
August 1971

Prepared for

Office of Air Programs
Environmental Protection Agency
Ann Arbor, Michigan 48103

Reproduced by
NATIONAL TECHNICAL
INFORMATION SERVICE
Springfield, Va. 22151

AIRESEARCH MANUFACTURING COMPANY
Los Angeles, California

94

BIBLIOGRAPHIC DATA SHEET

1. Report No.
APTD-0959

2.

3. Recipient's Accession No.

4. Title and Subtitle
Compact Condenser for Rankine Cycle Engine

5. Report Date
August 1971

6.

7. Author(s)
S. Wong, J. D. Duncan, D. W. Graumann, et al

8. Performing Organization Rept. No. 71-7464

9. Performing Organization Name and Address
AiResearch Manufacturing Company
The Garrett Corporation
Los Angeles, California

10. Project/Task/Work Unit No.

11. Contract/Grant No.
EHS 70-123

12. Sponsoring Organization Name and Address
ENVIRONMENTAL PROTECTION AGENCY
Office of Air Programs
Ann Arbor, Michigan 48103

13. Type of Report & Period Covered
Final

14.

15. Supplementary Notes

16. Abstracts

The goal of this study was to develop heat transfer designs or techniques that will allow construction of condensers for automobile Rankine-cycle engines that have frontal area, volume, and fan horsepower requirements which are not appreciably greater than those of present automobile radiators. The first phase of the study included a parametric study of air-side heat transfer surfaces using available heat transfer data. Plain, ring dimpled, and finned tubes as well as plain, strip, offset, louvered, wavy, and perforated plate-fin surfaces were evaluated. A perforated plate-fin gave the best analytical results when the fin thickness was changed from 0.012 in. to 0.004 in. A small test core utilizing the new perforated fin design was fabricated and tested. The performance of this core did not achieve the calculated performance. Ten more test cores were fabricated and tested with a range of perforation sizes and spacings. Several of these perforated fins yielded better overall performance than the best plain fin. Full size condensers were sized and the best perforated fin gave an optimum condenser which was 2 percent over the volume goal and 3 percent over the frontal area goal. A cost analysis was performed based on the optimized condensers.

17. Key Words and Document Analysis. 17a. Descriptors

Air pollution
Automobile engines
Rankine cycle
Condensers (liquefiers)
Heat transfer
Cost analysis

17b. Identifiers/Open-Ended Terms

17c. COSATI Field/Group 13B

18. Availability Statement
Unlimited

19. Security Class (This Report)
UNCLASSIFIED

20. Security Class (This Page)
UNCLASSIFIED

21. No. of Pages
94

22. Price

FORM NTIS-35 (10-70)

USCOMM-DC 40329-P71

Final Report

COMPACT CONDENSER FOR RANKINE CYCLE ENGINE

71-7464
August 1971

Prepared by

S. Wong
J. D. Duncan
D. W. Graumann
J. C. Gibson
J. J. Killackey

Prepared for

Office of Air Programs
Environmental Protection Agency
Ann Arbor, Michigan 48103

GARRETT

AIRESEARCH MANUFACTURING COMPANY
Los Angeles, California

FOREWORD

This report describes research conducted by the AiResearch Manufacturing Company, a division of The Garrett Corporation, Los Angeles, California, for the Office of Air Programs, Environmental Protection Agency, under contract number EHS 70-123. The work was performed under the direction of Mr. K. O. Parker of AiResearch and Mr. William Zeber of OAP.

CONTENTS

Section		Page
1	INTRODUCTION AND SUMMARY	1-1
	Introduction	1-1
	Summary	1-1
2	CONCLUSIONS AND RECOMMENDATIONS	2-1
	Conclusions	2-1
	Recommendations	2-1
3	PARAMETRIC STUDY	3-1
	Design Considerations	3-1
	Analysis	3-3
	Results	3-15
4	PARAMETRIC STUDY TEST CORE	4-1
	Core Fabrication	4-1
	Testing	4-3
	Test Results	4-5
5	PERFORATED PLATE-FIN MATRICES	5-1
	Review of Available Data	5-1
	Perforation Geometry Selection	5-2
	Fabrication	5-3
	Testing	5-17
	Test Results	5-17
6	APPLICATION TO FULL-SIZE CONDENSER	6-1
	Optimized Condensers	6-1
	Cost Analysis	6-2
7	REFERENCES	7-1

ILLUSTRATIONS

Figure		Page
2-1	Condenser Design for Various Air-Side Fins	2-2
3-1	Core Frontal Area and Air Side Volume vs Air Effectiveness for Rectangular Offset Fin	3-6
3-2	Core Frontal Area and Air Side Volume vs Air Effectiveness for Perforated Fin	3-7
3-3	Compact Condenser Study, Plate-Fin (Plain Triangular and Louvered)	3-20
3-4	Compact Condenser Study, Plate-Fin (Rectangular Offset and Wavy)	3-21
3-5	Compact Condenser Study, Plate-Fin (Perforated)	3-22
3-6	Variation of Frontal Area with Fins/In. and Fin Height for a Perforated Fin	3-24
3-7	Summary of Solutions (Frontal Area and Volume) for Various Air Fin Configurations	3-26
4-1	Test Core for f and j Factors (22 Fins per Inch Perforated 0.004 Aluminum Material)	4-2
4-2	Test Setup Schematic	4-4
4-3	Performance Parameters 22 FPI Perforated Fin	4-7
5-1	Perforated Fin Materials for Cores 1 and 3	5-4
5-2	Perforated Fin Materials for Cores 5 and 7	5-5
5-3	Perforated Fin Materials for Cores 9 and 11	5-6
5-4	Perforated Fin Materials for Cores 13 and 15	5-7
5-5	Perforated Fin Materials for Cores 17 and 19	5-8
5-6	Perforated Fins and Materials (0.030-in. Diameter Holes for Cores 1 and 3)	5-9
5-7	Perforated Fins and Materials (0.060-in. Diameter Holes for Cores 5 and 7)	5-10
5-8	Perforated Fins and Materials (0.015-in. Slots for Cores 9 and 11)	5-11

ILLUSTRATIONS (Continued)

Figure		Page
5-9	Perforated Fins and Materials (0.030-in. Slots for Cores 13 and 15)	5-12
5-10	Perforated Fins and Materials (0.060-in. Slots for Cores 17 and 19)	5-13
5-11	Overall View of Core During Stacking	5-15
5-12	Close-up View of Core During Stacking	5-15
5-13	Core in Brazing Fixture, Ready for Placement in Argon Retort	5-16
5-14	Test Setup Showing Water Flow Rate Measuring System and Thermocouple Measuring Apparatus	5-18
5-15	Test Setup Showing Test Core Mounted in Ducting	5-19
5-16	Turbulator Design	5-20
5-17	Pitot Tube Locations During Velocity Profile Traverse of Upstream Duct	5-21
5-18	Upstream Duct Velocity Profiles	5-22
5-19	Performance Parameters for the -0 Perforated Fin	5-24
5-20	Performance Parameters for the -1 Perforated Fin	5-25
5-21	Performance Parameters for the -3 Perforated Fin	5-26
5-22	Performance Parameters for the -5 Perforated Fin	5-27
5-23	Performance Parameters for the -7 Perforated Fin	5-28
5-24	Performance Parameters for the -9 Perforated Fin	5-29
5-25	Performance Parameters for the -11 Perforated Fin	5-30
5-26	Performance Parameters for the -13 Perforated Fin	5-31
5-27	Performance Parameters for the -15 Perforated Fin	5-32
5-28	Performance Parameters for the -17 Perforated Fin	5-33
5-29	Performance Parameters for the -19 Perforated Fin	5-34

ILLUSTRATIONS (Continued)

Figure		Page
5-30	Summary of Minimum Frontal Area Solutions for Perforated Fins	5-35
5-31	Effect of Upstream Turbulence on Condenser Minimum Frontal Area Solutions	5-38
5-32	Condenser Solutions for Selected Fins	5-39
6-1	Summary of Cost Analysis	6-5

TABLES

Table		Page
4-1	Condenser Designs with Perforated Fin	4-8
6-1	Condenser Cost Analysis	6-6

SECTION I

INTRODUCTION AND SUMMARY

INTRODUCTION

A critical problem for a Rankine-cycle power system is the large size of the condenser when its design is based on the heat transfer technology presently used in the automotive industries. The frontal area, volume, and fan horsepower requirements of condensers have been excessively large and have been factors in limiting the applicability of Rankine-cycle power systems to automobiles. Instead of increasing the physical size and/or fan power to obtain the required heat rejection capacity, the present study explored the use of more efficient heat transfer designs to obtain greater capacity in units of the same size.

The goal of this study for the Office of Air Programs (OAP) is to develop heat transfer designs or techniques that will allow construction of condensers for automobile Rankine-cycle engines that have frontal area, volume, and fan horsepower requirements which are not appreciably greater than those of present automobile radiators.

SUMMARY

The first phase of the study included a parametric study of air-side heat transfer surfaces using available heat transfer data. Plain, ring dimpled, and finned tubes as well as plain, strip, offset, louvered, wavy, and perforated plate-fin surfaces were evaluated. A perforated plate-fin gave the best analytical results when the fin thickness was changed from 0.012 in. (the thickness of the fin for which the basic data had been obtained) to 0.004 in. Further reductions in condenser size were obtained by modifying the fin height and the fin pitch from that of the tested fin. It was recognized that while the perforation size and spacing were identical to that of the tested fin, the fact that the thickness, height, and pitch were different introduced uncertainties into the design. A small test core utilizing this new perforated fin design was fabricated and tested. The performance of this core did not achieve the calculated performance and, in fact, was not as good as that calculated for a plain fin. This result was surprising since all other data available in the literature indicated that perforated surfaces were greatly superior to plain surfaces. These other data, however, did not extensively investigate the effect of the perforation variations. Therefore, ten more test cores were fabricated and tested with a range of perforation sizes and spacings. All cores had the same air fin height and the same fin pitch as the first test core.

Several of these perforated fins yielded better overall performance than the best plain fin. Further improvements were observed during testing with the introduction of turbulence upstream of the test cores. Full-size condensers were sized, and the best perforated fin gave an optimum condenser which was 2 percent over the volume goal and 3 percent over the frontal area goal at the design heat load of 1.5×10^6 Btu/hr. A cost analysis was performed based on the optimized condensers.

SECTION 2

CONCLUSIONS AND RECOMMENDATIONS

CONCLUSIONS

Results of the compact condenser program are summarized on Figure 2-1. The new perforated fin developed as part of this program has resulted in a substantial reduction in condenser volume. Perforated fins can reduce the condenser size by a factor of two compared to a design using current automobile radiator fins. Compared to a design using the best of the current aerospace heat transfer fins, the perforated fin can reduce the volume by 50 percent which must be considered as a breakthrough in heat exchanger design.

The reduction in condenser volume not only minimizes the installation problems, but yields a comparable savings in material costs.

The perforated fin condenser face area is within 6 percent of the OAP face area goal. With the addition of upstream turbulence, as would be generated by the vehicle grill, the test data indicate that the face area can be reduced within 3.4 percent of the OAP goal. Also, an analysis of the test data indicated that even further performance improvements may be achieved by further optimization of the slot spacing.

Using perforated fins the condenser for a 125 hp Rankine-cycle engine can be conveniently fitted into a current automobile engine compartment.

RECOMMENDATIONS

The use of a perforated fin does not a priori produce an optimized condenser. A study should be performed to realistically assess the tradeoffs between condenser size, condenser fin geometry, cooling air fan power consumption, and cost using an actual installation with inlet grill and exit duct pressure losses and flow blockage induced by an actual power plant. All elements must be considered to arrive at a truly optimum Rankine-cycle condenser/fan system installation.

In general, the perforated fin performance improved when the percent of open area increased from 12.5 percent to 25 percent. It is obvious that as the open area increases, there will be a point at which the performance will start to degrade. The best performance may be achieved at an open area greater than 25 percent, or it is possible that the best performance is achieved at an open area between 12.5 and 25 percent. It is recommended therefore, that perforated fins of 16.7 and 33.3 percent open area and 0.030-in. wide slots be tested with and without upstream turbulence to determine if a better perforation spacing exists.

Results of the parametric study indicate that a plain rectangular fin could be a reasonable solution for some applications. It is recommended

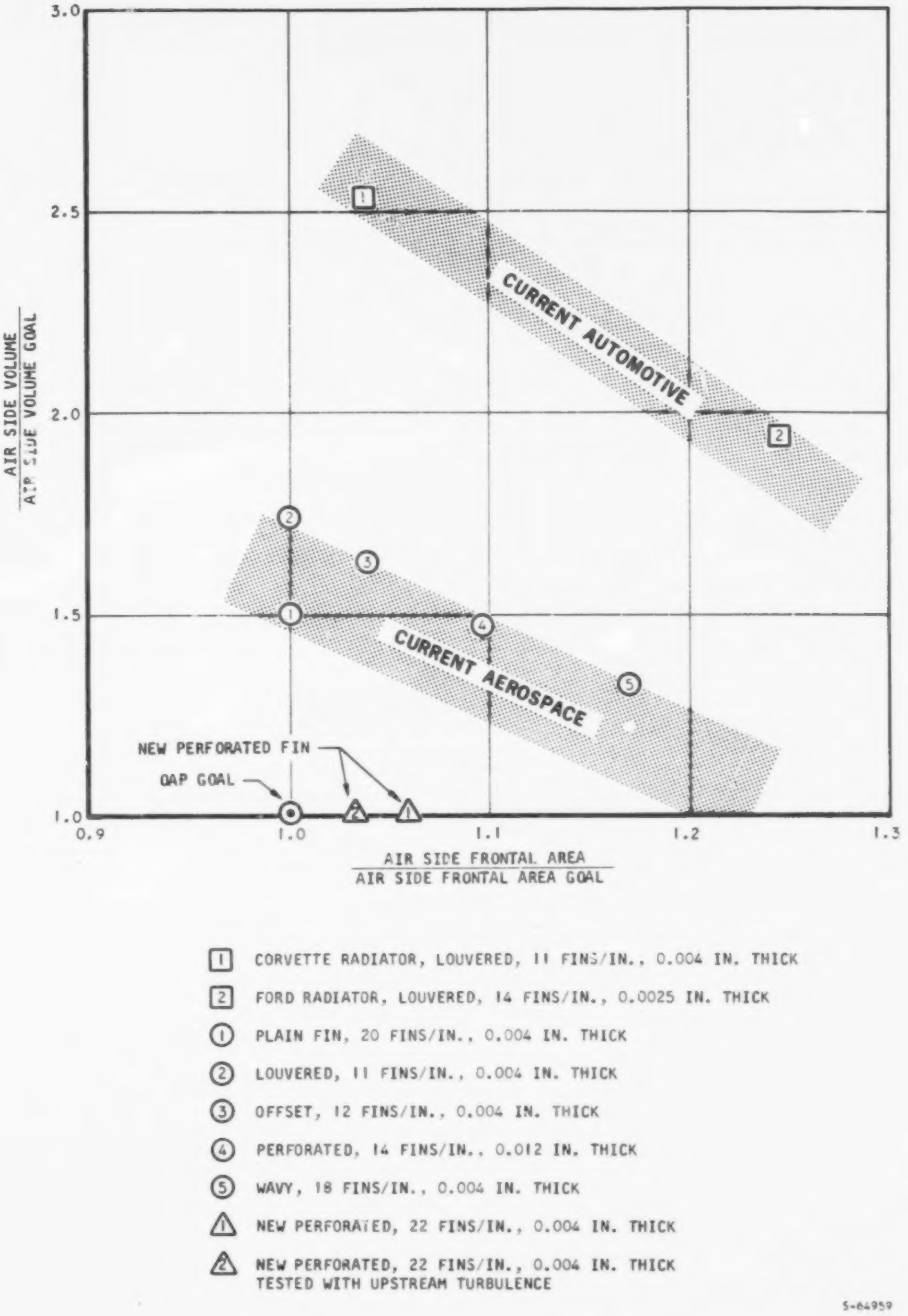

Figure 2-1. Condenser Designs for Various Air-Side Fins

therefore that a small plain fin test core using the same basic fin geometry and fabrication techniques as the perforated fin test cores be built and tested. Tests should be run with and without upstream turbulence and the results compared to the perforated fin data.

Finally, to verify the application of the perforated fin test data to a full-size condenser, it is recommended that a full size condenser using the best perforated fin be designed, built, and performance tested.

SECTION 3

PARAMETRIC STUDY

DESIGN CONSIDERATIONS

The design specifications for the parametric study of air side surfaces are as follows:

Heat rejection	0.5 million to 2.5 million Btu/hr
Parametric study design point	1.5 million Btu/hr
Air frontal area (vapor side and air side)	3.7 sq ft per million Btu/hr, or 6.0 sq ft total
Volume (air side only)	1.0 cu ft per million Btu/hr
Fan power (ideal air power)	6 hp per million Btu/hr
Inlet cooling air temperature	95^0F
Vapor condensing temperature	220^0F
Condensing side heat transfer coefficient	2000 Btu/(hr)(ft^2)(^{0}F)

A sea level pressure of 29.92 in. Hg abs was assumed.

This 1.5 million Btu/hr heat load selected for the parametric study design point is the average of the minimum and maximum heat loads. However, as long as no constraints are imposed on the shape of the core by the condensing side requirements or by the dimensional limitations, the results from the design point study will be the same for all loads because the available fan power is directly proportional to the heat load.

For example, if a core of frontal area A and airflow length L has a heat rejection HR at an airflow W and air horsepower AHP, the heat rejection can be increased directly by adding identical cores in parallel on the air side. For N cores in parallel, the total air frontal area becomes (N)(A), and a heat rejection of (N)(HR) is attained with an airflow of (N)(W). This additional airflow is available because the air pressure drop is constant for the parallel cores, and the available air horsepower varies directly with the heat rejection. The available core frontal area at the parametric study design point is (3.7)(1.5) or 5.55 sq ft (799.2 sq in.). This area was presumed to be the effective frontal area of the core. That is, the side plates and side strips enclosing the air fins or tubes in an actual core were not included. The fact that an actual core has an integral number of whole fin rows or tube rows was also neglected.

Since the available airflow and air pressure drop for the study are specified in the form of ideal fan air horsepower, there is no temperature rise across the fan. The fan could be located in the most advantageous position for the study; consequently, AiResearch presumed that the fan is upstream of the condenser and thus is operating at the point of maximum air density. Air horsepower is the product of the volumetric flow and the available pressure drop; the available air weight flow thus is a direct function of the fan air density at any particular pressure drop, and is, therefore, maximum at the maximum air density. Since the best airflows for the condenser correspond to relatively high air side temperature effectivenesses, the reduction in core volume due to the greater mean temperature difference in heat transfer of the higher density flow rate is more significant than the increase in frontal area required by the higher density flow rate.

In the analysis of the tubular surfaces for flow inside or outside the tubes, the vapor side surface was simply the plain round tube surface on the other side of the tube. In the analysis of the plate-fin surfaces, however, a plate-fin surface had to be selected for the condensing side. The only parameters on the condensing side specified for the study were the heat transfer coefficient and the condensing temperature. A low-height compact plate-fin surface was therefore selected for the condensing side fin in all the plate-fin designs. This fin was a stainless steel rectangular fin with 20 fins/in., a 0.050-in. height, a 1/10-in. offset length, and a fin thickness of 0.002 in. Stainless steel was originally selected for its compatibility with the condenser working fluid. The fin is a production AiResearch heat transfer surface and was deemed low enough in height to give maximum area to the air side area and yet not so low as to offer difficulties in fabrication and brazing.

At the start of the study, the volume requirement was specified as core volume. On this basis, the maximum airflow length was (1.5)(12)/5.55 or 3.243 in. However, after the study had progressed far enough to indicate that the plate-fin surfaces were the best choice, the volume criterion was revised to apply only to the air side volume of the core when the best plate-fin surface was chosen.

After the parametric study was completed, permission was received from the Project Officer to build the entire core of aluminum instead of using stainless steel for the condensing fin and copper for the air fin. As a consequence, the condensing fin thickness was increased to 0.004 in. for the aluminum material.

ANALYSIS

Types of Surfaces Evaluated

In the parametric study, the surfaces evaluated were flow inside plain round tubes and ring dimpled round tubes, flow outside plain round tubes and circular finned round tubes, flow through continuous fins outside flat tubes, and flow through plate-fin surfaces. The plate-fin surfaces were plain, strip, offset, louvered, wavy, and perforated. The perforated plate-fin surface was selected as the optimum type for this study on the basis of its air frontal area and air volume.

All the plate-fin surfaces were evaluated for fin thicknesses of 0.004 and 0.006 in. and in single, double, and triple sandwich construction. The multi-sandwich construction consists of more than one fin row or layer in each air passage between the tube plates enclosing the condensing passages. Each air fin row is separated from any adjacent air fin row in the same air passage by a splitter plate. This type of construction is a simple way of obtaining more than one surface configuration from one fin surface; the compactness of the fin is maintained, but its air pressure drop characteristics are changed by the changing heights of the air passage of the multi-sandwich construction. All the plate-fin surfaces presented in Kays and London "Compact Heat Exchangers" and the plate-fin surfaces in the AiResearch inventory were evaluated in this manner, although the available data are generally for one construction and one fin thickness.

Many of the plain and offset fin surfaces in "Compact Heat Exchangers" are from cores supplied to Stanford University by AiResearch. As a result, the surfaces in "Compact Heat Exchangers" and in the AiResearch inventory of plate-fin surface data are the same surfaces and use the same Stanford test data. The test data, however, were reduced by Stanford University and by AiResearch in a different manner because of the different emphasis on the use of the data. Since the AiResearch plate-fin computer programs are based on the AiResearch type of data reduction, the AiResearch curves were used where there was a difference in the results. This difference was significant only in the offset fin surfaces.

Computer Programs Used in the Analysis

Analysis of the round tube surfaces (both plain and ring dimpled) for flow inside the tubes was performed with a simple computer program that neglected the tube end losses, flow acceleration, compressibility, and condensing side conductance.

Analysis of the plain tube and circular fin tube banks with flow outside the tubes was performed with an AiResearch computer program that included flow acceleration pressure drops, surface temperature efficiencies, and the condensing side conductance. In runs with AiResearch performance data, approximate end loss coefficients were used.

Analysis of the plate-fin surfaces was performed by an AiResearch heat exchanger design computer program, which included core inlet and entrance losses, flow acceleration losses, compressibility effects, surface temperature efficiencies, and the condensing side heat-transfer conductance. The core end losses were approximated by the use of values of 0.19 for contraction and 0.07 for expansion for all of the surfaces to avoid the tedious work of using the exact loss coefficients for all of the same surface types.

The last two heat exchanger computer programs are two-fluid heat exchanger design programs; the condensing side, therefore, had to be simulated by a high water flow giving a temperature drop of 1°F. The heat transfer factor for the condensing side was adjusted so that the calculated heat transfer coefficient was always the 2000 Btu/(hr)(ft^2)(°F) specified.

An AiResearch plate-fin performance computer program was used to check the final solutions. Since the design computer programs were not able to handle the finned flat tubes, these surfaces were checked by an AiResearch general heat exchanger performance computer program, which estimated the performance in the available air frontal area and total core volume.

The plate-fin heat exchanger design program was used extensively in this study because the plate-fin surfaces proved to be the best. The computer program used for the plate-fin heat exchanger designs is a counterflow design program for the pure counterflow section of a heat exchanger. It designed the heat exchangers by an iteration procedure for a large number of plate-fin surfaces at a time. The friction factor (f) and the Colburn heat transfer factor (j) for each of the surfaces are in tabular form as a function of the heat exchanger Reynolds number. When given the required performance, fluid properties, fin information, and heat exchanger structural details, the fin information for each table could be modified by input problem data. Perfect gas behavior and normal operating temperature and pressure levels were assumed for the air. Density for the core friction pressure drop is the reciprocal of the average specific volume. Checks are made for thermodynamically impossible problems, and the core and duct Mach numbers are calculated. The specific heat ratio for air in the compressibility equations is calculated from the air specific heat and molecular weight by means of perfect gas relations. Fin efficiencies are determined by iteration.

The use of a counterflow plate-fin heat exchanger design program for a crossflow condenser is possible because the only requirements specified for the condensing side are the heat transfer coefficient and condensing temperature and there is no condensing side pressure drop requirement. This lack of a design pressure drop for the condensing side made the use of the AiResearch crossflow plate-fin heat exchanger design program inconvenient to use. In contrast, due to the loss of one degree of freedom in the design analysis by the constraint in the counterflow program that both fluids have the same flow width and flow length, the allowable pressure drop is usually met only by one of the fluids (the air in the study) and is only partially used up on the other side (the condensing side in the study). Since the condensing temperature is constant and the condensing side velocity is not a factor in the study, it was immaterial whether the computer program took the condensing side as a parallel to the airflow or as crosswise to the airflow.

Effects of Various Parameters on Condenser Configuration

In the study it was decided to use airflow increments based on increments of air temperature effectiveness. Any airflow rate value would be correct only for the parametric study design point heat load. However, the corresponding air temperature effectiveness would be valid for all heat loads. In addition, air temperature effectiveness can range only from zero to unity, while the airflow can vary from zero to a large value.

When the surfaces were examined over a wide range of air temperature effectivenesses (airflows), there was generally an effectiveness (airflow) at which the air frontal area reached a minimum for each surface. The curve was relatively flat in the region of the minimum. In contrast, no point of inflection occurred in the curves of the air volume and airflow length; both parameters always decreased as the effectiveness decreased (airflow increased).

It was felt that the minimum-volume unit would result from utilization of all of the available air frontal area. There were two approaches in reaching this goal. In the more restrictive surfaces, the air temperature effectiveness (and thereby the airflow) was varied to find the point for the minimum air frontal area. This procedure was necessary for surfaces whose minimum air frontal areas were equal to or larger than the allowable. For the less restrictive surfaces, the minimum air frontal area was less than the allowable. For these fins, the air temperature effectiveness was decreased (the airflow increased) until the allowable air frontal area was reached. This decrease in effectiveness caused a decrease in the air volume.

Figures 3-1 and 3-2 show the variation of air total frontal area and air side volume with the air temperature effectiveness for the design point heat rejection. Figure 3-1 is for the best rectangular offset fin and represents the case where the minimum air frontal area of the surface is more than the available area. Figure 3-2 is for the perforated fin with 0.004-in. fin thickness (the best heat transfer surface in the parametric study) and illustrates the case where the minimum air frontal area is below the available area so that the latter can be reached with a reduction in volume by decreasing the effectiveness (increasing the air weight flow).

In all cases, the solutions were achieved by varying the air effectiveness in increments of 0.005 in the area of the point of solution. Generally, the best airflow for a surface depended on its restrictiveness. The looser surfaces had higher optimum airflows (lower air temperature effectiveness) than the more restrictive surfaces. The air temperature effectiveness for the restrictive surface minimum frontal area was generally at 0.865. It was 0.770 for plain fin 19.86 and 0.700 for perforated fin 13.95, the two best existing surfaces in the study.

In the plate-fin surface computer runs, the air side fin thermal conductivity was set at 100 Btu/(hr)(ft)(^{0}F). Some aluminum fin stocks have this value of thermal conductivity, while others have a value of around 110. The value of 100 is also considered reasonable for the copper material originally selected for the air fin when stainless steel construction was deemed

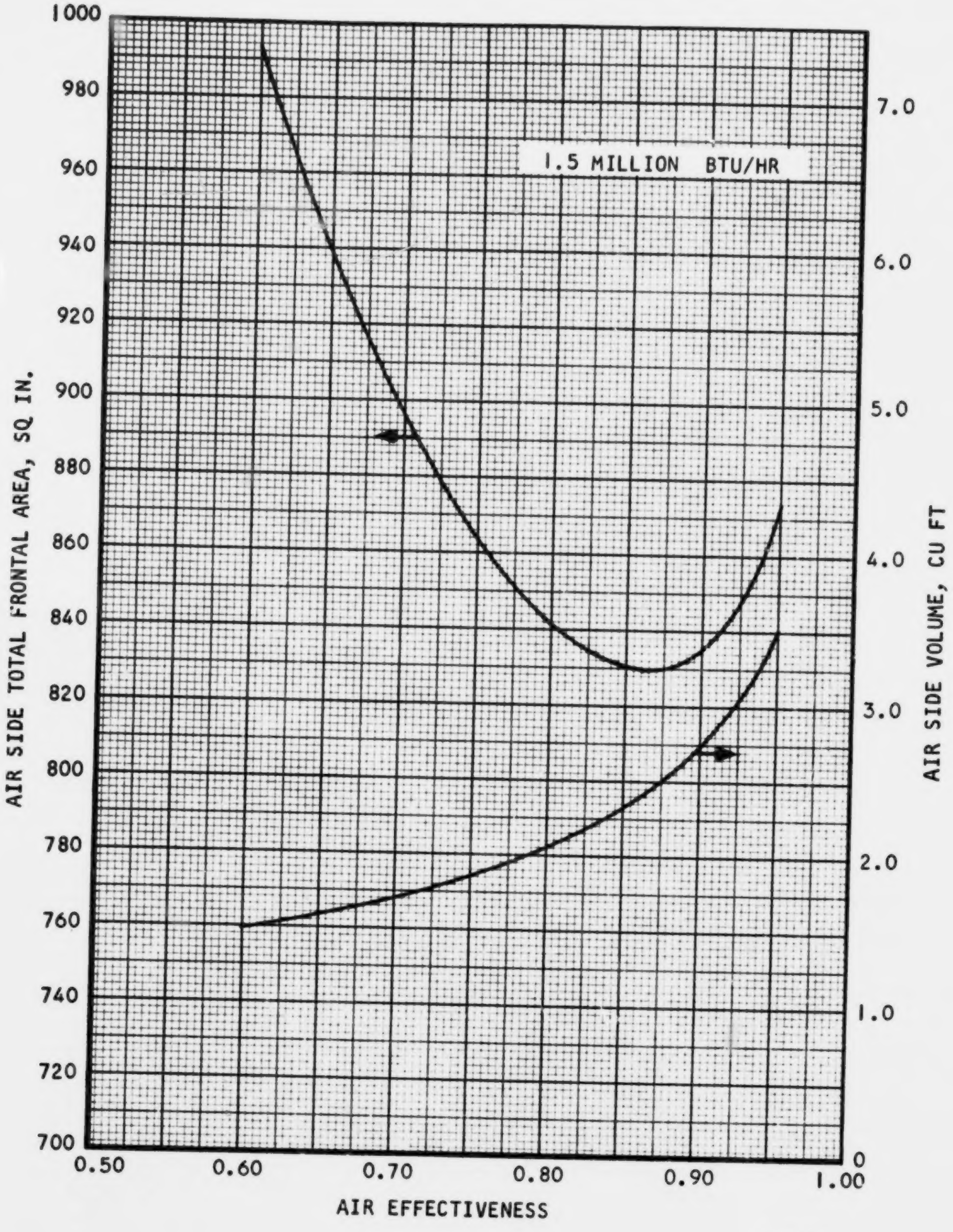

Figure 3-1. Core Frontal Area and Air Side Volume vs Air Effectiveness for Rectangular Offset Fin

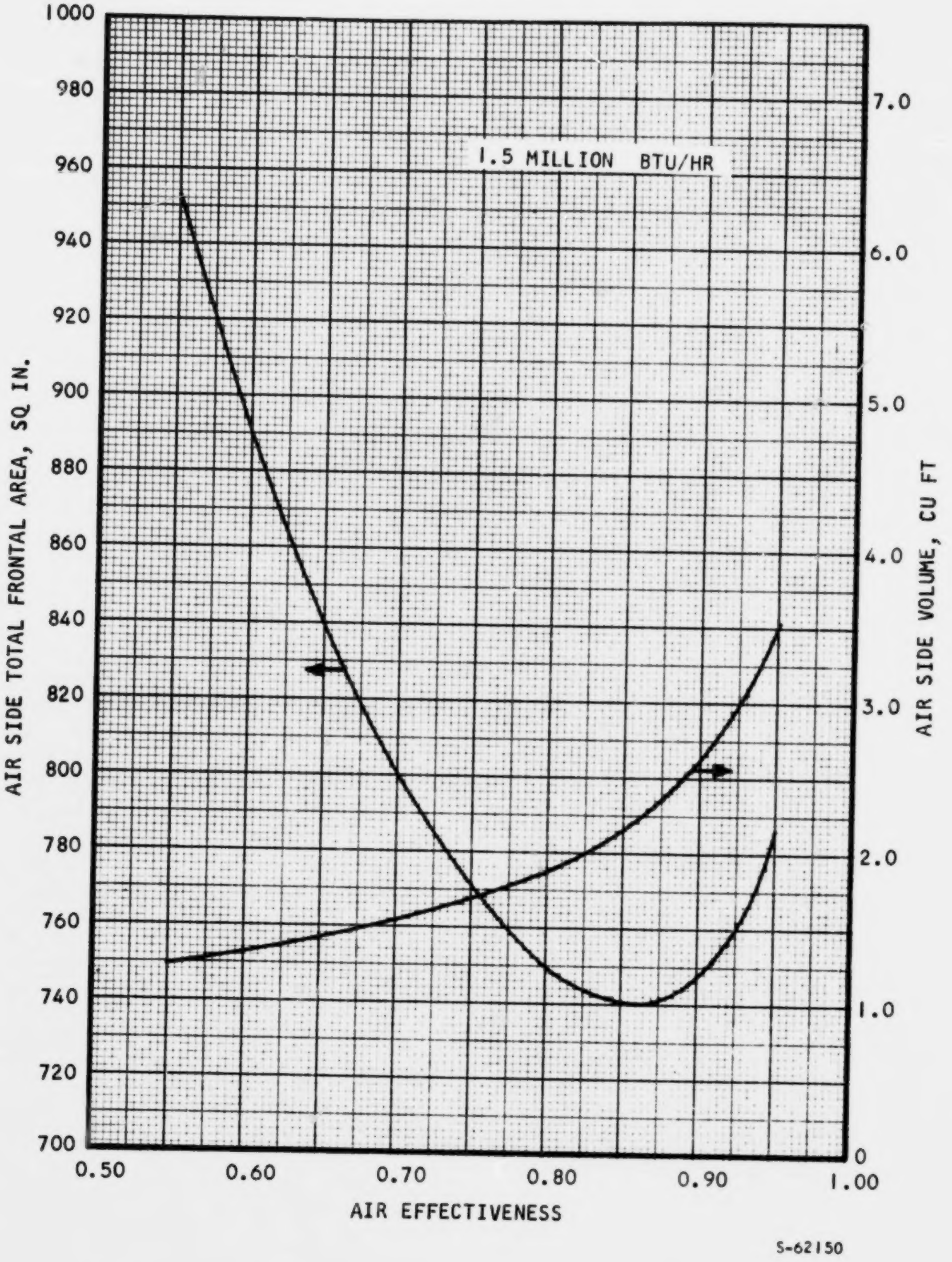

Figure 3-2. Core Frontal Area and Air Side Volume vs Air Effectiveness for Theoretical Perforated Fin

necessary for compatibility with the thiophene fluid. It was anticipated that the much higher thermal conductivity of the copper material would not be achieved by the fin after fabrication of the core because the brazing material might alloy with the fin and seriously reduce the effective thermal conductivity of the copper.

Fin thickness had a significant effect on the results. A thickness of 0.004 in. was chosen as the minimum practical gauge for the air fin because aluminum was a possible heat exchanger material. Although high fins have been made of thin copper (e.g., 0.002 in. in AiResearch heat exchangers for the environmental control system of the Lockheed C-5A airplane), it was felt that a thicker fin would be more rugged. The plate-fin surfaces were all also run at 0.006 in. thicknesses, but the solutions all were larger in face area, though smaller in volume, than the thinner fin results. A final check on the effect of the 0.006-in. fin thickness was to rerun the new perforated fin and a new plain fin with this gauge. The results agreed with those of the earlier runs. The conclusion is that the higher fin efficiency of the thicker fins was not enough to compensate for the face area increase caused by the higher pressure drop of the thicker fin. Another example of the effect of fin thickness is the perforated fin 13.95. The actual fin for which data was available was made of 0.012-in. material. Its air face area was too large. When the fin gauge was reduced to the 0.004 in. used in the study, the perforated fin became the best fin. A check of the effect of the gauge change from 0.012 to 0.004 in. was made by rerunning the rectangular offset fins with fin thicknesses of 0.012 in. The results confirmed that most of the perforated fin improvement was due to the fin thickness change.

At the design point of the study, the Reynolds number of the best plain fin, plain plate-fin 19.86, was 2120. It was 3539 for perforated fin 13.95. These are transition range Reynolds numbers, which point out the impracticability of following the advice of some writers not to design heat exchangers in the transition region. The reason for this advice is the uncertainty in the performance of long plain surfaces whose f and j curves show a transitional dip in this range. However, plain plate-fin 19.86 is not a very long fin. It was made in two pieces and had a length-to-hydraulic diameter ratio of 35.0, where the length is the uninterrupted fin flow length of 2.51 in. When all the plain fins investigated in the study were reanalyzed at the geometry of the 19.86 fin, only the results with the f and j curves of plain plate-fin 11.1 proved better. Plate-fin 11.1 had a length-to-diameter ratio of 20.6. The next best plain fin data was plain-fin 10.27T, which had a length-to-diameter ratio of 16.6. These results show that some turbulence is needed in the transitional Reynolds number range to get the best designs. As a result, if the plain plate-fin 19.86 solution had been selected, it would have to be built with the air fin being made in two pieces in the airflow direction and not in the one piece that is desirable for manufacturing simplicity and lower cost. The best available fin, perforated plate-fin 13.95, also had turbulence created by the perforations. This turbulence is efficient at the higher Reynolds numbers, but is less efficient at lower Reynolds numbers. If the design conditions were changed so that the design point Reynolds number was substantially reduced, another plate-fin surface would very likely prove to be a better fin for the new conditions than perforated fin 13.95.

Heat Transfer Surface Comparison Factors

The optimum heat transfer surface for any application depends on the particular requirements of that application. No one heat transfer surface is superior to all others for all applications. The selection of the best heat transfer surface for an application depends on a large number of variables: types of surface, surface geometry, surface performance characteristics, heat exchanger material, operating temperature level, flow rates, type of fluids, heat transfer rate, pressure drops, envelope constraints, allowable weight, cost, and other factors. To facilitate the quick comparison of many surfaces and different types of surfaces, various approximate relations or factors have been derived in the heat transfer literature from the standard heat transfer equations.

It must be emphasized that such approximate comparison factors cannot be used to design actual heat exchangers because many simplifying assumptions are made in the derivation of the relations. For example, core entrance and exit losses and flow acceleration losses are usually neglected. Fin efficiencies as well as fin blockage also are often neglected. As a result, their usefulness in practical applications is to act as a screen, and the final decision must be based on actual heat exchanger designs using the most promising surfaces.

The usual approach is to start with the standard heat transfer and pressure drop relations

$$j = \frac{h}{Gc_p} Pr^{2/3} = \frac{h}{(W/A_c)c_p} Pr^{2/3} = \frac{hA_c}{Wc_p} Pr^{2/3}$$

$$f = \frac{\Delta P}{\frac{L}{r_h}\frac{G^2}{2g\rho}} = \frac{\Delta P}{\frac{L}{r_h}\frac{(W/A_c)^2}{2g\rho}}$$

$$Re = \frac{4r_hG}{\mu} = \frac{4r_hW}{\mu A_c}$$

which, together with the definition of hydraulic radius ($r_h = A_c L/A$) as used by Kays and London in "Compact Heat Exchangers" can be manipulated into different arrangements of the various variables to obtain different surface comparison factors. The following nomenclature is in consistent units:

A	heat transfer surface area
A_c	free flow area
A_{fr}	frontal area
c_p	specific heat at constant pressure
f	Fanning friction factor
g	conversion factor
G	mass velocity, W/A_c
h	heat transfer coefficient
j	Colburn heat transfer factor
L	flow length
NTU	number of heat transfer units, UA/Wc_p (hA/Wc_p for one side)
Pr	Prandtl number
Re	Reynolds number
r_h	hydraulic radius, A_cL/A
U	overall heat transfer coefficient based on A
V	volume, $A_{fr}L$
W	weight flow rate
ΔP	friction pressure drop
η_o	surface temperature efficiency
ρ	density

1. NTU, Number of Heat Transfer Units

NTU is a measure of the heat transfer effectiveness. If the weight flow is held constant, NTU directly reflects the heat transfer capacity. With h from the definition of j and noting that $A/A_c = L/r_h$ from the definition of r_h:

$$NTU = \eta_o \, j \, \frac{L}{r_h} \, \frac{1}{Pr^{2/3}}$$

Hence, for a given condition and a fixed flow length, NTU varies directly with the ratio of the heat transfer factor j and the hydraulic radius r_h.

2. NTU/V, NTU Per Unit Volume

The NTU per unit volume is of interest. Dividing NTU by the volume V, where $V = A_{fr} L$:

$$NTU/V = \eta_o \, \frac{j}{r_h} \, \frac{1}{A_{fr}} \, \frac{1}{Pr^{2/3}}$$

for a fixed frontal area and a given condition, NTU/V is a direct function of j/r_h, which can be considered as a measure of the restrictiveness of a surface.

3. NTU/ΔP, NTU Per Unit Pressure Drop

The ratio of the NTU to the pressure drop is an indication of the efficiency of the pressure drop in heat transfer:

$$NTU/\Delta P = \eta_o \, \frac{j}{f} \, \frac{2g\rho}{Pr^{2/3}} \, \frac{A_c^2}{W^2}$$

The efficiency of the pressure drop in heat transfer is therefore indicated by the ratio j/f, which is known as the "goodness factor." The higher this j/f ratio is, the more efficient the surface is in its use of the friction loss incurred across the surface itself.

4. A_c, Free Flow Area

AiResearch prefers to use f/j, the reciprocal of the goodness factor, because the free flow area required by any surface varies directly as the square root of the ratio of f to j; the higher this ratio is, the more the free flow area that is required by the surface. The f/j ratio is a parameter in the equation for free flow area A_c derived by Dr. John L. Mason of AiResearch. From the definitions of the heat transfer factor j and the friction factor f, G and L/r_h are replaced by their equivalents W/A_c and A/A_c, respectively, and the free flow area is then solved for:

$$A_c = \sqrt{\frac{1}{2g} \, \frac{Pr^{2/3}}{c_p} \, \frac{f}{j} \, \frac{WhA}{\rho \Delta P}}$$

This relation is called the impossibility equation because it was derived to prove that certain conditions specified in a heat exchanger problem statement are impossible to meet with any heat exchanger. (It proved that is probably impossible to meet the maximum heat rejection point of this study.) For example, the heat transfer conductance (hA) cannot be less than the overall heat transfer conductance (UA), $\underline{\Delta}P$ cannot be greater than the available overall pressure drop, and f/j is not less than 2.19 for gas flow in smooth passages. When these values are substituted into the impossibility equation, along with the appropriate fluid properties and the fluid flow rate, the minimum free flow area required to meet the heat transfer and pressure drop requirements can be determined. If this minimum attainable free flow area is greater than the available face area specified in the problem statement, the problem statement is obviously impossible. This means that no heat exchanger can be designed to meet the problem statement and that the problem statement must be modified in order to obtain a solution.

The equation is also used to estimate the required free flow area (and thereby the face area) for a heat exchanger by making assumptions for the thermal conductance ratio, the fin effectiveness of an extended surface heat exchanger, and the ratio of the friction pressure drop to the available pressure drop. This procedure is the basis for the initial iteration in all AiResearch heat exchanger design computer programs.

Standard equations for turbulent flow of gases in plain round tubes as given in McAdams "Heat Transmission" (3rd edition) are:

$$f = 0.046/Re^{0.2}$$

$$j = 0.021/Re^{0.2}$$

The f/j ratio is therefore 0.046/0.021 or 2.19. This turbulent flow value is a lower limit that is not reached by the reliable air test data of any other heat transfer surface. Any data that achieves this limit is normally considered questionable because any surface that creates more turbulence than flow inside a plain round tube must have parasitic losses that are not usable for heat transfer.

An example of such questionable data is plain plate-fin surface 5.3 in Kays and London "Compact Heat Exchangers," which has an f of 0.00806 and a j of 0.00397 (f/j of 2.03) at a Reynolds number of 8000. The f is questionable because the entrance and exit losses deducted from the measured overall core pressure drops to obtain the friction losses for f were relatively large.

Application of Impossibility Equation

1. Plate-Fin Heat Exchanger

A simple computer program was written to apply the Mason impossibility equation to the design point conditions of this study. In one computer run, the f/j ratio of 2.19 was used along with the ideal assumptions of all prime surface, all pressure drop used for friction, and zero resistance for the wall and the condensing side. A range of air side effectivenesses was run in increments of 0.005. In the neighborhood of the minimum free flow area, the results were:

Air Effectiveness	Airflow, lb/min	Air Free Flow Area, sq in.
0.830	1000.38	442.28
0.835	994.38	442.09
0.840	988.45	441.96
0.845*	982.59*	441.91*
0.850	976.80	441.95
0.855	971.08	442.06
0.860	965.42	442.27

The air effectiveness is therefore 0.845 at the minimum free flow area of 441.91 sq in. The corresponding airflow is 982.59 lb/min, the inlet volumetric flow is 13,733 cfm, and the available pressure drop is 4.166 in. H_2O, which corresponds to an available heat exchanger corrected pressure drop ($\sigma\Delta P$) of 3.576 in H_2O at the NASA standard atmosphere density of 0.0765 lb/cu ft (29.92 in. Hg abs pressure and 59°F temperature). Based on the standard fan air density of 0.075 lb/cu ft (29.92 in. Hg abs pressure and 70°F temperature), the required fan pressure rise at standard fan conditions ($\Delta P/\sigma$) is 4.46 in. H_2O.

The available effective air frontal face area is 799.2 sq in. The corresponding free flow-to-frontal area ratio is therefore 441.91/799.2 or 0.553. Therefore, it would be impossible for any heat transfer surface with an air free flow-to-frontal area ratio of less than 0.553 to meet the design conditions within the design frontal area, and such surfaces were analyzed in the study to show the validity of this screening value. Note that this value of 0.553 does not allow for the space required by the surface itself or by the condensing side, so the required value for an actual heat exchanger would be higher than 0.553.

For plate-fin surfaces with the fin blockage neglected, the minimum air fin passage height for a condensing fin height of 0.050 in. and tube plate thickness of 0.006 in. is 0.075 in. for a free flow-to-frontal area ratio of 0.553. This value is too low to serve as a criterion in screening plate-fin surfaces.

Another run was made under the same conditions but with the fan located downstream of the heat exchanger. The results were:

Air effectiveness	0.830
Minimum free flow area	486.14 sq in.
Airflow	1000.38 lb/min
Outlet volumetric flow	16,737 cfm
Available pressure drop	3.418 in. H_2O
Available heat exchanger $\sigma\Delta P$	2.911 in. H_2O
Required fan $\Delta P/\sigma$	4.29 in. H_2O

---

*Minimum free flow area

At the maximum heat load of 2.5 million Btu/hr, the values are the same as those for the 1.5 million Btu/hr except that the free flow areas and volumetric flows are directly increased by the ratio of the heat loads (2.5/1.5). The required minimum free flow area with the fan upstream is 736.52 sq in., and the available air frontal area is 864 sq in. (6.0 x 144); therefore, the minimum free flow-to-frontal area ratio is 0.852. Since the free flow-to-frontal area ratio for only the fin passage of the new perforated fin selected for the condenser is 0.900, it is probably impossible to meet the maximum heat rejection requirement within the maximum available air frontal area of 6.0 sq ft. With the fan located downstream of the heat exchanger, the minimum free flow area rises to 810.24 sq. in. and the minimum free flow-to-frontal area ratio is 0.938 for the maximum heat rejection point.

2. Tubular Heat Exchanger

In flow outside plain round tubes, the minimum free flow area cannot be greater than the transverse flow area. For a transverse spacing of X_T tube diameters in an infinite heat exchanger, the free flow area gap between adjacent tubes is one tube diameter less, or X_T-1. The frontal area for the tube is X_T, so the core free flow area-to-frontal area ratio is $(X_T-1)/X_T$. For the minimum value of 0.553, X_T is 2.237, which means that a surface with air flowing outside the tubes in a bank of plain round tubes or finned circular tubes must have a transverse tube spacing of at least 2.237 tube diameters and a free flow-to-frontal area ratio of at least 0.553. The diameter of the tube does not affect this ratio.

Of the 10 plain (bare) tube test surfaces reported in Kays and London "Compact Heat Exchangers," the free flow-to-frontal area ratio ranged from 0.200 to 0.414. This last value is for surface S2.00-1.00, which is a staggered arrangement with an X_T of 2.00 and X_L of 1.00. The only surface with an X_T above 2.237 is surface S2.50-0.75, which has a free flow-to-frontal area of only 0.366.

Of the 16 surfaces of circular finned tubes, five had free flow-to-frontal area ratios higher than 0.553, but they had f/j ratios that are substantially above 2.19. As a result, their minimum required free flow-to-frontal area ratio is higher than the minimum of 0.553 as shown:

Surface	Available Free Flow-to-Frontal Area Ratio	Required Free Flow-to-Frontal Area Ratio
CF-8.7-5/8J(B)	0.628	0.837
CF-9.05/3/4J(B)	0.572	0.828
CF-9.05-3/4J(C)	0.688	0.939
CF-9.05-3/4J(E)	0.571	0.845
CF-8.8-1.0J(B)	0.642	0.746

With this adjustment in f/j, none of the five surfaces meet the minimum free flow area requirement. To confirm this analysis, surface CF-8.8-1.0J(B), which has the lowest free flow area requirements, was analyzed. The results confirmed the above analytical conclusion.

Effect of Reynolds Number Transitional Range

It is essential to have heat transfer factor and friction factor data for a surface before it can be analyzed for use in heat exchangers. It is also important to know the source of the data and how the data was obtained. The lowest pressure drop in-line bare tube surface presented in Kays and London "Compact Heat Exchangers" is based on Grimison's correlation and has a transverse spacing of 2.00 tube diameters and a longitudinal spacing of 1.25 tube diameters. The data is presented by Kays and London in order to include compact arrangements of interest not covered by their test cores. This surface would be called I-2.00-1.25 if it had been tested by Kays and London. AiResearch has test data for this spacing. When a tube diameter of 0.100 in. was used with both sets of j and f curves, the following differing results were obtained:

	Grimison	AiResearch
Air total frontal area, sq in.	1085	1312
Airflow length, in.	6.0	8.48
Total volume, cu ft	3.77	6.43

The Reynolds number is approximately 3000, which is the low Reynolds number end of the curve presented in "Compact Heat Exchangers." The AiResearch curve has a dip which shows that this Reynolds number is in the transitional range between laminar and turbulent flow. The shape of friction factor curve in "Compact Heat Exchangers" confirms that there is a transition. However, Grimison made his correlation with only turbulent flow data and purposely did not use the available transitional Reynolds number data in his correlation because most of the data did not show a transition and he was primarily interested in turbulent flow performance.

RESULTS

Flow Inside Round Tubes

Flow inside round tubes is not a practical configuration for this application because too many tubes are required and there are no structural supports on the condensing fluid side. Plain tube surface ST-1 of Kays and London was used to calculate the performance of a tube bundle with air flowing inside the tubes. The tube wall thickness was 0.004 in. The tube bundle was arranged in an equilateral triangular pattern with a clearance between tubes of 0.020 in. Fractional tubes were presumed possible. The condensing side resistance, entrance and exit pressure losses, and flow acceleration were neglected. The tube diameter was increased until an available tubing size was found at which the air frontal area was acceptable and the desired heat transfer was achieved. The solution has a 3/16-in.-diameter tube, 20.3 in. long. The air frontal area was 727.7 sq in., the volume was 5.8 cu ft. At the next lower tube diameter of 0.150 in., the tube length was 24.2 in., the frontal area was 861.3 sq in., and the volume was 7.64 cu ft. It is seen that the volume as well as the frontal area increased with decreasing tube diameter. It is usually expected that the volume will decrease with the tube diameter, however in this particular case the Reynolds number was in the transitional range between laminar and turbulent flow. In this region the f and j increase with the Reynolds number rather than decrease, and the net effect was an increase in the volume for a smaller tube diameter.

Much better results were obtained with AiResearch data for flow inside a plain round tube with turbulence in the air at the inlet, surface PLNTD. This data more closely represents the actual situation where the fan is presumed to be upstream of the condenser. The extent of the transitional dip is less. As a result, with a tube diameter of 0.100 in., the frontal area was 879.8 sq in. and the total volume was 2.21 cu ft. The airflow length was 8.20 in. A larger tube diameter would produce a smaller frontal area, and the airflow length would increase.

The 0.100-in. tube diameter was also used for ring dimpled tubes over a range of 16 dimple depths. The best ring dimple was chosen on the basis of its minimum volume because there was no inflection point for either frontal area or flow length as a function of the dimple depth, and the inflection point for flow length was at the highest frontal areas. The total volume was reduced to 1.35 cu ft but the frontal area soared to 1101 sq in.

Flow Outside Round Tubes

In flow outside round tubes, the calculated minimum required transverse spacing was 2.37 tube diameters, and the minimum required free flow area-to-frontal area ratio for a f/j value of 2.19 was 0.553. None of the bare tube surfaces in "Compact Heat Exchangers" met these criteria. Surface S-2.00-1.00 has a free flow area-to-frontal area ratio of 0.414, the largest value. The surface is a staggered tube bank with 0.375-in. diameter tubes, a transverse spacing of 2.00 tube diameters and a longitudinal spacing of 1.00 tube diameters. The surface with the greatest transverse spacing is surface S-2.50-0.75, which is a staggered tube bank with a tube diameter of 0.375-in., a transverse spacing of 2.50 tube diameters, and a longitudinal spacing of 0.75 tube diameters. Its free flow area-to-frontal area ratio, however, is only 0.366. Both surfaces were evaluated with their 0.375-in. diameter tube and with a tube diameter of 0.100 in., because the study showed that the air frontal area decreased with the tube diameter instead of increasing as was found with flow inside round tubes. The reduction in total volume is great with the smaller tube but the air frontal area is still excessive as the impossibility equation had predicted. The transverse spacing of surface S-2.00-1.00 was extended to 3.50 tube diameters by using AiResearch surface SB350100, which is a staggered tube bank of bare tubes with a transverse spacing of 3.50 tube diameters and a longitudinal spacing of 1.00 tube diameters. Its frontal area was still excessive. To see what a very compact tubular surface would do, AiResearch surface SB125100 was used. This surface differs from SB350100 only in having a transverse spacing of 1.25 tube diameters. The total volume was reduced but the frontal area increased as expected.

Surface	Air Frontal Area, sq in.	Total Volume, cu ft
S-2.00-1.00 (0.375-in. OD)	2192	15.7
S-2.00-1.00 (0.100-in. OD)	1914	2.22
S-2.50-0.75 (0.375-in. OD)	2473	14.49
S-2.50-0.75 (0.100-in. OD)	2135	2.23
SB350100 (0.100-in. OD)	1587	6.52
SB125100 (0.100-in. OD)	2886	1.34

Since a lower pressure drop surface was necessary, in-line tube banks were next examined. The only surfaces in "Compact Heat Exchangers" with a transverse spacing as high as 2.00 tube diameters is not Kays and London test data but is based on Grimison's correlation. The least restrictive of these surfaces is called "A," but can be called surface IB200125, which denotes an in-line bare tube bank with a transverse spacing of 2.00 tube diameters and a longitudinal spacing of 1.25 tube diameters. The frontal area of this surface is less than the staggered arrangements but is still excessive. However, as discussed previously, the Grimison correlation is not adequate here because the point of operation is in the transitional Reynolds number range and the Grimison correlation was made for turbulent flow. For comparison, an analysis was made with AiResearch data for this configuration, which shows a curve transition in this Reynolds number area.

Surface	Air Frontal Area, sq in.	Total Volume, cu ft
IB200125 (Grimison)	1085	3.77
IB200125 (AiResearch)	1312	6.43

A check of the finned circular tube surfaces in "Compact Heat Exchangers" indicated that none had sufficient flow area. Two of the least compact surfaces were run. As expected, they were still too restrictive even though their free flow-to-frontal area ratios were up to 0.688. The AiResearch finned circular surfaces are much more compact than the most compact finned circular tube surfaces in "Compact Heat Exchangers," so they are even less suited for this application.

Surface	Air Frontal Area, sq in.	Total Volume, cu ft
CF-9.05-3/4J(C)(0.774-in. OD)	1332	32.15
CF-9.05-3/4J(C)(0.100-in. OD)	1198	13.46
CF-8.8-1.0J(B)(1.024-in. OD)	1303	30.88
CF-8.8-1.0J(B)(0.100-in. OD)	1137	8.60

Plate-Fin Surfaces

The plate-fin surfaces proved to be the best surfaces when both the frontal area and volume requirements were considered. All these surfaces in "Compact Heat Exchangers," as well as all the AiResearch surfaces, were analyzed. They were analyzed in 0.004- and 0.006-in. fin thicknesses and in multiple sandwich arrangements even though their data are for only one sandwich arrangement. The 0.004-in. fin thickness was superior to the 0.006-in. fin thickness.

The best of the plain plate-fin surfaces was plain fin plate-fin 19.86, which has 19.86 fins per inch, a plate spacing of 0.250 in., a fin flow length of 2.51 in. and whose data is for a 0.006-in. thick fin.

After the available surfaces were surveyed, all of the plain plate-fin data was rerun, but with the geometry of the best plain fin imposed in order to determine if a better solution could be obtained with the best plain fin geometry and other sets of plain fin f and j data. Only one set of plain plate-fin f and j tables was found to give better results than the f and j data of the original plain plate-fin 19.86. This fin was plain plate-fin 11.1. The improvement was slight.

The next step was to use the f and j data of plain plate-fin 19.86 but to vary the fin height and the fin pitch to see if a better new fin could be found. For ease in fabrication, the fins per inch were varied in integral number of fins per inch, and the fin height was varied in 0.001-in. increments about the point of solution. The airflow was varied by increments of 0.005 in. about the air effectiveness found best for plain plate-fin 19.86.

As the number of fins per inch increased, the fin height had to be increased in order to keep the fin from becoming too restrictive. Each increase in fins per inch reduced the air volume required at a progressively decreasing rate. Finally, a fins-per-inch value was reached at which the air volume decrease was negligible or the allowable air frontal area was exceeded, irrespective of the air fin height.

The best of the louvered plate-fin surfaces was surface 3/4-11.1, which has 11.1 fins per inch, a plate spacing of 0.250 in., a louver length of 3/4 in., and was tested with a fin thickness of 0.006 in. Besides the louvered fin surfaces in "Compact Heat Exchanger," two other louvered plate-fin surfaces were analyzed. One is the composite louvered surface in the Chevrolet Corvette radiator, and one is the Ford louvered surface used in the condenser of the Thermo Electron Rankine-cycle system for automobiles.

The Corvette radiator air fin may be described as a composite of Kays and London louvered plate-fin surfaces 3/16-11.1, 3/8-11.1, and 1/2-11.1 with approximately 10.7 fins per inch and a fin height of 0.45 in. The louver lengths in the airflow direction were 0.1875, 0.375, 0.375, 0.500, 0.500, 0.375, 0.375, and 0.1875 in. The fin thickness was not given so a value of 0.004 in. was used for fin thickness. The j and f tables for these three Kays and London reported surfaces were used with the fin height and fins per inch of the Corvette fin. The results for the three fins were plotted against the louver length, and values for the Corvette fin were obtained from curves drawn through the points at a weighted average louver length of 0.39 in. A more accurate interpolation would probably have been on the basis of the length-to-hydraulic diameter ratio; the face area would be higher and the air volume less.

Details on the Ford fin were obtained from the Thermo Electron report, which also presented f and j curves for the fin from which tables of f and j values were prepared for the AiResearch computer program. The Ford fin has 14 fins per inch, a height of 0.500 in. (scaled from the drawing in the report), a louver length of 1/16 in., and a thickness of 0.0025 in. This fin was run both at this thickness of 0.0025 in. and the 0.004 used for the fins in the study. Both fins were inferior to the best fin of this study.

Figure 3-3 plots the design point air total frontal area and the air side volume for the best plain plate-fin surface (plain-fin plate-fin surface 19.86) and the best louvered plate-fin surface (louvered plate-fin surface 3/4-11.1) as a function of air weight flow in the area of the point of solution.

The strip and offset fins were lumped together. The best fin in this group was surface 12R-0.178-0.178(0) as a double sandwich fin. This surface has 12 rectangular fins per inch, a plate spacing of 0.178 in., an offset length of 0.178 in., and was tested with 0.004-in. aluminum fin stock. The surface is the same as strip-fin plate-fin surface 1/6-12.18(D) in "Compact Heat Exchangers." Somewhat different results were obtained with the Kays and London curves and the AiResearch curves although both sets of j and f curves are derived from the same Stanford University test data on the AiResearch core. The discrepancies are due to differences in the evaluation of the raw test data and the test core surface parameters. For example, the Kays and London curves yield a frontal area of 806.0 sq in., while the AiResearch curves give 828.8. The AiResearch curves invariably resulted in larger face area cores. Since the AiResearch computer design programs are based on the AiResearch method of data reduction, the AiResearch curves were used where there was any disagreement.

Of the three wavy fins in "Compact Heat Exchangers," the best was wavy fin plate-fin surface 17.8-3/8W, which has 17.8 fins per inch, a plate spacing of 0.413 in., a wave length of 3/8 in., a double amplitude of 0.0775 in., and was tested in 0.006-in. aluminum fin stock. The AiResearch data on other wavy plate-fin surfaces are for much more restrictive surfaces so this data was not used.

Figure 3-4 is a plot of the air side total frontal area and air side volume at the design point for the best rectangular offset surface (surface 12R-0.178-0.178(0)) and the best wavy fin surface (wavy fin plate-fin surface 17.8-3/8W).

NOTES:

1. 1.5×10^6 BTU/HR
   9 AIR HP
2. CONDENSING H OF 2000 BTU/(HR)(SQ FT)(°F)

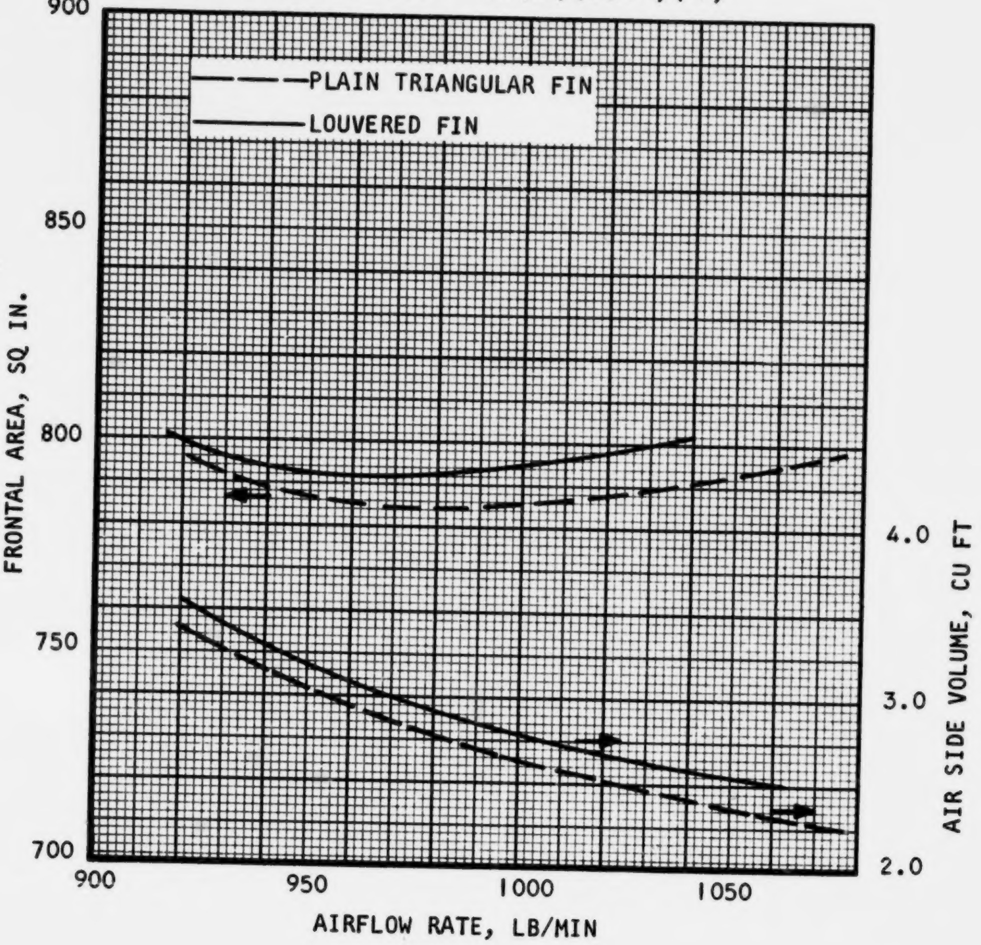

S-62153

Figure 3-3. Compact Condenser Study, Plate-Fin (Plain Triangular and Louvered)

NOTES:

1. 1.5×10^6 BTU/HR
   9 AIR HP
2. CONDENSING H OF 2000 BTU/(HR)(SQ FT)(°F)

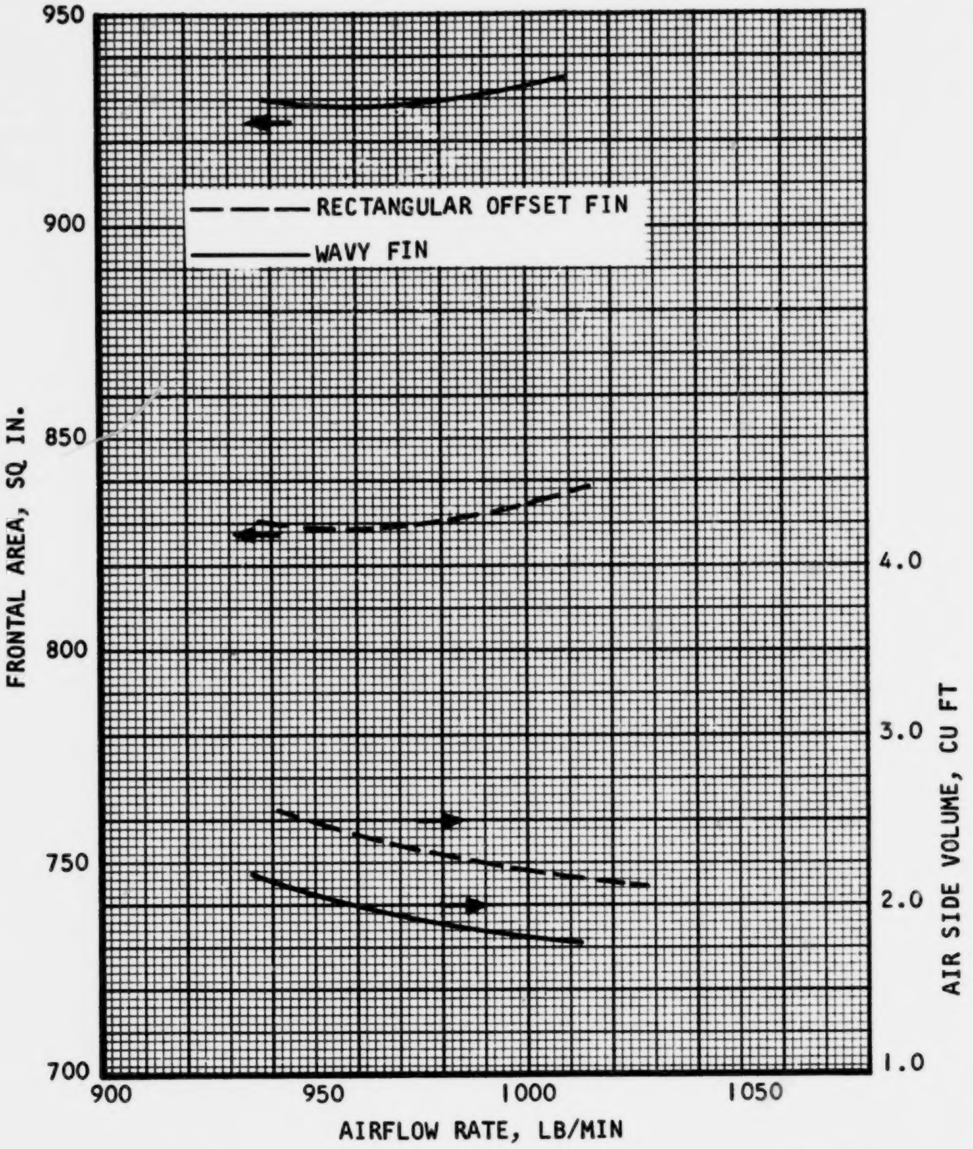

S-62151

Figure 3-4. Compact Condenser Study, Plate-Fin (Rectangular Offset and Wavy)

NOTES:

1. 1.5×10^6 BTU/HR
   9 AIR HP

2. CONDENSING H OF 2000 BTU/(HR)(SQ FT)(°F)

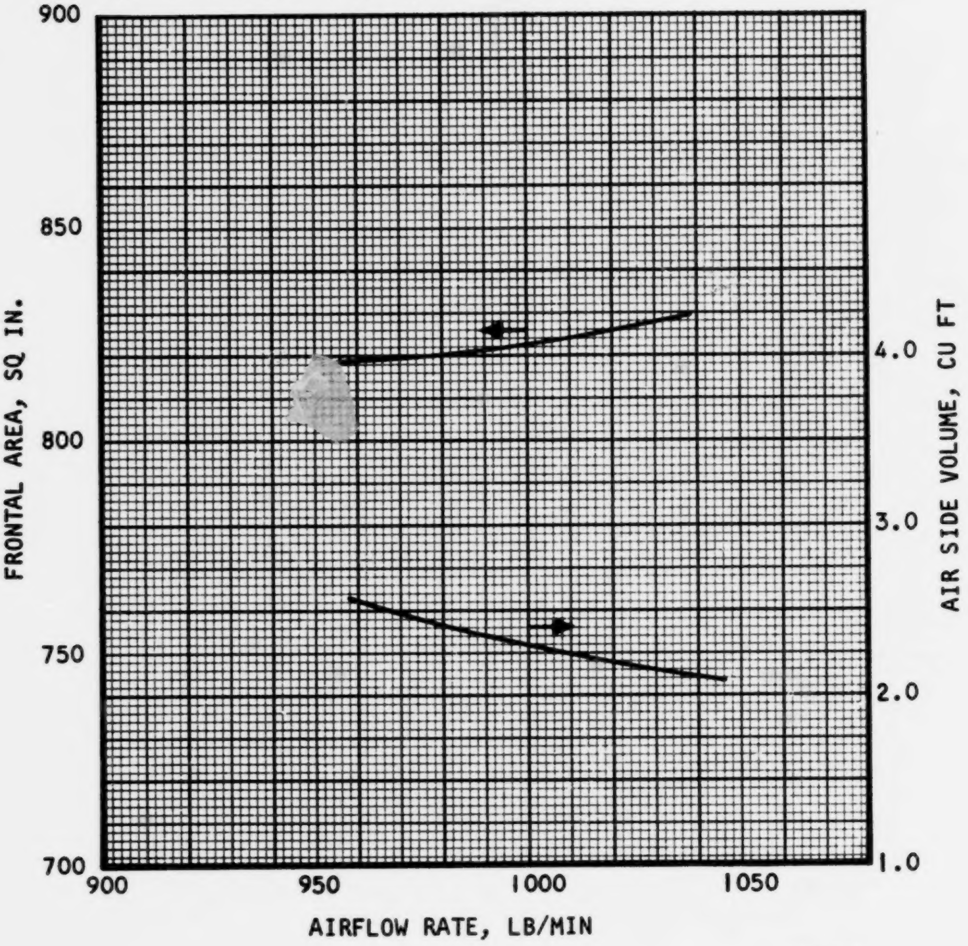

S-62155

Figure 3-5. Compact Condenser Study, Plate-Fin (Perforated)

A perforated fin was found to be the best surface in this study for the condenser at the specified conditions. The data in "Compact Heat Exchangers" for perforated fin plate-fin surface 13.95(P) is for a fin that has 13.95 fins per inch, a plate spacing of 0.200 in., perforations of 0.079-in. diameter spaced 32 per sq in. on a square pattern, and tested with 0.012-in. aluminum fin stock.

The calculated results with this thickness were not as good as those of plain plate-fin 19.86 at a thickness of 0.004 in. However, when the perforated fin was analyzed with the 0.004-in. fin thickness, the perforated fin provided the smallest volume of all of the solutions.

The perforated fin performance with 0.004-in. fin thickness was calculated by using the Kays and London f and j data for the 0.012-in. fin, but with the geometry of the 0.004-in. fin. The area lost by the perforations was deducted and the area of the rims of the perforations was added. The fin efficiency was calculated on the basis of the fin being nonperforated. The data of the 0.012-in. fin was also obtained in this manner according to Stanford University Technical Report No. 39, "The Heat Transfer and Flow Characteristics of a Wavy Fin, a Strip Fin, and a Perforated Fin Heat Transfer Surface," by W. M. Kays.

The air side frontal area and volume are shown in Figure 3-5 for perforated plate-fin surface 13.95(P) with a 0.012-in. fin thickness.

The procedure of varying the fin height and the number of fins per inch in order to find a better perforated fin was followed just as for the plain fin, but since this fin is a rectangular fin, the number of fins per inch was increased by increments of two fins per inch. This limitation was desirable because a rectangular fin with an even number of fins per inch is easier to cut into sections for a heat exchanger in the airflow width direction. The results of this analysis are shown in Figure 3-6. All points on the lines shown meet the heat transfer and pressure drop requirements of the design point. At a given frontal area, the incentive for increasing the number of fins per inch is a decrease in the air side volume. For this reason, a fin geometry of 22 fins/in with a plate spacing of 0.326 in. was selected as the theoretically best perforated fin. An additional increase in the number of fins per inch is not possible without exceeding the air side frontal area goal of 799 sq in. at the design point.

Although there is uncertainty due to the fin thickness and fin geometry changes, the estimated results are promising enough to warrant the selection of the perforated surface for the condenser test core.

The new perforated fin was selected as the new fin for the condenser. It should be noted that there are uncertainties in its design besides the obvious one of using the f and j data of one geometry and one thickness for another geometry at another fin thickness. Other factors are that the original test data of perforated plate-fin 13.95 was calculated on the basis of the fin efficiency of an unperforated fin, and the edges of the perforations were included in the heat transfer area. Other data in the literature on perforated material were examined, but they were not applicable because: (1) they were obtained with blowdown transient rig testing, which limits the accurate range of the test data to the laminar flow range, (2) the test data was all in the laminar flow range, or (3) the perforations were considered too small to be practical for a Rankine-cycle engine condenser.

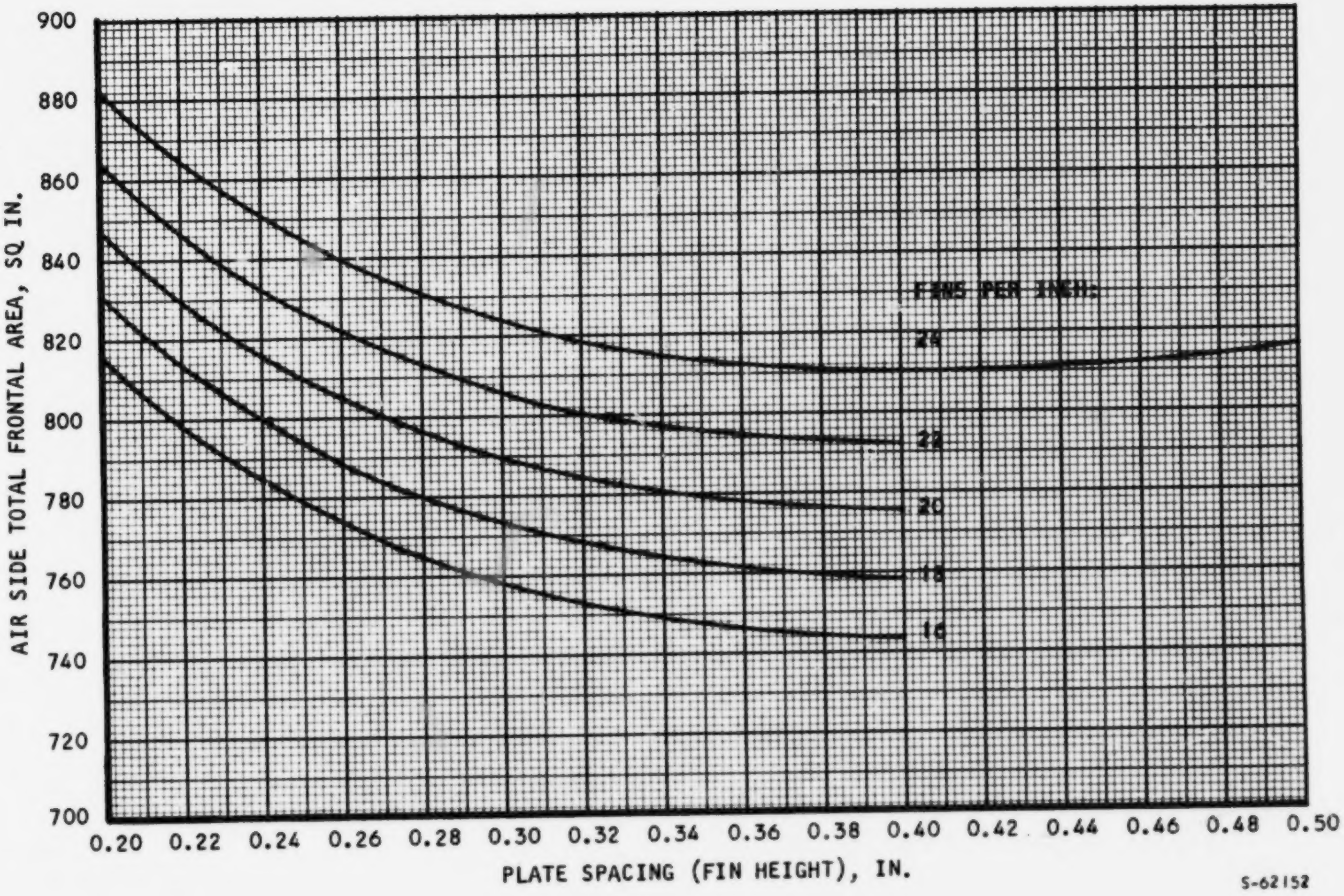

Figure 3-6. Variation of Frontal Area with Fins/In. and Fin Height for a Perforated Fin

Summary of Parametric Study Results

Figure 3-7 plots the air side volume as a function of the air total frontal area for the various surfaces analyzed in terms of a million Btu/hr heat load. Note that the frontal area is in sq ft instead of sq in. as in the other parts of the report. Also plotted in Figure 3-7 are the Corvette radiator surface, the Ford louvered fin surface in 0.0025-in. and 0.004-in. thicknesses, perforated fin plate-fin surface 13.95(P) in its original 0.012-in. thickness and in a 0.004-in. thickness, and the new perforated fin (22 fins per inch and 0.326-in. height).

Optimum condensers over the range of heat rejection rates of the study were determined using the existing heat transfer data. The following condensers were selected: (1) assuming face area as the primary goal, and (2) a compromise between face area and air side volume.

FACE AREA PRIME CONSIDERATION

Heat Rejection Rate, Btu/hr	Goal		Results	
	Area, sq in.	Volume, cu ft	Area, sq in.	Volume, cu ft
0.5×10^6	266	0.5	266	0.74
1.0×10^6	533	1.0	533	1.44
1.5×10^6	799	1.5	799	2.20
2.0×10^6	864	2.0	870	9.25
2.5×10^6	864	2.5	1040	15.50

The solutions for 0.5×10^6 to 1.5×10^6 Btu/hr use plain triangular air fin 19.86 and meet the face area requirement but exceed the volume by 48 percent. The solutions for 2.0×10^6 and 2.5×10^6 Btu/hr use plain rectangular air fin 6.2. This fin was selected because it comes the closest to the 6 sq ft face area limit. The volumes for these solutions are unreasonable, and therefore, compromise solutions were selected.

COMPROMISE BETWEEN FACE AREA AND VOLUME

Heat Rejection Rate, Btu/hr	Goal		Results	
	Area, sq in.	Volume, cu ft	Area, sq in.	Volume, cu ft
2.0×10^6	864	2.0	1045	3.84
2.5×10^6	864	2.5	1300	4.80

The compromise solutions also use the 19.86 plain triangular fin on the air side. The tabulated solutions represent the minimum frontal area with the 19.86 plain triangular fin and exceed the volume goal by a maximum of 92 percent.

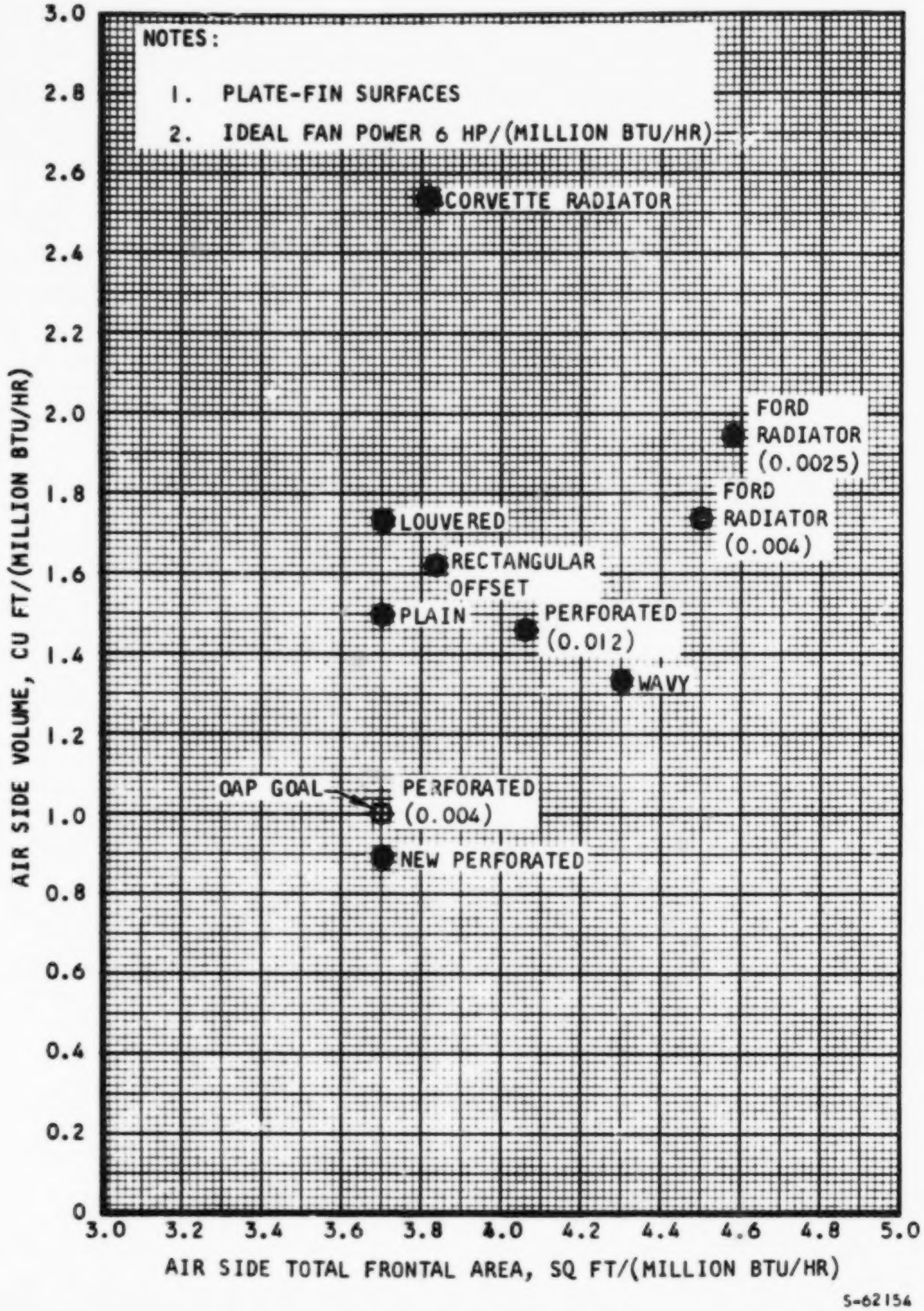

Figure 3-7. Summary of Solutions (Frontal Area and Volume) for Various Air Fin Configurations

SECTION 4

PARAMETRIC STUDY TEST CORE

CORE FABRICATION

A test core was fabricated (See Section 5) and tested to verify the performance of the new perforated fin defined in the parametric study. The selected air fin was based on heat transfer performance data in the literature for a fin made with 0.012-in.-thick perforated material. The fin thickness was reduced to 0.004-in. because the analysis indicated that this thinner gauge was required for the fin to meet the problem constraints. The perforation hole size and spacing were available commercially in thicker material. However, perforated material suppliers indicated that their present tooling would not produce the perforated material in the 0.004-in. material. Therefore, a punch press die to produce the chosen perforated material was designed and fabricated.

The aluminum test core built from the new perforated material is shown in Figure 4-1. The flow configuration is single-pass crossflow. The core is constructed from (1) ten air side sandwiches using the selected 22 fins per inch perforated rectangular fin surface, (2) eleven water side sandwiches using a 20 fins per inch offset rectangular fin surface, (3) separating tube plates, and (4) edge bars. The air fin flow length was the same as the selected air fin of the condenser. The core air face area was dictated by the required air Reynolds number range and the capacity of the laboratory test setup air supply.

The test core was stacked and fluxless brazed without any difficulties. The fabricated core was inspected with the following average dimensions: air sandwich flow width of 3.902 in., an air fin flow length of 3.38 in., and a total height of 4.13 in. The height over the air fins was 3.888 in., giving an effective air frontal area of 15.17 in.^{2}.

The air fins were counted in each passage. The air fin flow length was obtained from two sample air fins. The water fin count and flow length were obtained from four sample water fins.

The height of the air fin passage was measured in many places, but the values were not considered reliable because of yielding of the tube plates under pressure of the measuring device. As a result, the stack height over all the air fins was measured, and the average air fin passage height was calculated, after deducting the nominal water fin heights and nominal tube plate thicknesses. The calculated value of 0.3253 was considered close enough to the nominal 0.326 for the latter to be used in the calculations. The air fin had 22.04 fins per inch so a value of 22.0 was used. The water fin had 20.3 fins per inch, and its nominal height of 0.050 in. was used.

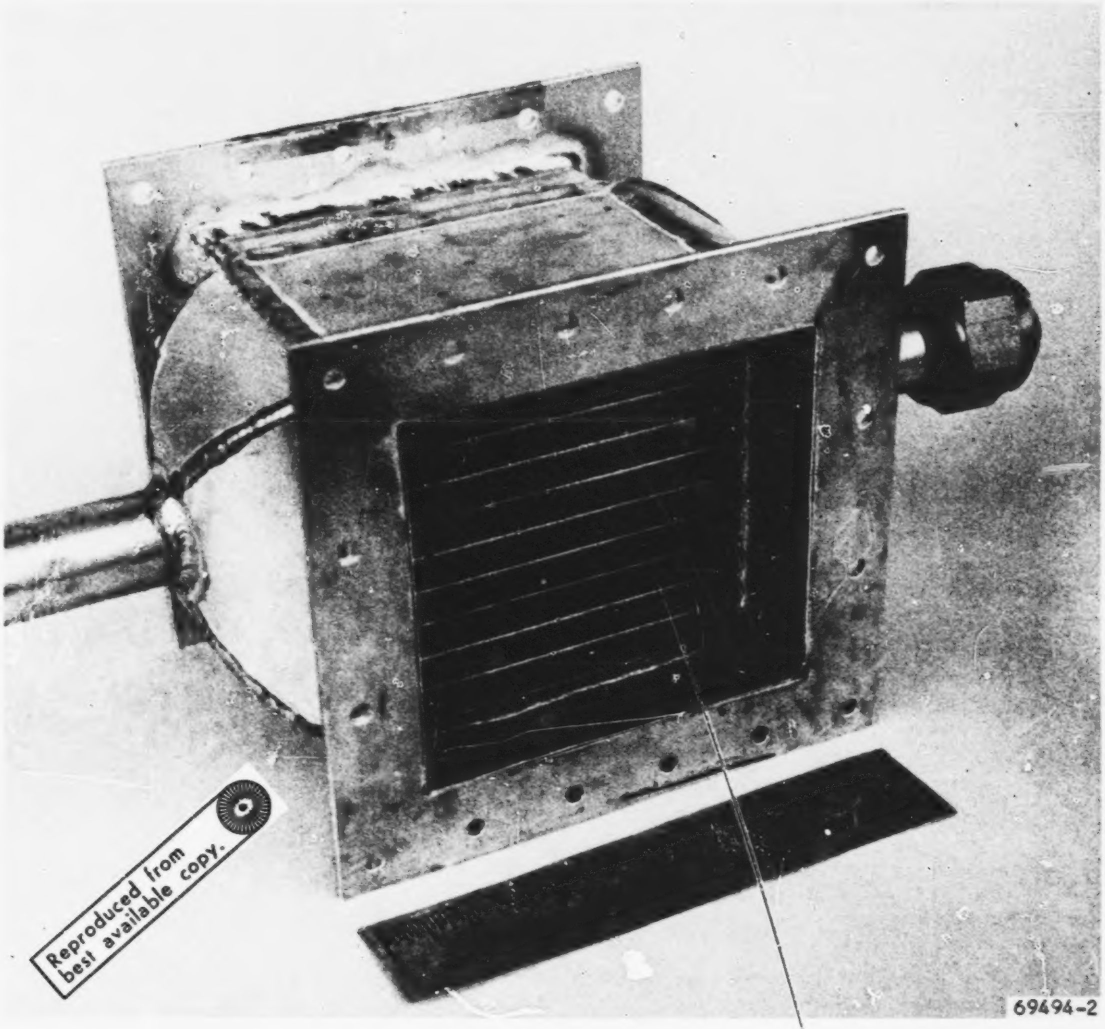

Reproduced from best available copy.

Figure 4-1. Test Core for f and j Factors (22 Fins per Inch Perforated 0.004 Aluminum Material)

The fin areas were calculated on the idealized model of rectangular fins. The edges of the perforations were included in the air fin area, and the air fin effectiveness was calculated on the basis of a solid straight fin; the data of Kays and London Perforated Fin 13.95 (P) was calculated in this manner. The overall fin length was used instead of the flow length of the core, and the heat transfer areas did not include the edge areas of the tube plates and core face cross strips that were exposed to the fluids at the inlet and outlet faces.

TESTING

Figure 4-2 is a schematic of the test setup. The air source was pressurized plant supply air, which had a moisture content of 8 grains per lb of dry air. The air weight flow rate was determined upstream of the core by a square-edged orifice plate in a 3-in. diameter pipe-flow measuring section; both met the requirements of the 1959 ASME Power Test Code for this type of flowmeter. Two orifice diameters were used: 2.0 and 1.5 in. The inlet air temperature was measured by a thermocouple, and the outlet air temperature was measured by four thermocouples after the air had been mixed in an insulated mixing device.

On the water side, the water was pumped from an open sump through a heat exchanger where it was heated by steam. The water then passed through a rotameter, which was used only to set the flow, and through a mixing device to the unit. After flowing up through the core, the water passed through another mixing device, through a filter, and through a weighing system back to the sump. The weight flow was determined by the weight-time method where the flow time for a specific weight of water was determined automatically to 0.01 sec. Weights varied from 22 to 12 lb and times from 30 to 66 sec.

Thermocouples were of special grade copper-constantan, which has an allowable tolerance of ±0.75°F. Temperatures were read by a direct reading potentiometer. Water temperature drop was measured by a differential thermocouple.

Air inlet static pressure and static pressure drops were measured by water manometers; inclined manometers were used to read all but the highest pressure drops to an accuracy of 0.01 in. of water. Wall pressure taps were located 3.0 in. upstream and 5.0 in. downstream of the faus of the test cores. Two taps located on opposite sides of the duct were used at each location and were connected to a common manometer to average the pressures. Water side pressure drops were measured in inches of water by differential pressure gauges and were used in the data reduction to calculate the frictional heating of the water.

Accuracy of the first data was indicated by the heat balances achieved. For all air flows except one above a Reynolds number of 1200, at least one run was obtained with a heat balance of not over 2 percent. Heat balances were poorer at lower flows. A heat balance of +4.5 percent was obtained at the lowest air flow, where a plus value indicated the water heat transfer rate was higher than the air heat transfer rate.

The performance characteristics of the optimum perforated fin were obtained from a water-to-air test. A water-to-air test was selected instead of a steam-to-air test because the water heat transfer coefficient could be more accurately determined and the water side heat transfer rate more easily obtained in a single phase fluid test.

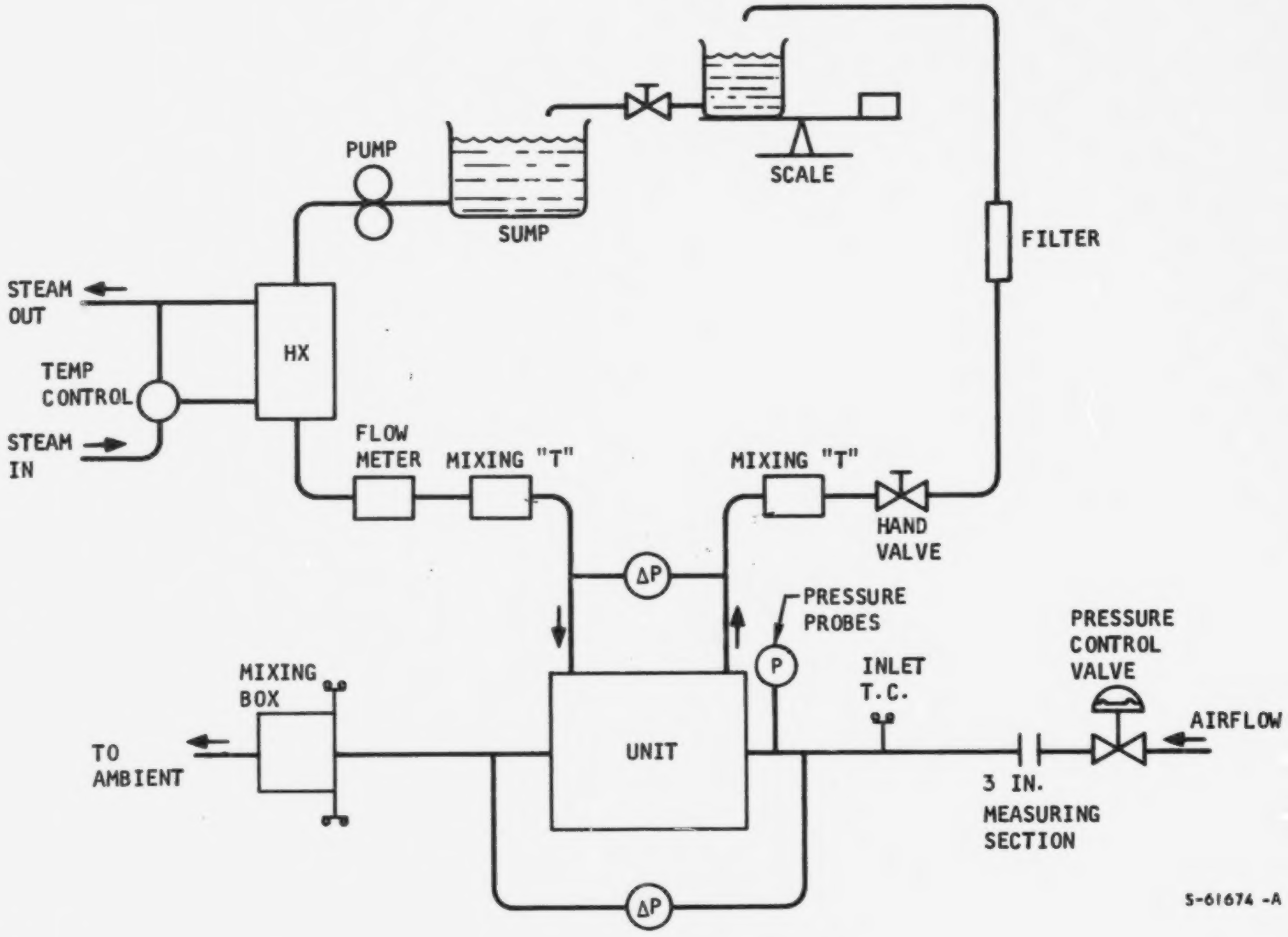
PUMP
SUMP
SCALE
FILTER
STEAM OUT
HX
TEMP CONTROL
STEAM IN
FLOW METER
MIXING "T"
MIXING "T"
HAND VALVE
ΔP
PRESSURE PROBES
P
PRESSURE CONTROL VALVE
MIXING BOX
INLET T.C.
AIRFLOW
TO AMBIENT
UNIT
3 IN. MEASURING SECTION
ΔP
5-61674 -A

Figure 4-2. Test Setup Schematic

Inlet temperature of the water was 188°F to 190°F, which is high enough for a good initial temperature difference, only 31°F below the design condensing temperature of 220°F, and safely below the boiling point of water. The air came from the unheated plant air supply with a temperature of 57°F to 78°F.

Selection of the water flow for each air flow point was based on three considerations. First, the water flow had to be low enough to yield a temperature change of at least 10°F in order to obtain an accurate water side heat transfer rate. Second, the water flow had to be high enough so that the water heat transfer conductance would be at least six times the anticipated air side conductance and reduce the effect of any uncertainty in the calculated water side conductance. Third, the water flow had to be high enough to reach the Reynolds number range where the difference between the Colburn heat transfer factors for air and water flows was negligible. The reason is the heat transfer factor curve for the water side fin was derived from an air test on a similar fin.

TEST RESULTS

The data was reduced by two existing AiResearch computer programs. The first program calculated the air flows and the air Fanning friction factors (f). The second program calculated the air Colburn heat transfer factors (j). The latter program is normally used to calculate f and j factors of liquid-to-liquid tests. As a check, the resulting curves of f and j were used with the AiResearch performance prediction program to calculate the test core performance at each of the air flow points; the agreement was satisfactory.

The flows, temperatures and heat transfer rates were computed from the test data. Each overall heat transfer conductance (UA) was obtained from

$$UA = Q/\Delta t_m$$

where Q is heat transfer rate and Δt_m is the mean temperature difference (for cross-flow with no mixing) from the test temperatures.

The water heat transfer conductance and the tube plate transverse conductance were calculated and deducted from the UA to obtain the air heat transfer conductance ($\eta_o hA$) from which the heat transfer coefficient (h) was obtained in an iterative calculation. At the maximum air flow, the calculated air conductance was 9.7 percent higher than the UA. The heat transfer factor was then calculated from h. Properties were evaluated at the bulk average temperature. The heat transfer factor for each air flow was calculated in this manner for a UA using the air side heat transfer rate and for a UA using the water side heat transfer rate. The two were then averaged for the curve. The Reynolds number was then calculated.

For the air friction factor, the core entrance and exit losses and the flow acceleration were deducted from the measured pressure loss, and the friction factor calculated. Abrupt area change turbulent flow loss coefficients of 0.178 and 0.06 were used for the entrance and exit losses, respectively. At the maximum air flow, the deducted losses were 14.6 percent of the overall pressure drop. The air density used for the friction factor was calculated with the average bulk values of pressure and temperature.

Figure 4-3 compares the test core f and j with those of Kays and London Perforated Plate-Fin Surface 13.95 (P) used in the design calculations. Both surfaces had the same size holes (0.079 in. dia), the same square pattern (32 holes per sq in.) and the same air flow length. However, the test fin was 0.004-in. thick and 0.326-in. high while Surface 13.95(P) was 0.012-in. thick and 0.200-in. high.

The test surface friction factor is higher than that of Surface 13.95(P) in the laminar region because the former has a higher fin passage aspect ratio. The lower heat transfer factor in the design range is apparently due to the lower turbulence from the shallower holes in the test fin. The friction factor apparently did not correspondingly reduce because of burrs at the edge of the holes. Contributing to the lower turbulence is the somewhat longer length-to-diameter (L/D) ratio of the test fin. As a result, the increase in j in the transitional Reynolds number range in the Kays and London test was not achieved in the AiResearch test.

The irregularity in the j curve at low flows may be an inherent performance characteristic of perforated fins because the Kays and London data also exhibit irregularities in this range (their Reynolds numbers 517 and 924, in particular).

A comparison of the two surfaces geometry follows:

	Surface 13.95 (P)	Test Fin
Fins per inch	13.95	22.0
Plate spacing, in.	0.200	0.326
Fin thickness, in.	0.012	0.004
Fin flow length, L, in.	3.375	3.38
Hydraulic diameter, D_h, in.	0.0986	0.0826
L/D_h	34.2	40.9
Total heat transfer area/volume between plates, β, ft^2/ft^3	381	524
Fin area/total area	0.705	0.872
Fin passage aspect ratio	3.15	7.75

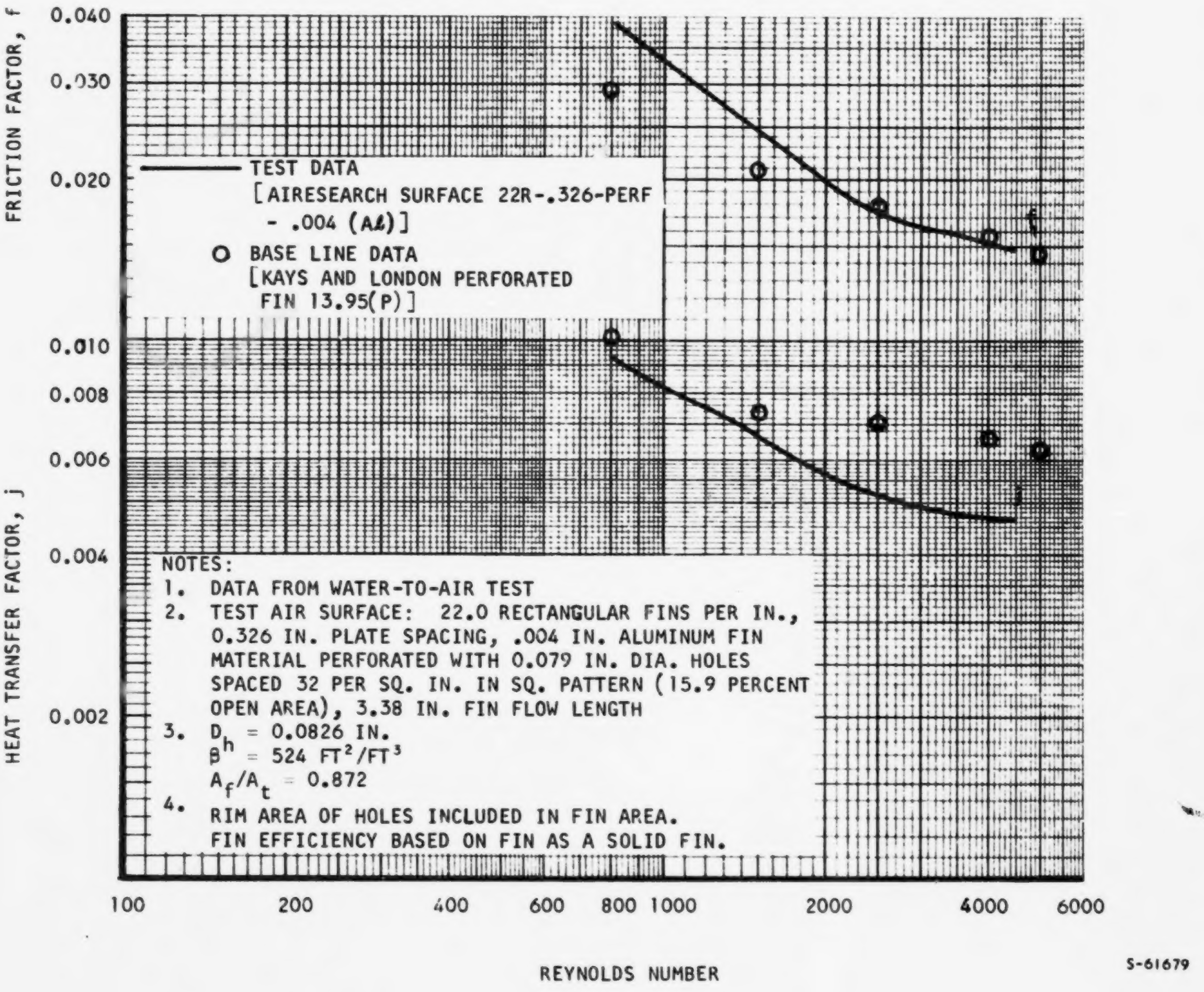

Figure 4-3. Performance Parameters 22 FPI Perforated Fin

The f and j data of the new perforated fin was used to design condenser cores at five heat rejection rates over the range of the study. These designs are shown in Table 4-1.

TABLE 4-1

CONDENSER DESIGNS WITH PERFORATED FIN

Heat Rejection Rate, Btu/hr	Goal		Results	
	Area, sq in.	Volume, cu ft	Area, sq in.	Volume, cu ft
0.5×10^6	266	0.5	279	0.87
1.0×10^6	533	1.0	559 ($3.88\ ft^2$)	1.73
1.5×10^6	799	1.5	838	2.60
2.0×10^6	864	2.0	1120	3.47
2.5×10^6	864	2.5	1395	4.34

Comparison of the 1.0×10^6 Btu/hr condenser core with cores sizes shown in Figure 3-7 indicates that the expected performance of this fin was not achieved. In fact, the plain fin yielded a smaller condenser than the new perforated fin. It was decided to investigate experimentally other perforated fin designs in order to realize the anticipated improved performance of a perforated fin design.

SECTION 5

PERFORATED PLATE-FIN MATRICES

The perforated air fin selected for the parametric study test core differed in height, pitch, and thickness from the perforated fin whose test data was used in the analysis. It was therefore anticipated that the selected fin test performance could be lower than calculated, but that its performance would still be superior to that of a plain fin. However, tests revealed that the performance of the selected fin was poorer than a plain fin. Since it was thought that the potential for reducing condenser core size using perforated fins still existed, the decision was made to investigate other perforated fin matrices. The selection and testing of these additional geometries is described in this section.

REVIEW OF AVAILABLE DATA

The available data in the heat transfer literature on perforated surfaces all indicate the improved performance of perforated surfaces over that of non-perforated surfaces. However, most of the data are not applicable to the particular requirements of the compact condenser. The data published by the U.S. Naval Postgraduate School is generally limited to the laminar flow region, whereas the operating point of the compact condenser is in the transitional Reynolds number range at approximately 1700. Their report NPS-59PC7081A, Heat Transfer and Flow Friction Characteristics of Several Plate-Fin Type Compact Heat Exchanger Surfaces, has one slotted perforated plate-fin surface of 0.0047 inch thick material. However, the slots are only 0.0023 inches wide and are spaced 0.0125 inches between centers in the air flow direction. These perforations are considered too small, and therefore subject to fouling, to be used in the compact condenser.

Twenty-five different matrices are covered in the Air Preheater Company report, Advanced Heat Exchanger Designs of Compact Heat Exchangers When Operating in a Marine Environment (Reference 1), which studied the heat transfer and flow friction characteristics of round hole and slotted hole perforated plate matrices. The tests were for heat transfer factor (j), friction factor (f) and/or noise data. Eight different round hole geometries and three different slotted hole geometries were tested. However, there were so many variables in the study that the effect of any one variable could not be definitely defined. The variables included four plate thicknesses (minimum of 0.015 inch), two different types of plates, three round hole sizes, two slot sizes, and various spacings. As a result, the only comparisons that could be made by the report to show the effect of one variable were in slot width, burrs, plate spacing and passage aspect ratio. It can be seen that only one of the direct comparisons involved the perforation geometry. The conclusions of The Air Preheater report were that more data was needed to properly define the effect of hole or slot size, open area, plate spacing and other parameters. They also recommended that plate-fin cores be tested to correlate the performance of perforated plates and perforated plate-fin surfaces. They concluded that round holes and slotted perforations had equal potential in heat exchanger design. It was also concluded that round hole perforations should not have an open area greater than 30 percent and that the size of the round holes was of minor importance.

The perforated plate-fin surface data reported by Kays (Reference 2) and summarized by Kays and London (Reference 3), was therefore the best available data on perforated surfaces that could be used in the design of the compact plate-fin condenser. The AiResearch perforated fin derived from the Kays and London data did not have the predicted heat transfer performance. The hole size and hole pattern were not factors because both surfaces had the same hole size and hole pattern. Additional Stanford data was furnished to AiResearch by Professor London of a test on a perforated plate in which the holes were made progressively larger with no change in the spacing. Comparison of this data with the AiResearch-Stanford test data comparison indicated that one common factor was that the heat transfer factor in both comparisons increased as the ratio of plate land-to-thickness decreased, where land is the distance between perforations in the flow direction.

PERFORATION GEOMETRY SELECTION

In the selection of the perforated patterns for the test cores, it was decided to start with a minimum slot width of 0.015 in. and a minimum land between slots in adjacent rows equal to the slot width. These criteria resulted in the spacing of 0.060 in. for the 0.015 in. wide slot. The maximum open area tested was 25 percent, which is less than the 30 percent limit for round perforations as suggested by the Air Preheater Company (Reference 1). By omitting alternate punches, the same perforation tool can be used to produce a pattern with the same size perforation but with twice the spacing for an open area of 12.5 percent. The slot width was then successively doubled and the same procedure followed to obtain widths of 0.015, 0.030, and 0.060 in. with two different spacing for each slot width. The slot widths therefore cover a four-fold range and the spacings cover an eight-fold range.

In the case of the round hole patterns, a staggered arrangement was selected for all configurations, based on the Air Preheater results. The hole diameters cover a two-fold range. (In the Air Preheater Company report where the hole diameters ranged from 0.020 in. to 0.125 in., they concluded that the hole diameter was of minor importance.) The starting geometry open area of the hole configuration equals the starting geometry open area in the slot configuration.

Ten perforated matrices were thus selected. The perforations were as follows:

Core	Perforation Type	Size of Perforations, in.	Spacing of Perforations, in.	Theoretical Percent Open Area	Actual Percent Open Area
1	Round	0.030 dia	0.057	25.0	23.3
3	Round	0.030 dia	0.114	6.3	5.93
5	Round	0.060 dia	0.114	25.0	24.6
7	Round	0.060 dia	0.228	6.3	6.36
9	Slotted	0.015 x 0.250	0.060	25.0	24.4
11	Slotted	0.015 x 0.250	0.120	12.5	12.4
13	Slotted	0.030 x 0.250	0.120	25.0	22.2
15	Slotted	0.030 x 0.250	0.240	12.5	11.5
17	Slotted	0.060 x 0.250	0.240	25.0	23.1
19	Slotted	0.060 x 0.250	0.480	12.5	12.4

The theoretical percent open area values are for the perforations in an infinite heat exchanger where edge effects are negligible. The actual percent open area values are for the perforations in the test cores where the perforations had to be in an air flow length of 3.38 in. A further limitation was that the air fin in the ten test cores was made in two pieces in the air flow dimension so that the air flow length of each piece was 1.69 in.

FABRICATION

Perforated Fin Material

The ten perforated fin patterns were fabricated from one master die with ten sets of interchangeable punch configurations. By adding (or removing) every other lance in a set, a different perforated configuration was fabricated. The dimensions of the perforated materials are presented in Figures 5-1 through 5-5.

The ten perforated fin configurations were formed into fins with a stack height of 0.326 in., and a spacing of 22 fins per inch. The resulting fins and samples of the perforated materials are shown in Figures 5-6 through 5-10.

Test Core Fabrication

The ten test cores were identical to the parametric study test core shown in Figure 4-1. Each core is constructed from (1) ten air side sandwiches using the selected 22-fins-per-inch perforated rectangular fin surface, (2) eleven water side sandwiches using a 20-fins-per-inch offset rectangular fin surface, (3) tube plates, (4) U-channels, and (5) rectangular header bars. The flat

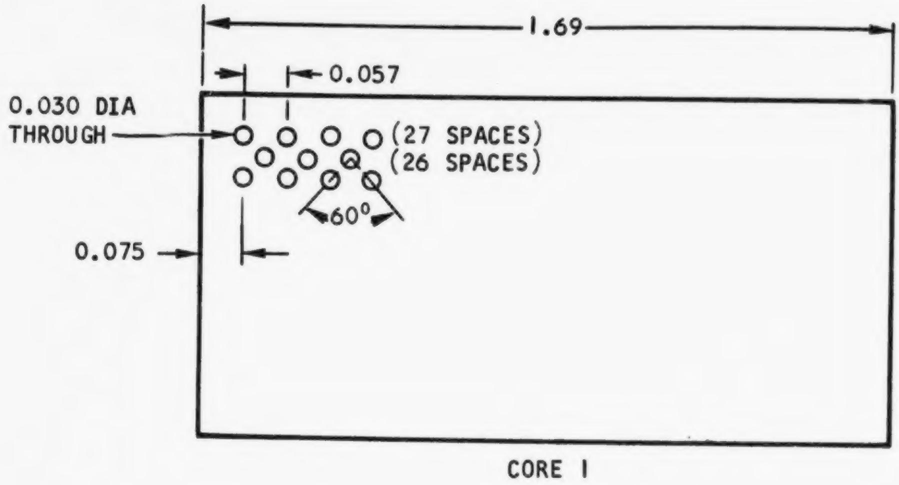
1.69
0.057
0.030 DIA
THROUGH
(27 SPACES)
(26 SPACES)
60°
0.075
CORE 1

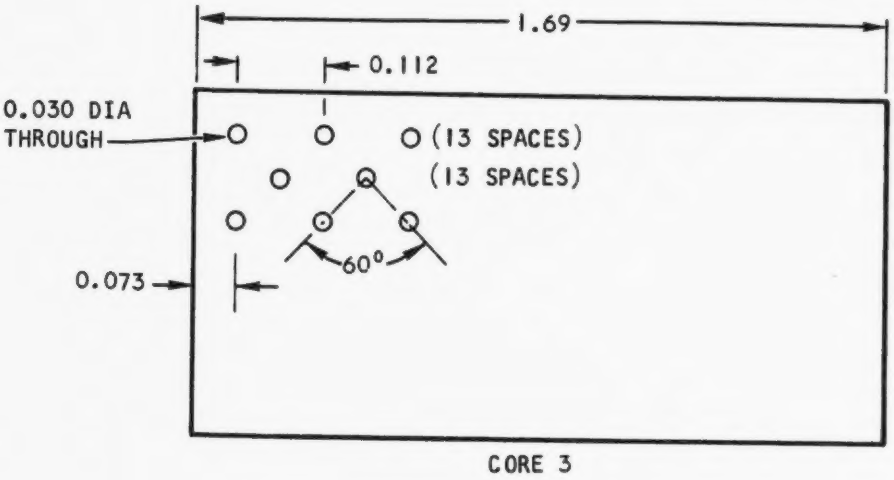
1.69
0.112
0.030 DIA
THROUGH
(13 SPACES)
(13 SPACES)
60°
0.073
CORE 3

NOTE: ALL DIMENSIONS ARE
IN INCHES

S-64795

Figure 5-1. Perforated Fin Materials for Cores 1 and 3

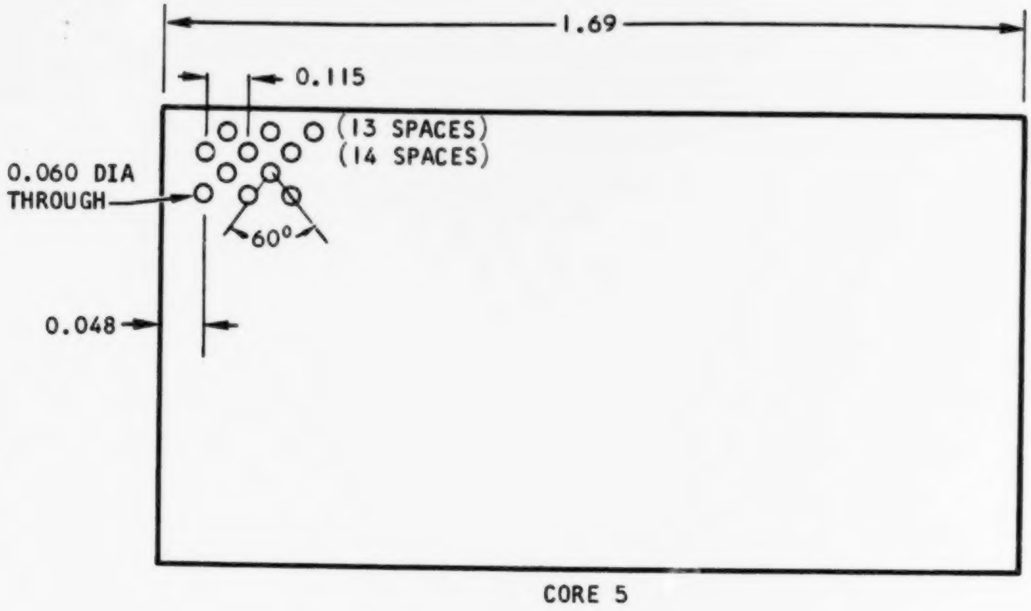
1.69
0.115
(13 SPACES)
(14 SPACES)
0.060 DIA THROUGH
60°
0.048
CORE 5

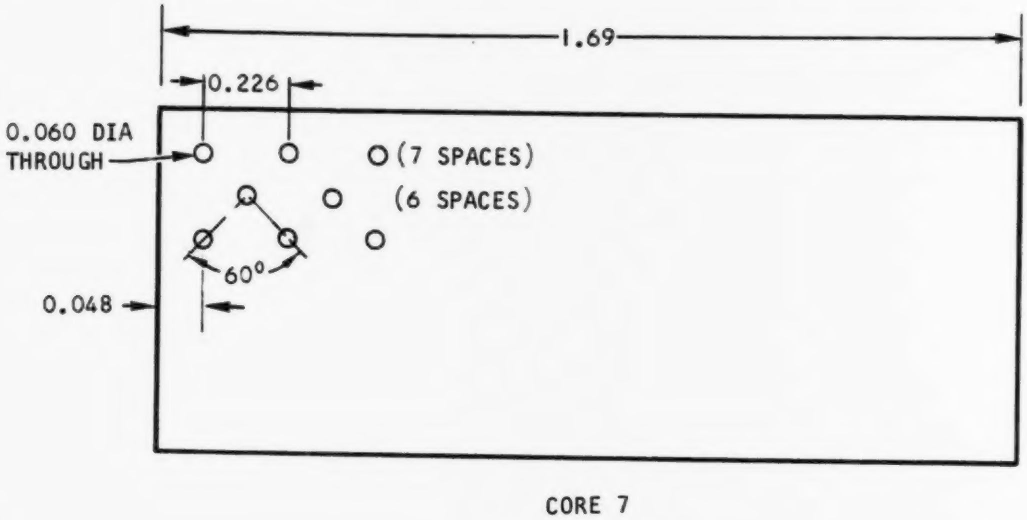
1.69
0.226
0.060 DIA THROUGH
(7 SPACES)
(6 SPACES)
60°
0.048
CORE 7

NOTE: ALL DIMENSIONS ARE IN INCHES

S-64796

Figure 5-2. Perforated Fin Materials for Cores 5 and 7

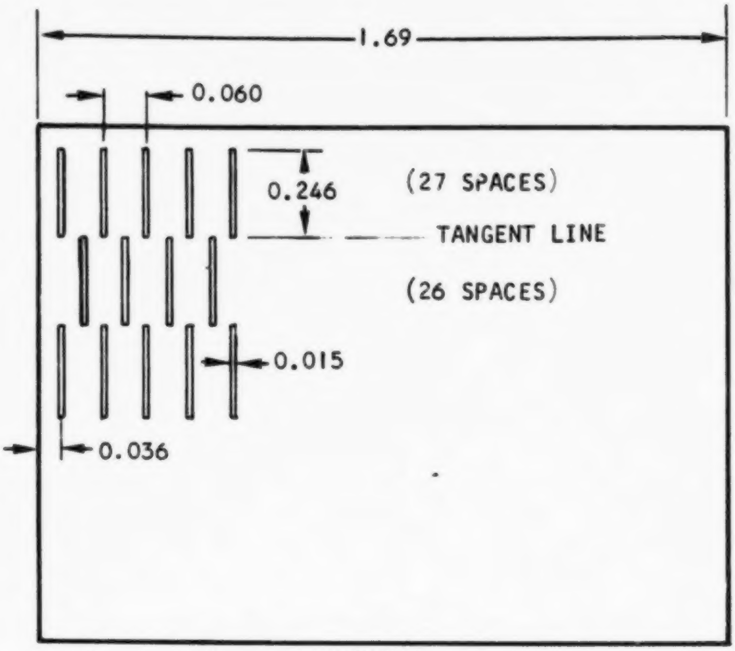
1.69
0.060
0.246
(27 SPACES)
TANGENT LINE
(26 SPACES)
0.015
0.036

CORE 9

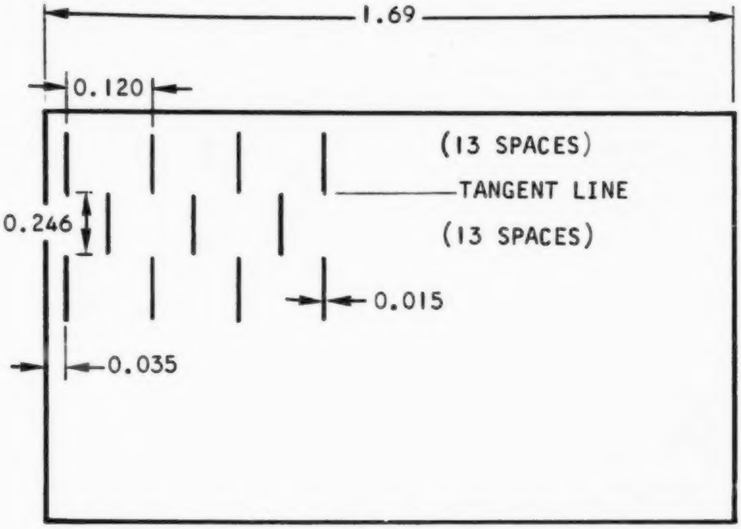
1.69
0.120
(13 SPACES)
TANGENT LINE
0.246
(13 SPACES)
0.015
0.035

CORE 11

NOTE: ALL DIMENSIONS ARE
IN INCHES

S-64793

Figure 5-3. Perforated Fin Materials for Cores 9 and 11

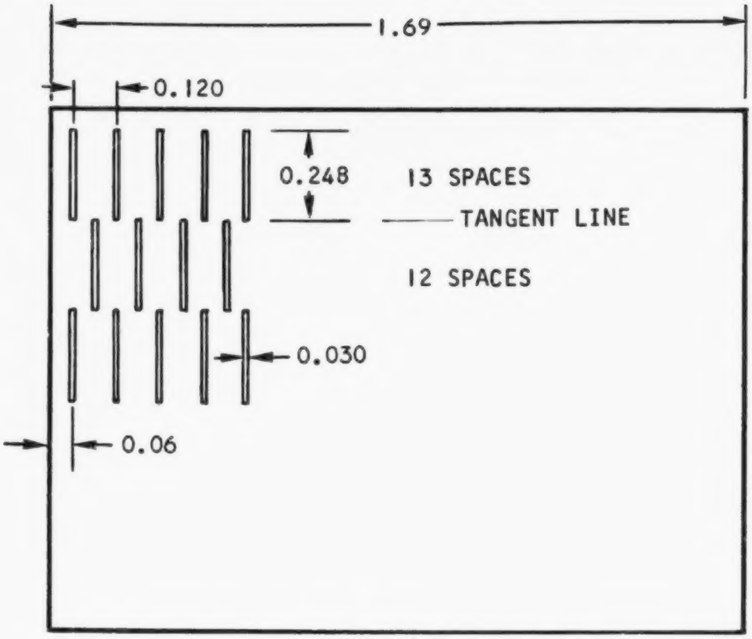
1.69
0.120
0.248
13 SPACES
TANGENT LINE
12 SPACES
0.030
0.06

CORE 13

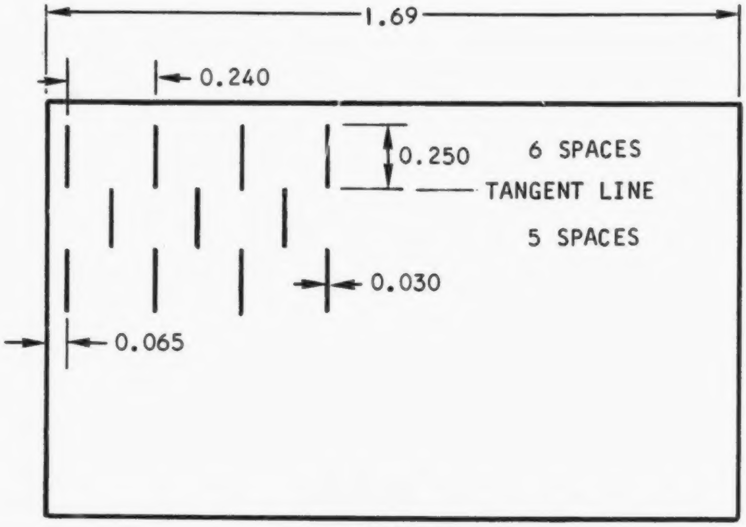
1.69
0.240
0.250
6 SPACES
TANGENT LINE
5 SPACES
0.030
0.065

CORE 15

NOTE: ALL DIMENSIONS ARE
IN INCHES

S-64794

Figure 5-4. Perforated Fin Materials for Cores 13 and 15

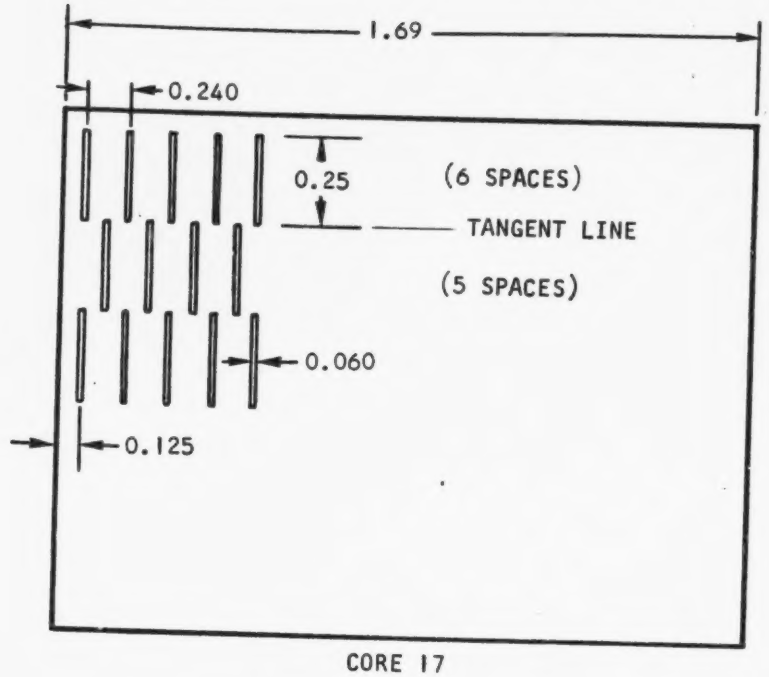
1.69
0.240
0.25
(6 SPACES)
TANGENT LINE
(5 SPACES)
0.060
0.125
CORE 17

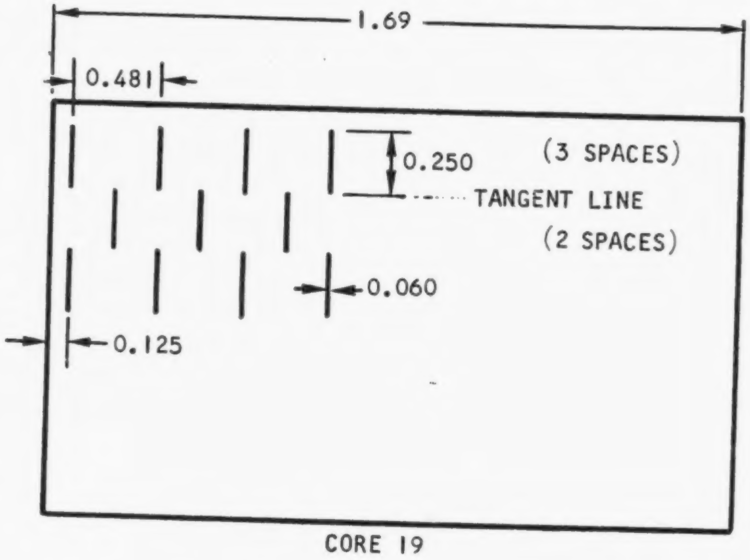
1.69
0.481
0.250
(3 SPACES)
TANGENT LINE
(2 SPACES)
0.060
0.125
CORE 19

NOTE: ALL DIMENSIONS ARE IN INCHES

S-64792

Figure 5-5. Perforated Fin Materials for Cores 17 and 19

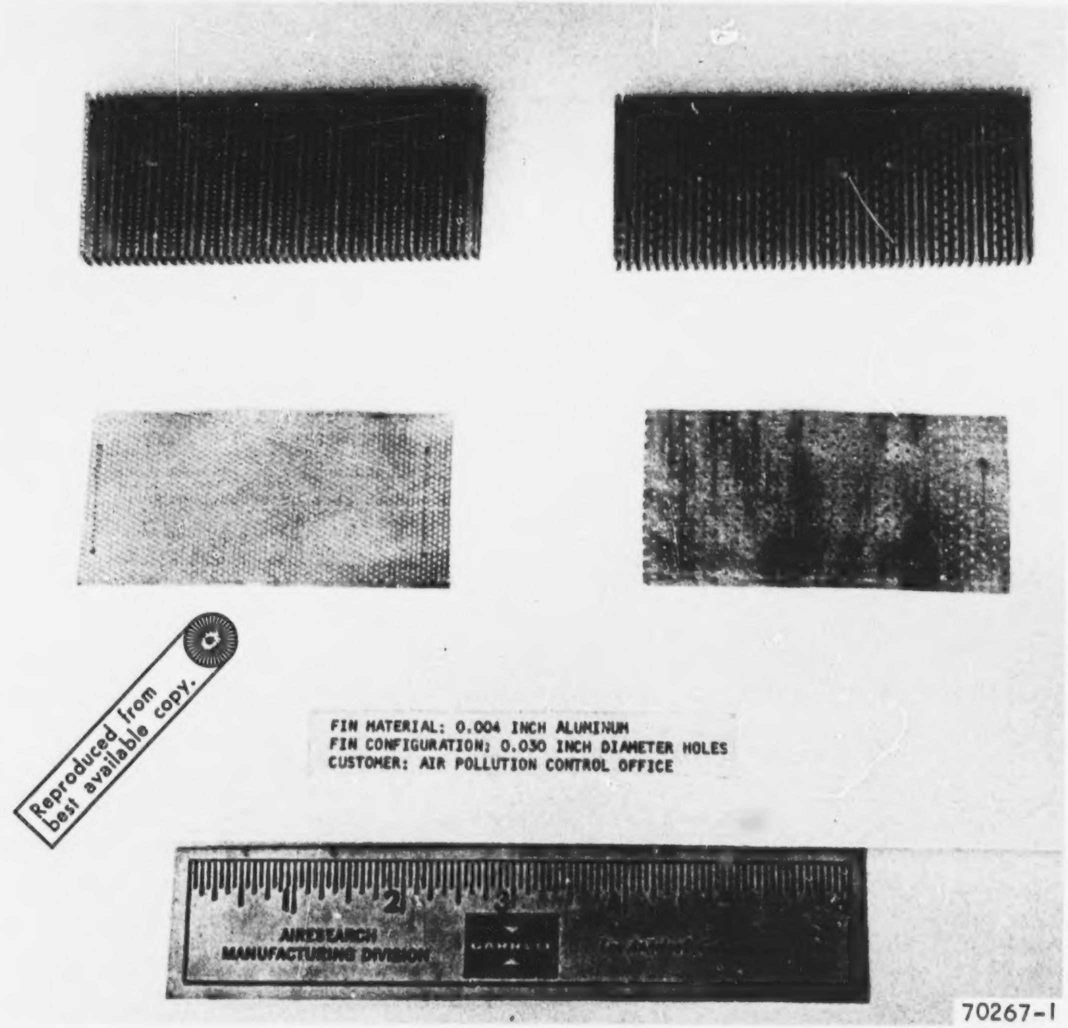
FIN MATERIAL: 0.004 INCH ALUMINUM
FIN CONFIGURATION: 0.030 INCH DIAMETER HOLES
CUSTOMER: AIR POLLUTION CONTROL OFFICE
AIRESEARCH
MANUFACTURING DIVISION
70267-1

Reproduced from best available copy.

Figure 5-6. Perforated Fins and Materials (0.030-in. Diameter Holes for Cores 1 and 3)

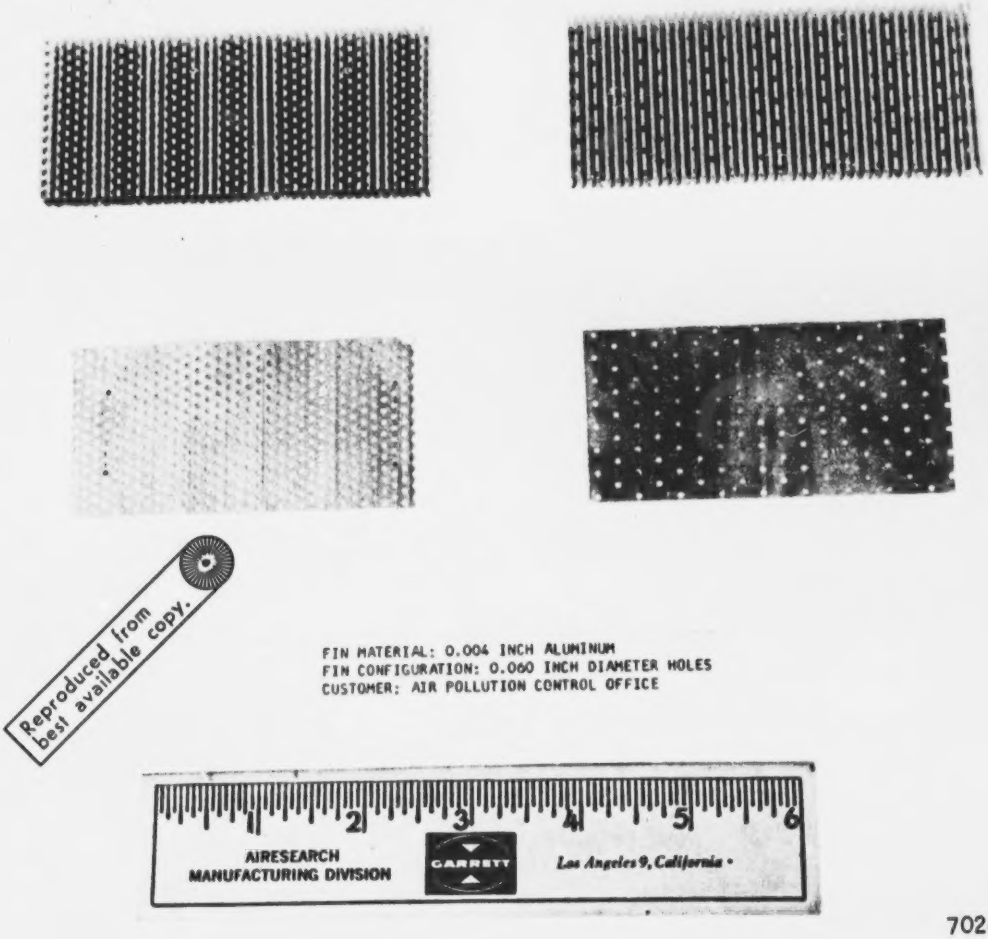
FIN MATERIAL: 0.004 INCH ALUMINUM
FIN CONFIGURATION: 0.060 INCH DIAMETER HOLES
CUSTOMER: AIR POLLUTION CONTROL OFFICE
1
2
3
4
5
6
AIRESEARCH
MANUFACTURING DIVISION
GARRETT
Los Angeles 9, California

Reproduced from
best available copy.

70267-6

Figure 5-7. Perforated Fins and Materials (0.060-in. Diameter Holes for Cores 5 and 7)

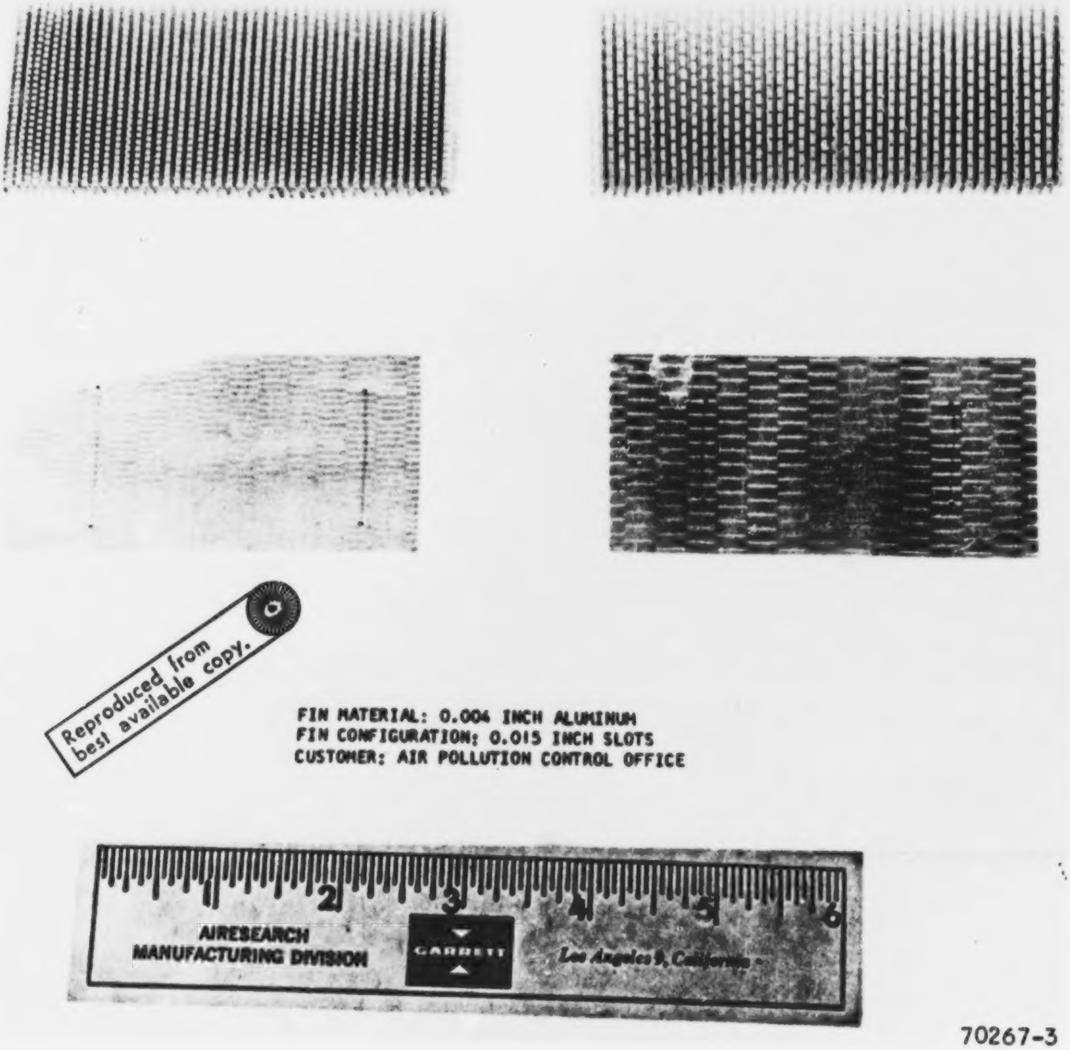
FIN MATERIAL: 0.004 INCH ALUMINUM
FIN CONFIGURATION: 0.015 INCH SLOTS
CUSTOMER: AIR POLLUTION CONTROL OFFICE
1
2
3
4
5
6
AIRESEARCH
MANUFACTURING DIVISION
GARRETT
Los Angeles 9, California

Reproduced from best available copy.

70267-3

Figure 5-8. Perforated Fins and Materials (0.015-in. Slots for Cores 9 and 11)

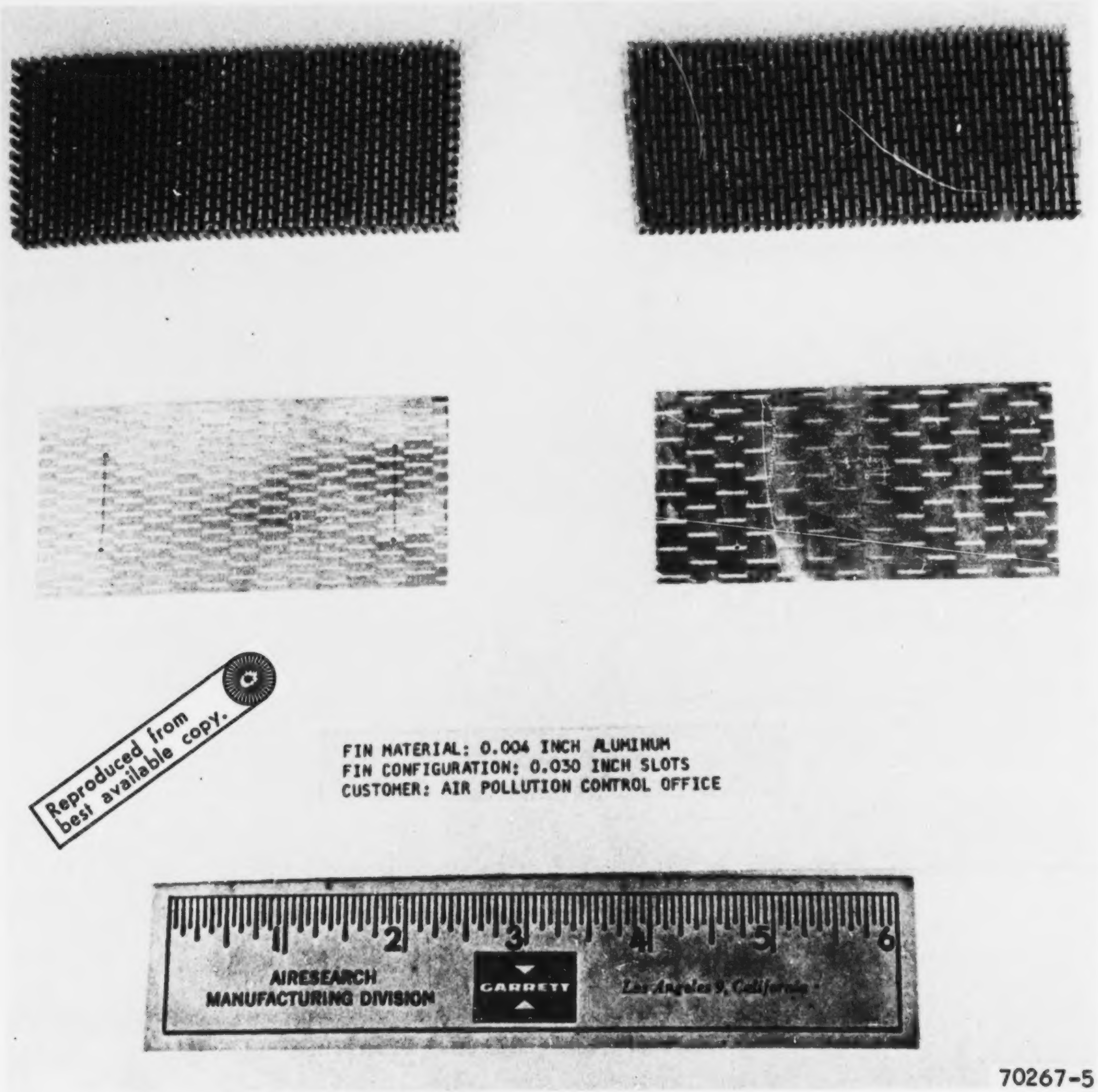
FIN MATERIAL: 0.004 INCH ALUMINUM
FIN CONFIGURATION: 0.030 INCH SLOTS
CUSTOMER: AIR POLLUTION CONTROL OFFICE
1
2
3
4
5
6
AIRESEARCH
MANUFACTURING DIVISION
GARRETT
Los Angeles 9, California
70267-5

Reproduced from best available copy.

Figure 5-9. Perforated Fins and Materials (0.030-in. Slots for Cores 13 and 15)

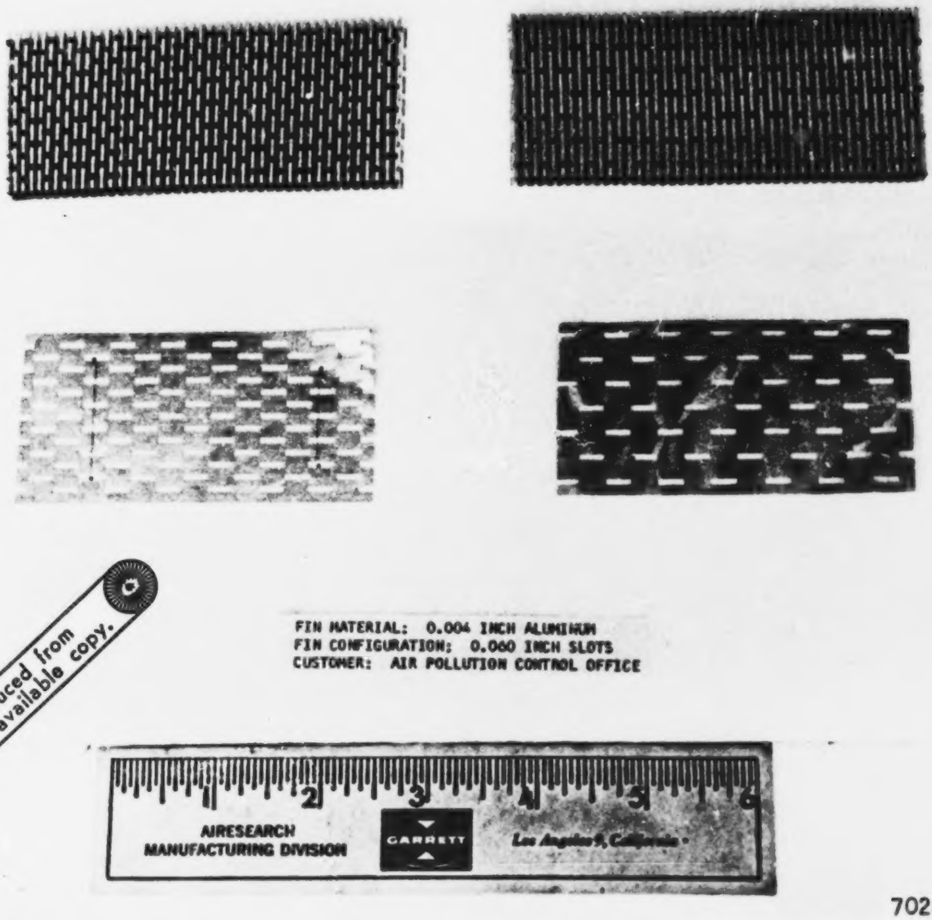
FIN MATERIAL: 0.004 INCH ALUMINUM
FIN CONFIGURATION: 0.060 INCH SLOTS
CUSTOMER: AIR POLLUTION CONTROL OFFICE
1
2
3
4
5
6
AIRESEARCH
MANUFACTURING DIVISION
GARRETT
Los Angeles 9, California

Reproduced from
best available copy.

70267-4

Figure 5-10. Perforated Fins and Materials (0.060-in. Slots for Cores 17 and 19

bottoms of the "U"-channels formed the sides of the air passages, and the rectangular bars formed the sides of the water passages.

The test cores were stacked and fluxless brazed in an argon retort without any difficulties. Views of the core in the brazing fixture during the stacking operations are presented in Figures 5-11 and 5-12. The core, assembled and instrumented with thermocouples installed for brazing, is shown in Figure 5-13. After brazing, picture-frame flanges were welded to the air faces of the core, and pans and ducts were welded to the water faces. A subsequent pressure test verified the integrity of the assembly.

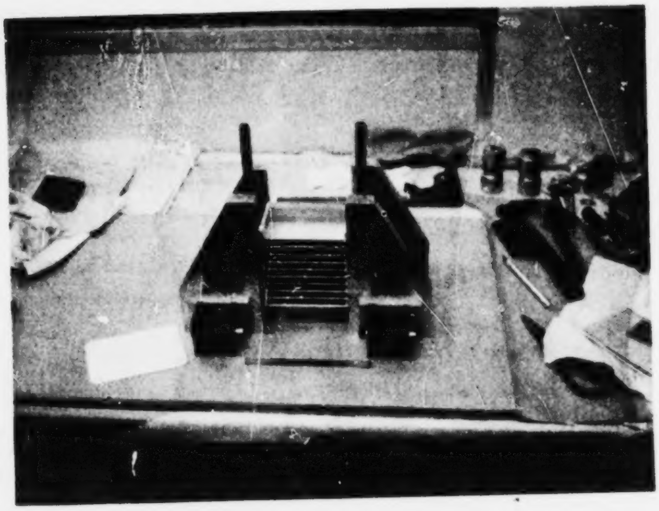

Figure 5-11. Overall View of Core During Stacking

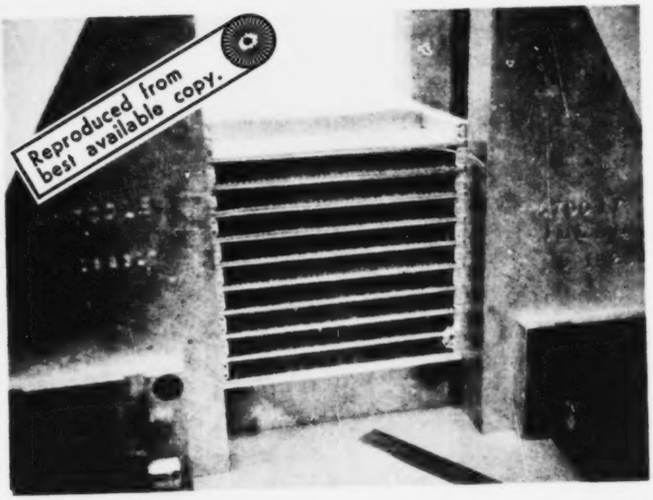
Reproduced from best available copy.

F-13581

Figure 5-12. Close-up View of Core During Stacking

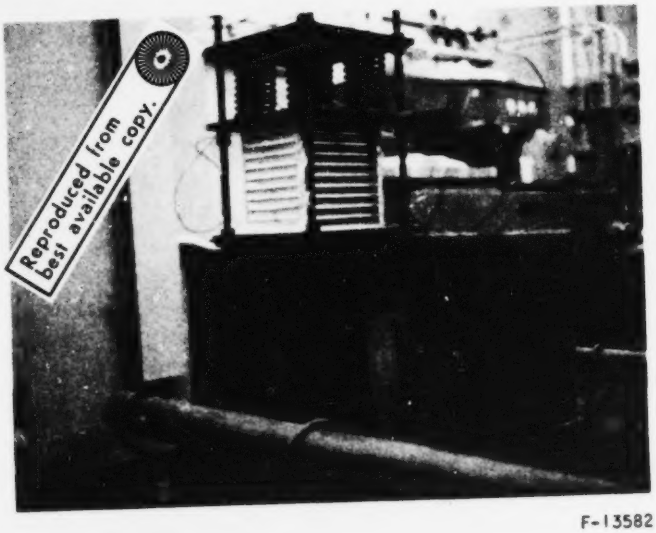
Reproduced from best available copy.

F-13582

Figure 5-13. Core in Brazing Fixture, Ready for Placement in Argon Retort

TESTING

The ten perforated fin test cores were performance tested in an air-water test setup similar to that shown in Figure 4-2. Photographs of the test setup are presented in Figures 5-14 and 5-15. The test setup was changed to incorporate traversing pressure probes upstream of the air inlet face of the core to measure the approaching air stream velocity. A thermocouple grid was installed downstream of the core to measure the temperature gradient of the air leaving the core.

In selected tests to determine the affect of turbulence, turbulator rods were installed upstream of the test section to determine the effect of turbulence on fin performance. Three 1/2-in.-diameter rods were placed 4 in. upstream of the face of the core as shown in Figure 5-16. The size and spacing of the turbulator rods was selected on the basis that the wakes of the air stream would be intersecting upstream of the test unit, resulting in a minimum variation in air velocity at the face of the core.

Temperature, pressure, and flowrates were determined in the same manner as for the parametric study test core as explained in Section 4. In measuring the water flow rate, the water collected was always 20 lb. Based on a solid fin hydraulic diameter, the Reynolds numbers of the eight air flows were approximately 840, 1250, 1600, 1950, 2400, 3000, 3750, and 4500.

TEST RESULTS

As was stated above, a traversing pressure probe was used to determine the velocity profile across the upstream duct during one of the runs. The probe was located 1.75 in. upstream of the core inlet face, and static and total pressures were measured at 16 locations on each traverse of the duct. The agreement between the average static pressure measured with the traversing probe and that measured at the duct wall taps was good; the maximum variation for all runs was 0.05 in. of water. Profiles were determined in five vertical planes and two horizontal planes as shown in Figure 5-17. Flat velocity distributions indicate uniform flow distribution which is essential when basic heat transfer and friction pressure drop data are being obtained. The measured velocity profiles are shown in Figure 5-18. The vertical scale is not an absolute velocity but rather an arbitrary scale of relative velocity which illustrates the velocity profiles. The profiles obtained were relatively uniform. The traverse at the far right side of the duct, run 105, indicates velocities approximately 10 to 15 percent lower than at the other locations and is therefore suspect. The two local velocities from the horizontal traverses which lie on the vertical plane of run 105 were higher than indicated in the 105 profile and indicate that the magnitude of run 105 is probably in error on the low side. The profiles obtained were thought to be uniform enough so that good data was obtained.

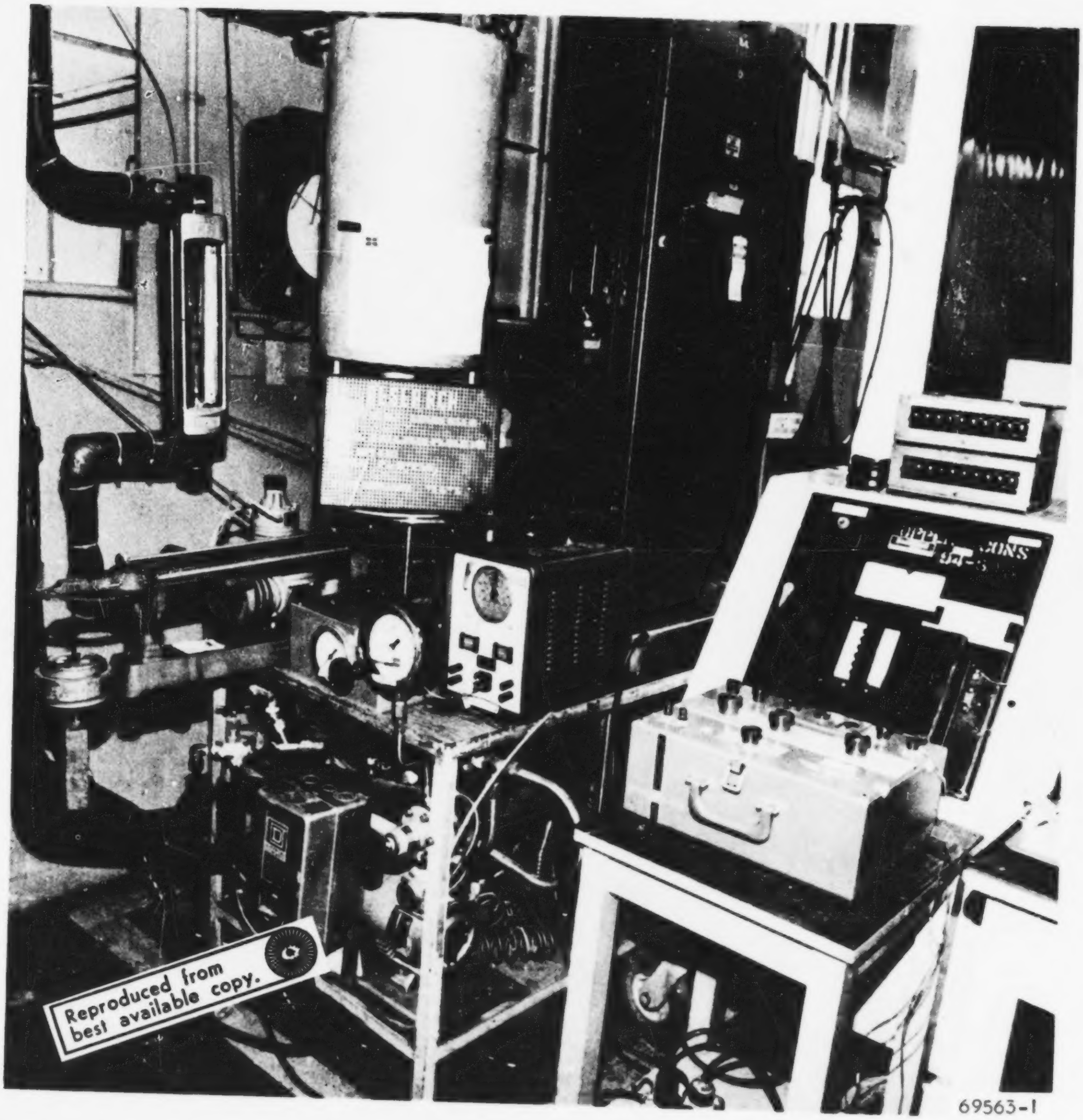

Reproduced from
best available copy.

69563-1

Figure 5-14. Test Setup Showing Water Flowrate Measuring System and Thermocouple Measuring Apparatus

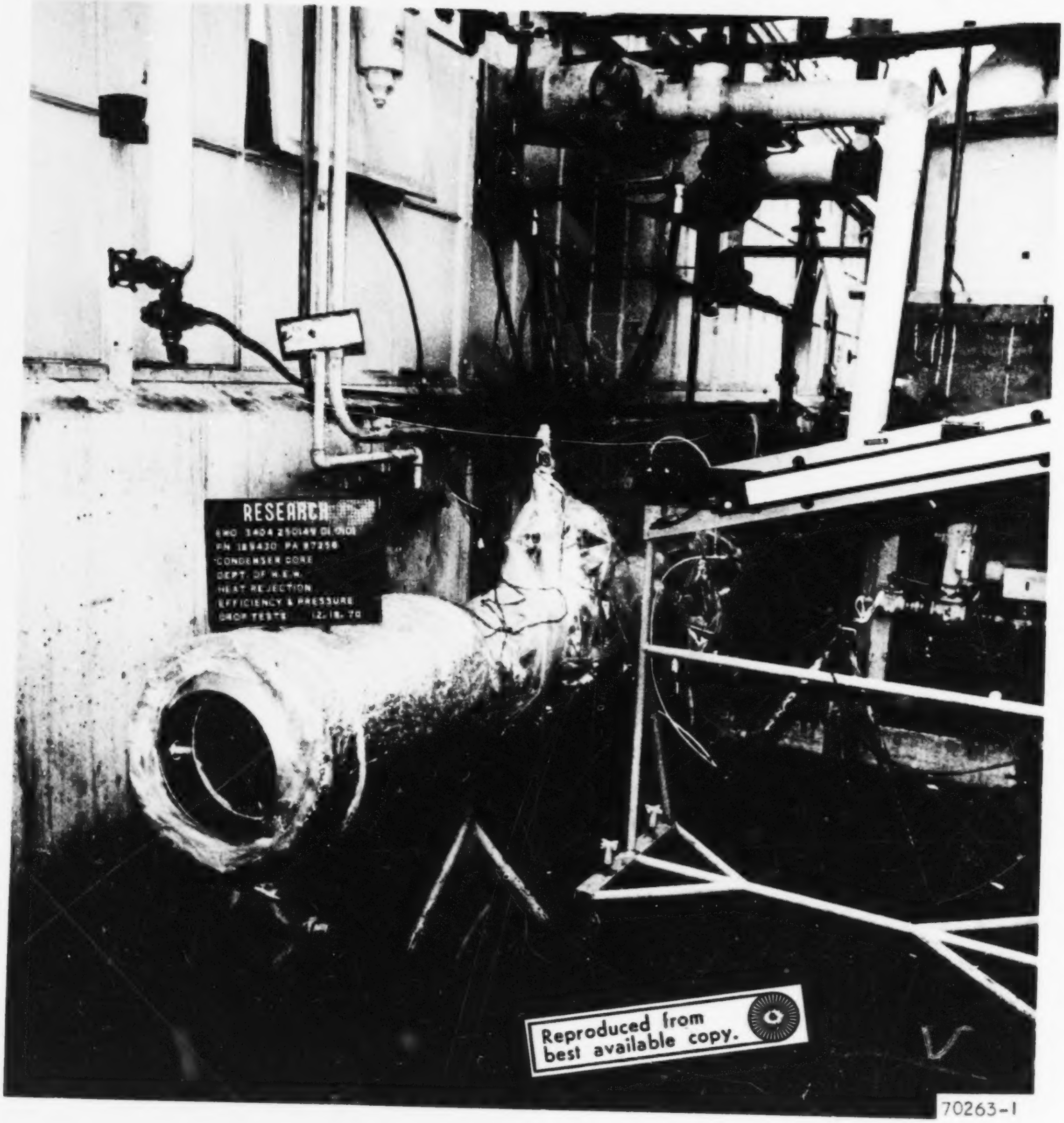
RESEARCH
EWO 3404 250149 01 0101
PN 185430 PA 87256
CONDENSER CORE
DEPT. OF H.E.W.
HEAT REJECTION
EFFICIENCY & PRESSURE
DROP TESTS 12.18.70

Reproduced from best available copy.

70263-1

Figure 5-15. Test Setup Showing Test Core Mounted in Ducting

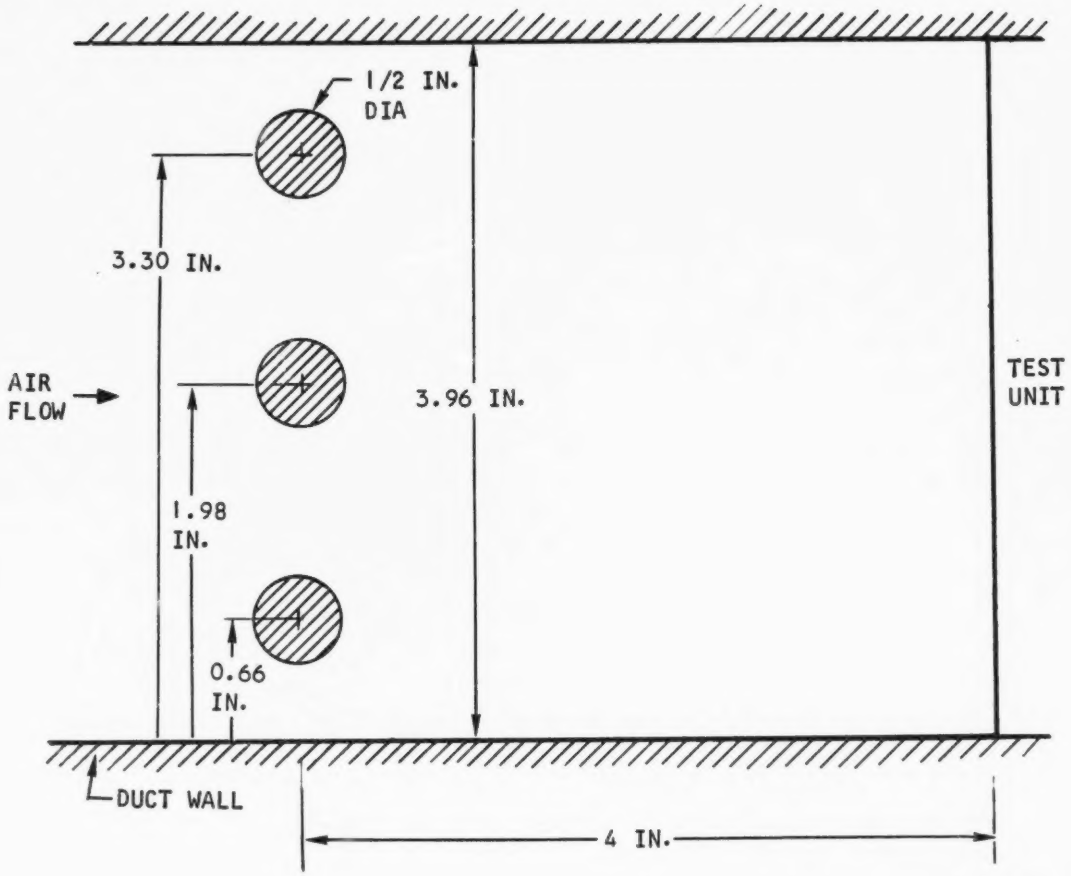
1/2 IN.
DIA
3.30 IN.
AIR
FLOW
3.96 IN.
TEST
UNIT
1.98
IN.
0.66
IN.
DUCT WALL
4 IN.
S-64774

Figure 5-16. Turbulator Design

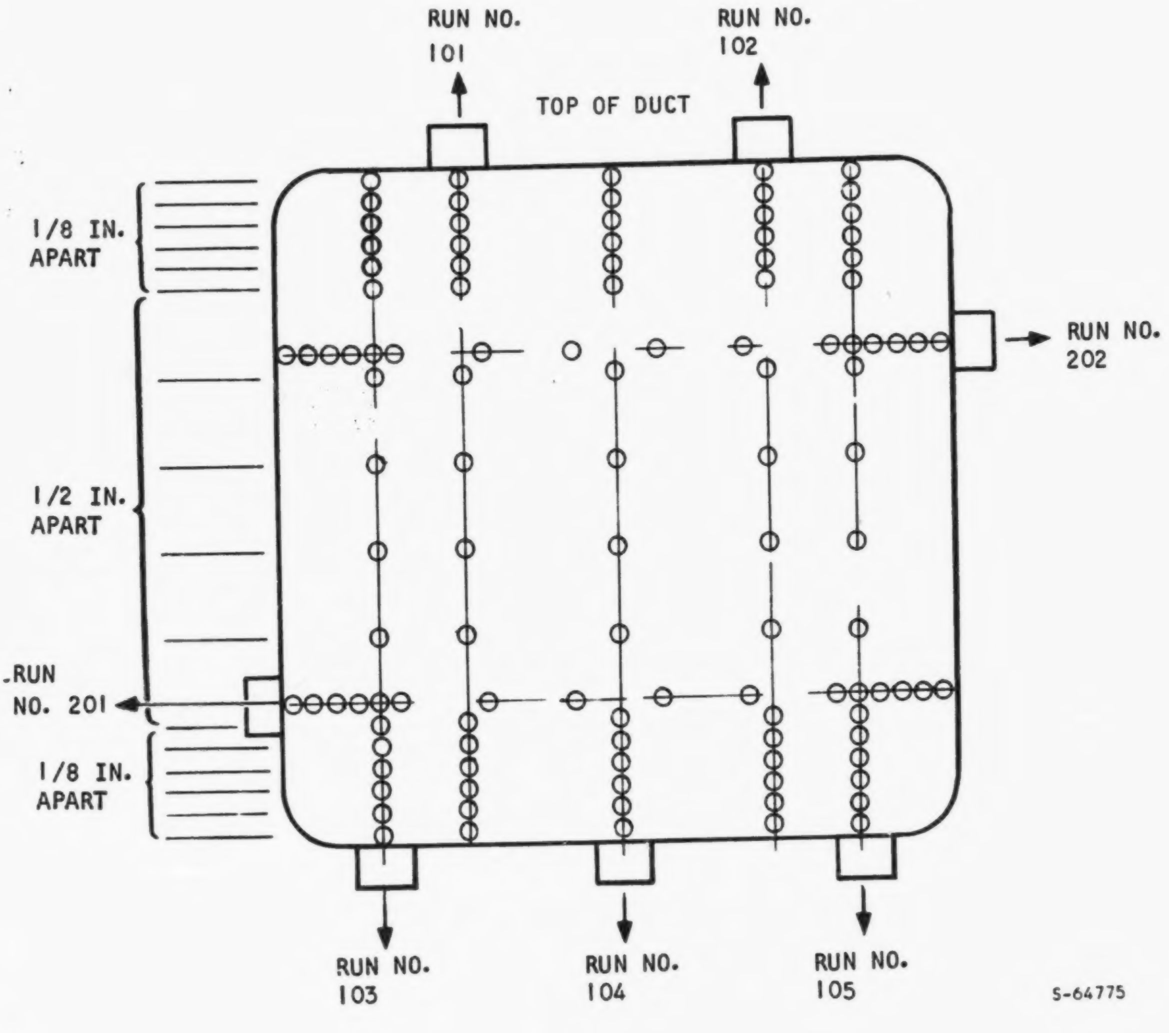
RUN NO. 101
RUN NO. 102
TOP OF DUCT
1/8 IN. APART
1/2 IN. APART
1/8 IN. APART
RUN NO. 202
RUN NO. 201
RUN NO. 103
RUN NO. 104
RUN NO. 105
S-64775

Figure 5-17. Pitot Tube Locations During Velocity Profile Traverse of Upstream Duct

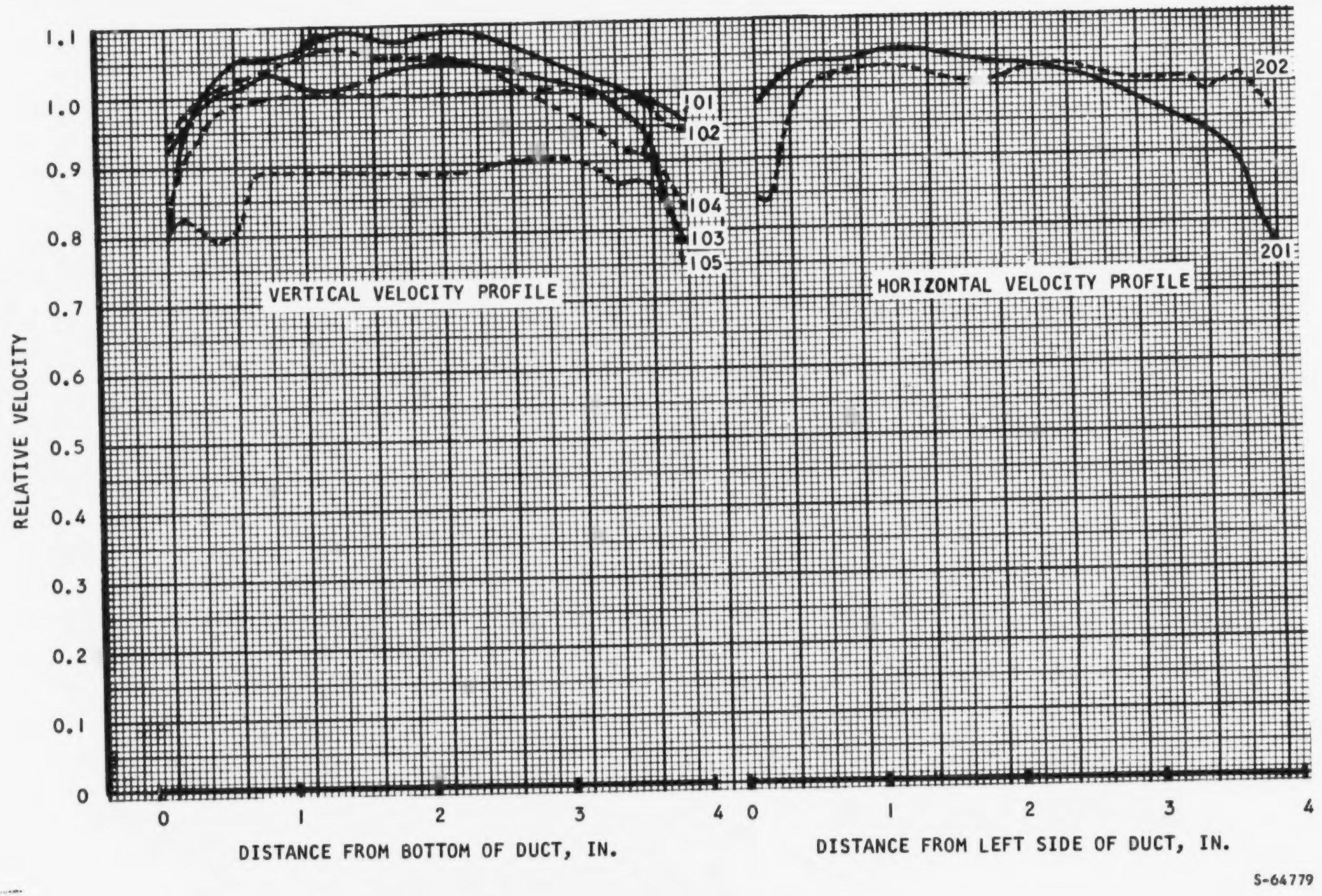

Figure 5-18. Upstream Duct Velocity Profiles

The test data for the ten cores were reduced on the basis of a solid fin-both in heat transfer area and in fin efficiency. In addition, the small variations between cores were neglected and the same dimensions were used for all the cores. The parametric study test core data was recalculated on the same basis. As a result, the curves can be compared directly. That is, at the same Reynolds number, the air flow in each core would be the same and the heat transfer and friction factors can be used to compare the heat transfer conductances and the pressure drops respectively. It would be impossible to make such direct comparisons if the effect of the perforations on the hydraulic diameter and the heat transfer area was included in the curves. Since the principal purpose of this study is to obtain the best air side surface, this procedure is acceptable.

Figures 5-19 through 5-29 present the heat transfer factors (j) and friction factors (f) for each of the eleven perforated surfaces. The surface identification, 22R-.326-PERF( )-.004(Al), is based on the AiResearch system for plate-fin surfaces where the 22 refers to the fins per inch, the R is for rectangular fin, the .326 is the plate spacing in inches, PERF refers to a perforated fin, .004 is the fin thickness, and Al is the fin material. In addition, for the purposes of this work, the perforated core identification is placed in the parentheses after PERF. Fluid properties including the density were evaluated at the bulk average temperature. The heat transfer area, hydraulic radius, and fin efficiency are based on those of a solid fin of the same geometry. The hydraulic diameter (D_h) is 0.07345 in., the area density (β) is 589 ft^2/ft^3 and the fin area-to-total area ratio (A_f/A_t) is 0.886.

Because of the low friction factor point in the core 13 data and the shape of some of the curves, it was decided to rerun some of the test cores. In addition, since the fan is presumed to be upstream of the core in the study, some of the test cores were retested with inlet turbulence. Note that even if the fan were downstream of the core, the air flow into the condenser would have turbulence from the automobile grill and from the lack of any straightening duct sections ahead of the condenser. The original test points are identified by circle symbols, rerun test points are shown by square symbols, and the test points with turbulence are represented by diamond symbols. The turbulence was created by a single row of circular rods upstream of the core.

The f and j data was used to size condensers at the parametric study design point heat rejection of 1.5×10^6 Btu/hr. The nondimensionalized core sizes are shown in Figure 5-30 for the data without upstream turbulence. The cores were nondimensionalized by dividing the air total frontal area and the air side volume by the area and volume design goals respectively. Also shown on the plot for comparison pruposes are the condenser sizes using the parametric study perforated fin (test core 0) and the best plain fin from the parametric study (19.86T). All points on Figure 5-30 except for the plain fin solution represent the minimum frontal area solutions. Lines of constant theoretical open area have been faired through the data for the slot perforations. Over the range of parameters applicable to this problem statement, the perforated fin performance was better at the higher percentage of open area. It is cautioned, however, that this trend cannot be extrapolated with confidence.

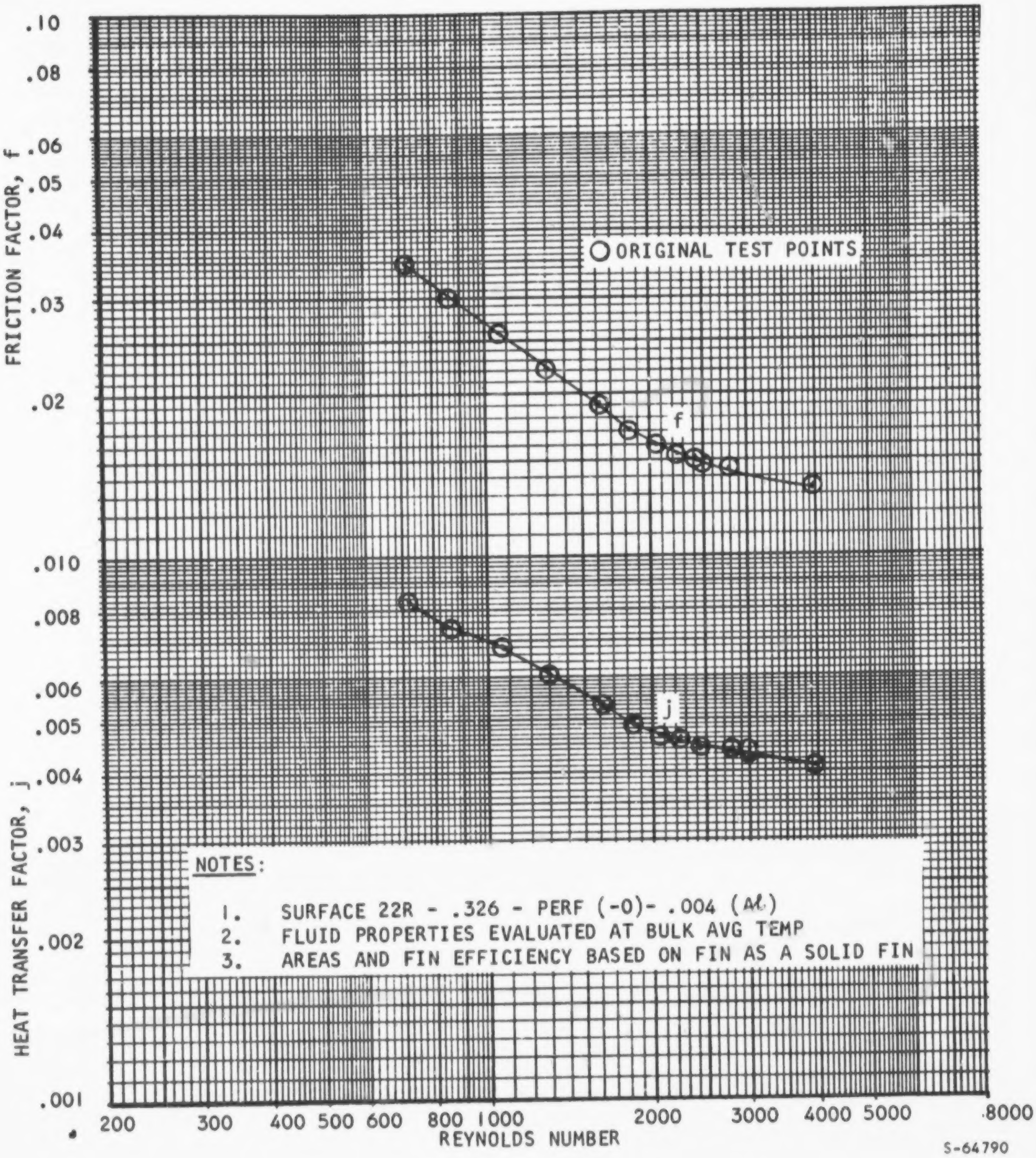

Figure 5-19. Performance Parameters for the -0 Perforated Fin

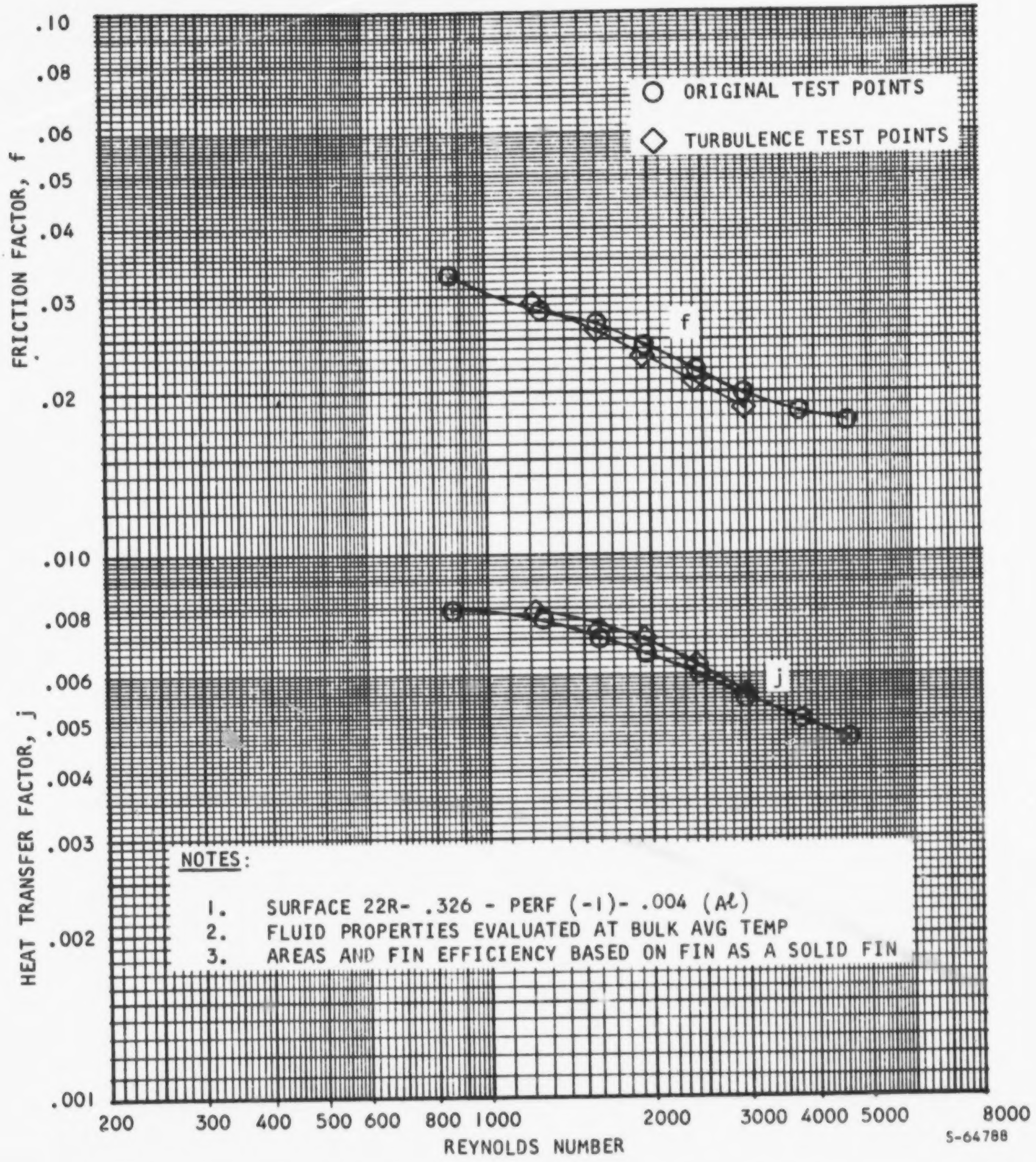

Figure 5-20. Performance Parameters for the -I Perforated Fin

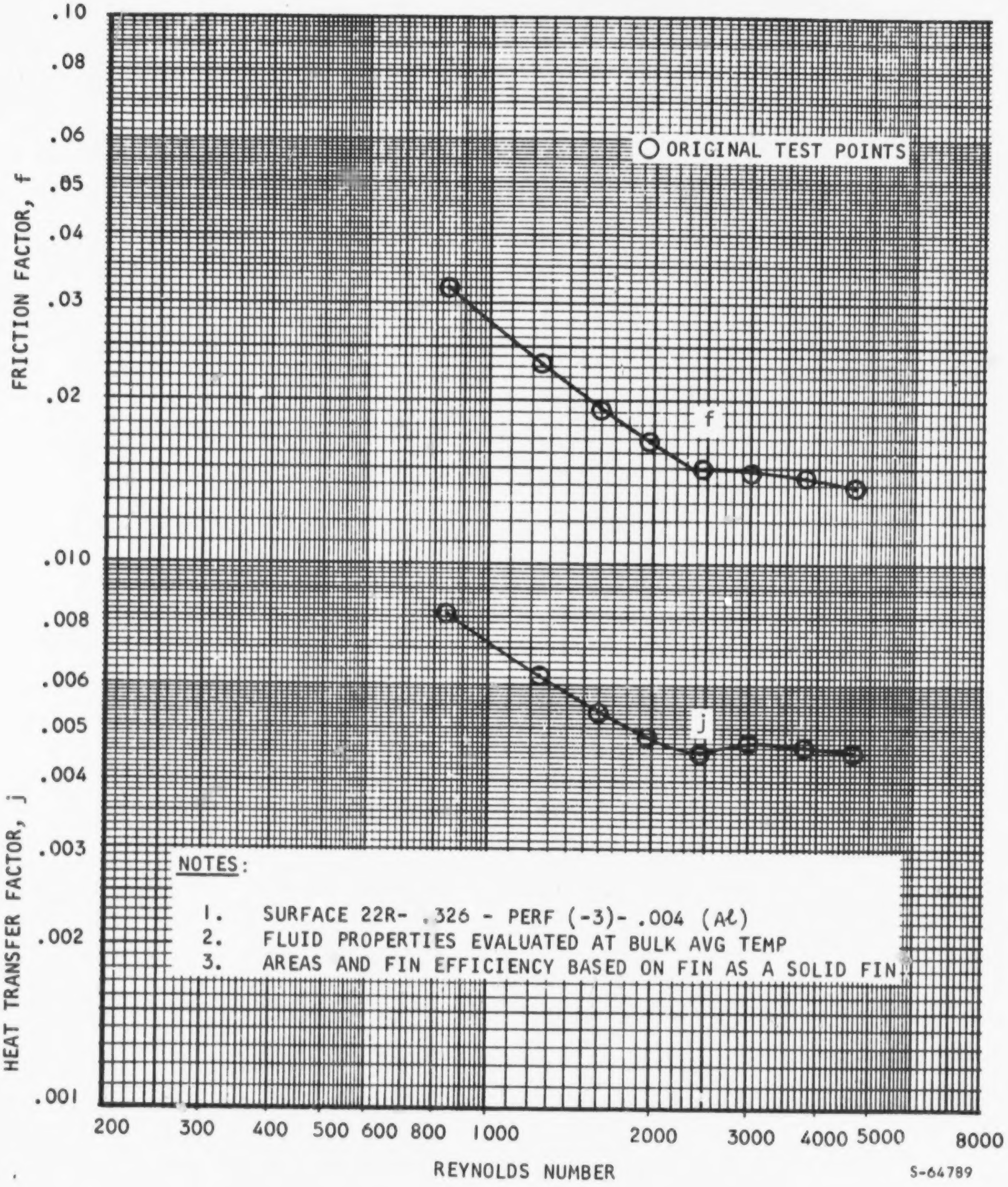

Figure 5-21. Performance Parameters for the -3 Perforated Fin

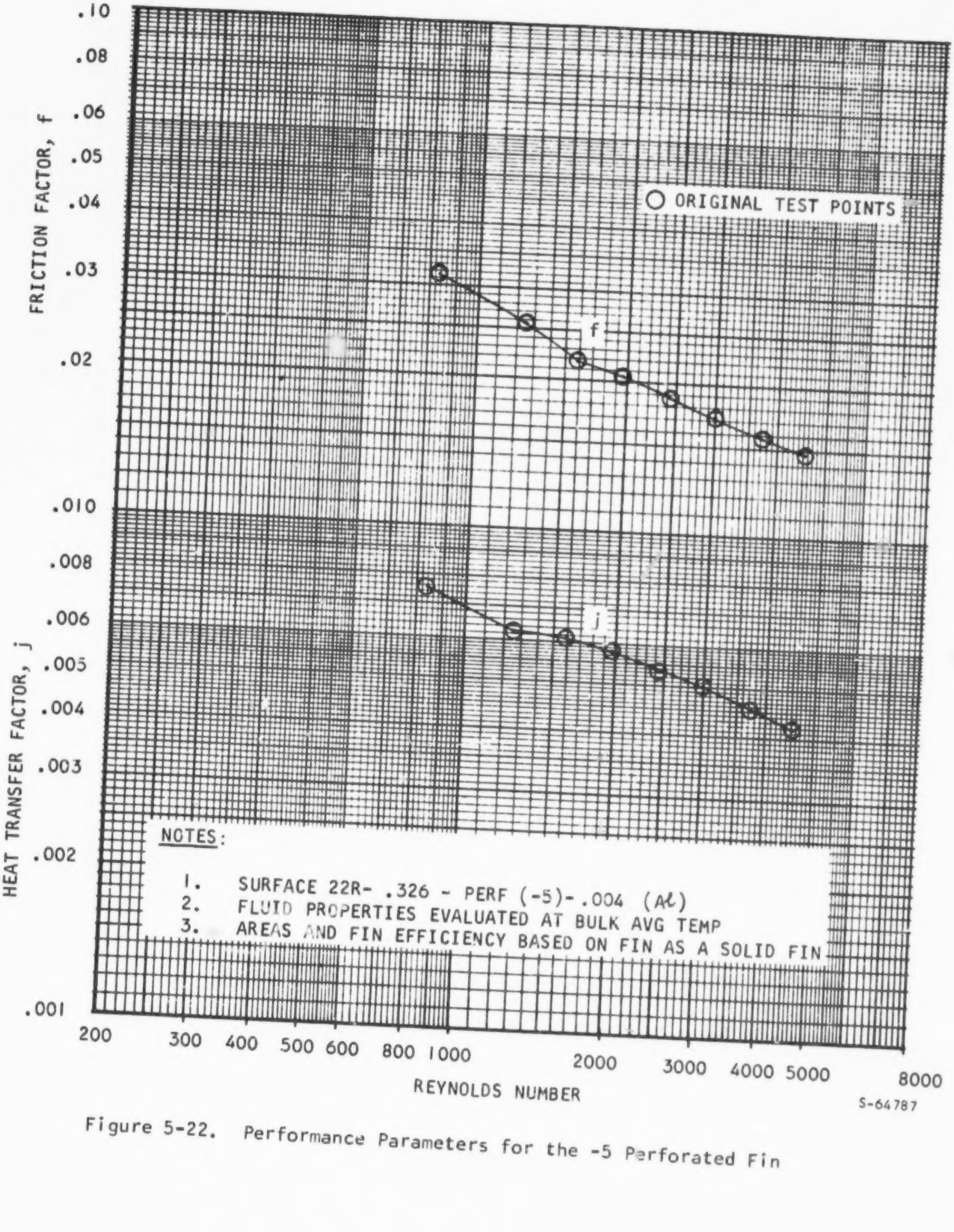

Figure 5-22. Performance Parameters for the -5 Perforated Fin

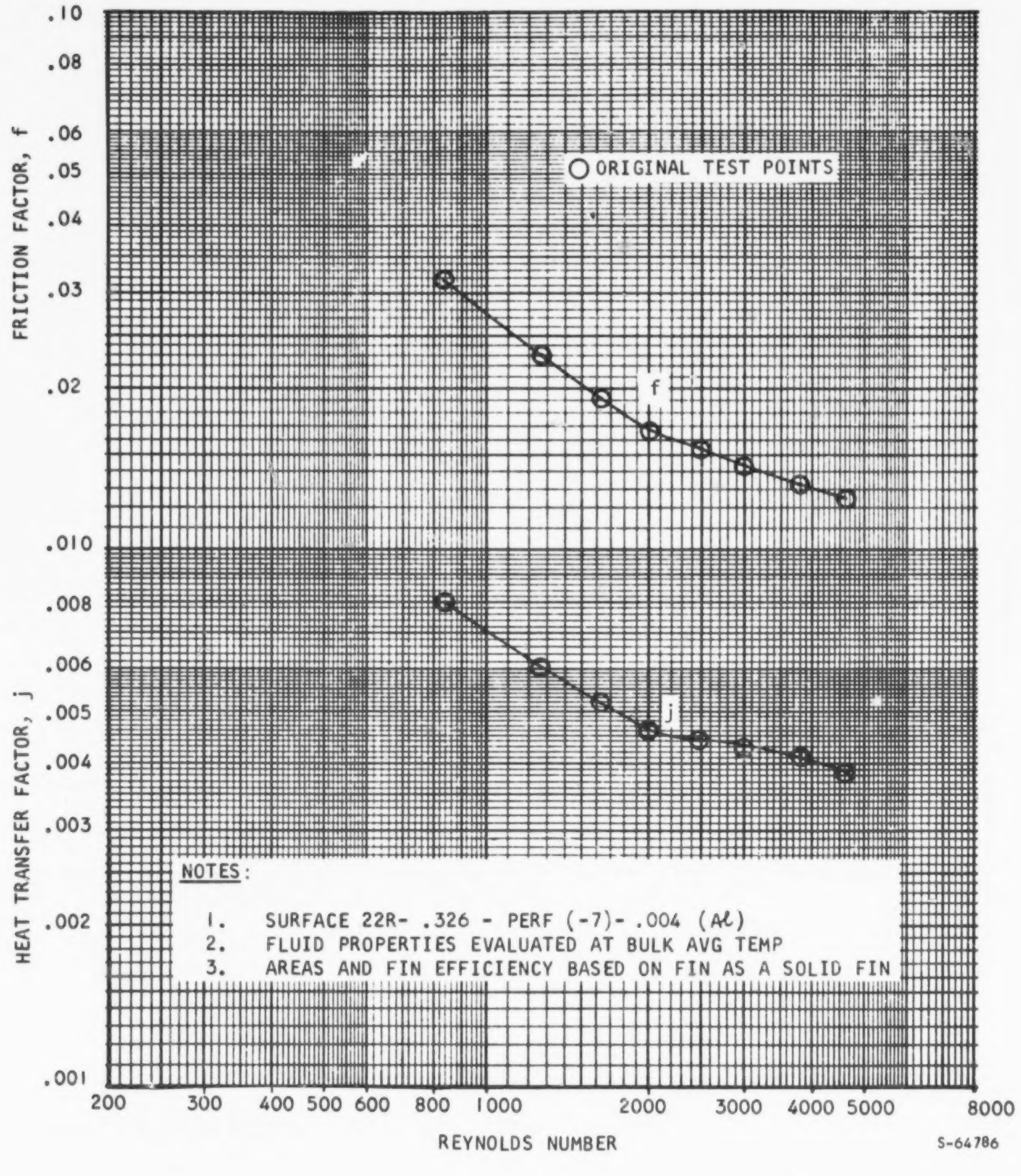

Figure 5-23. Performance Parameters for the -7 Perforated Fin

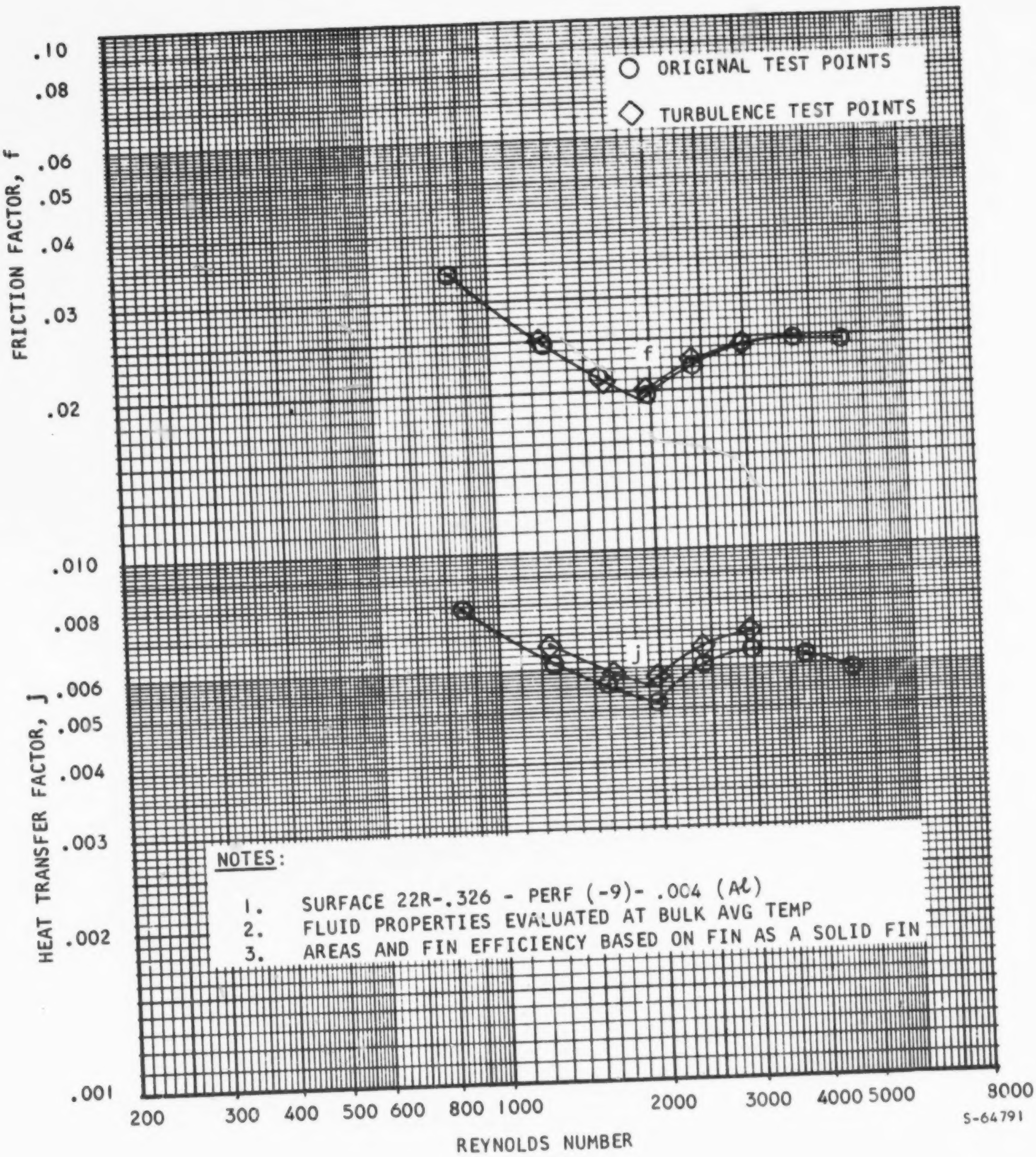

Figure 5-24. Performance Parameters for the -9 Perforated Fin

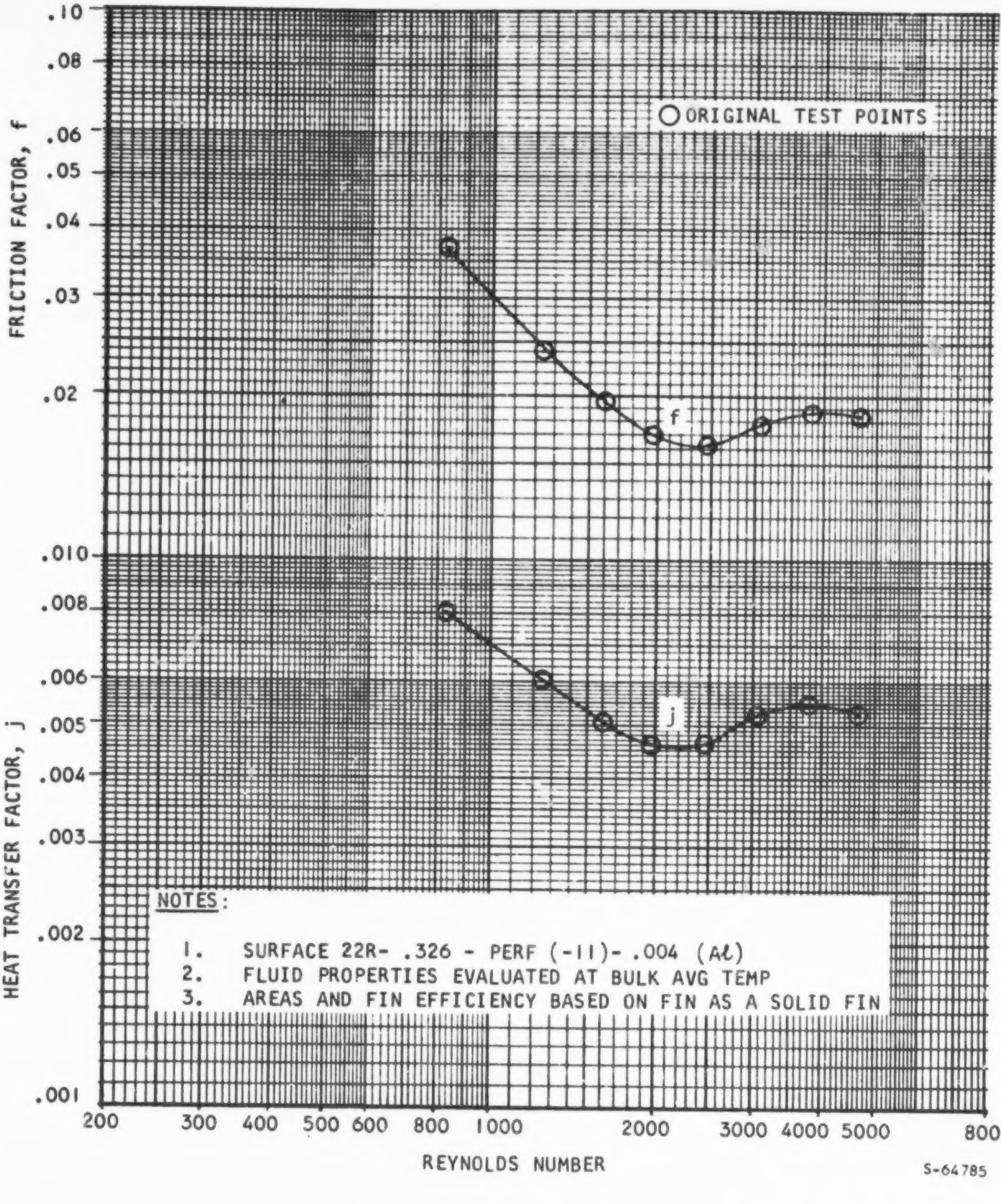

Figure 5-25. Performance Parameters for the -11 Perforated Fin

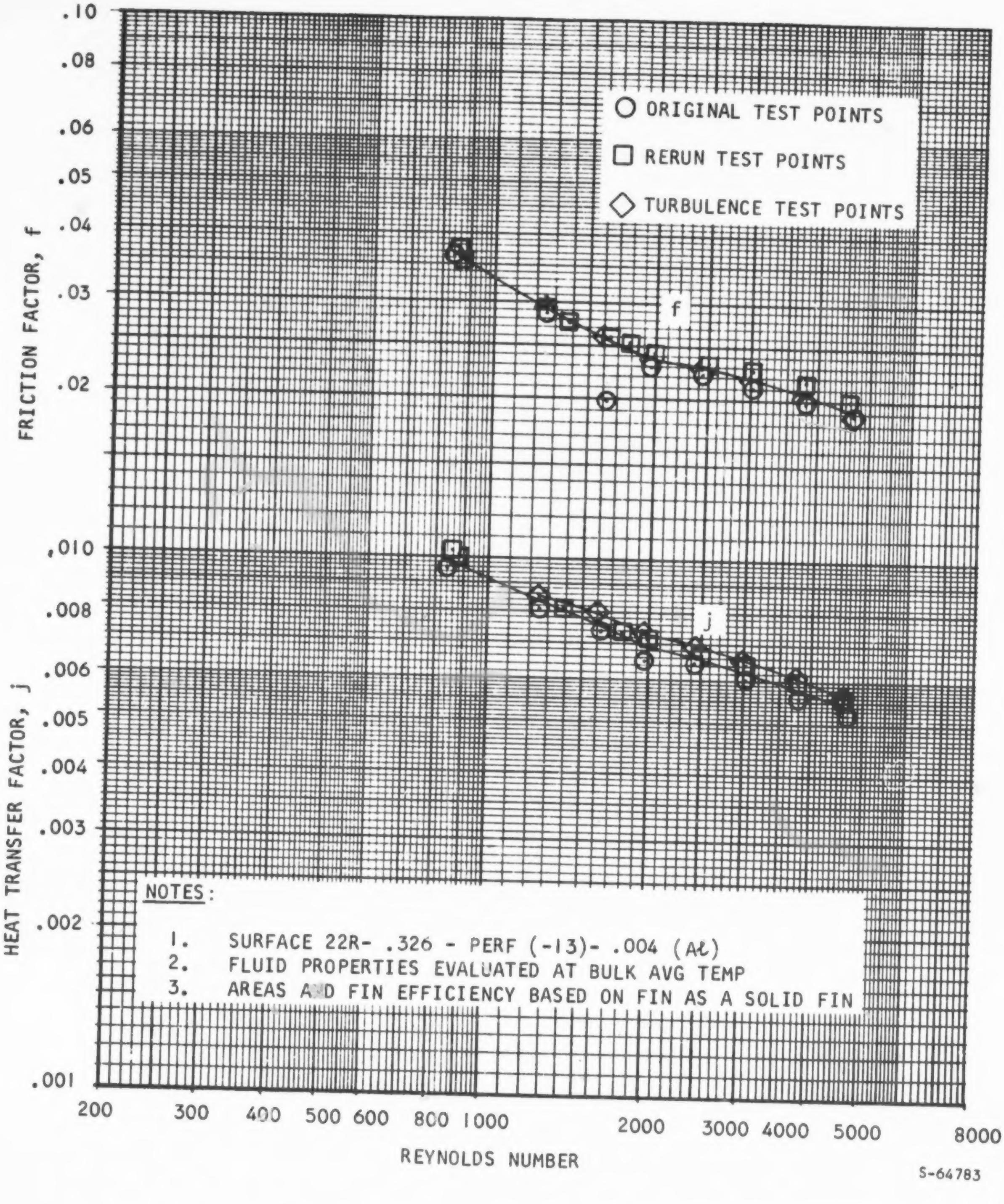

Figure 5-26. Performance Parameters for the -13 Perforated Fin

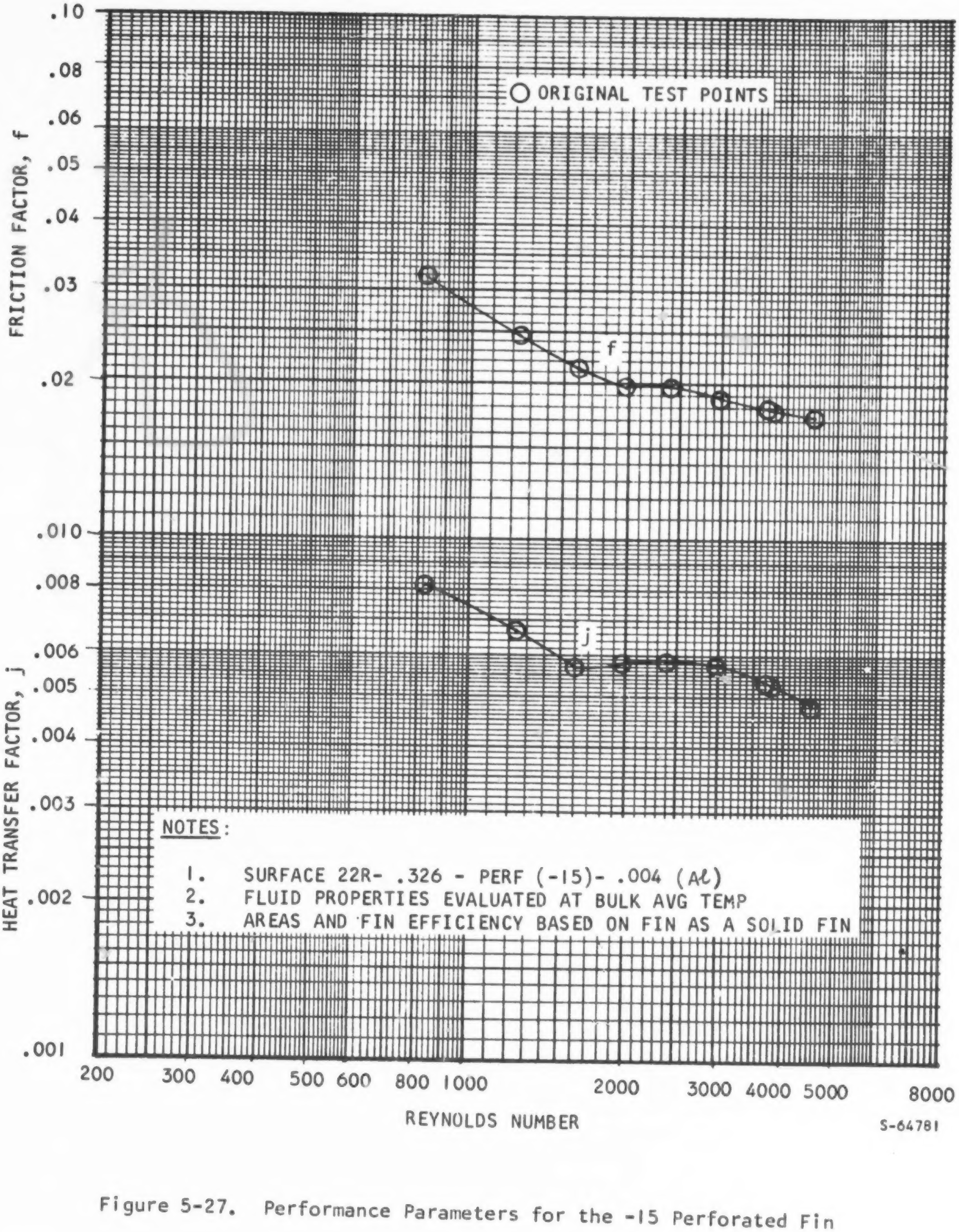

NOTES:

1. SURFACE 22R- .326 - PERF (-15)- .004 (Aℓ)
2. FLUID PROPERTIES EVALUATED AT BULK AVG TEMP
3. AREAS AND FIN EFFICIENCY BASED ON FIN AS A SOLID FIN

Figure 5-27. Performance Parameters for the -15 Perforated Fin

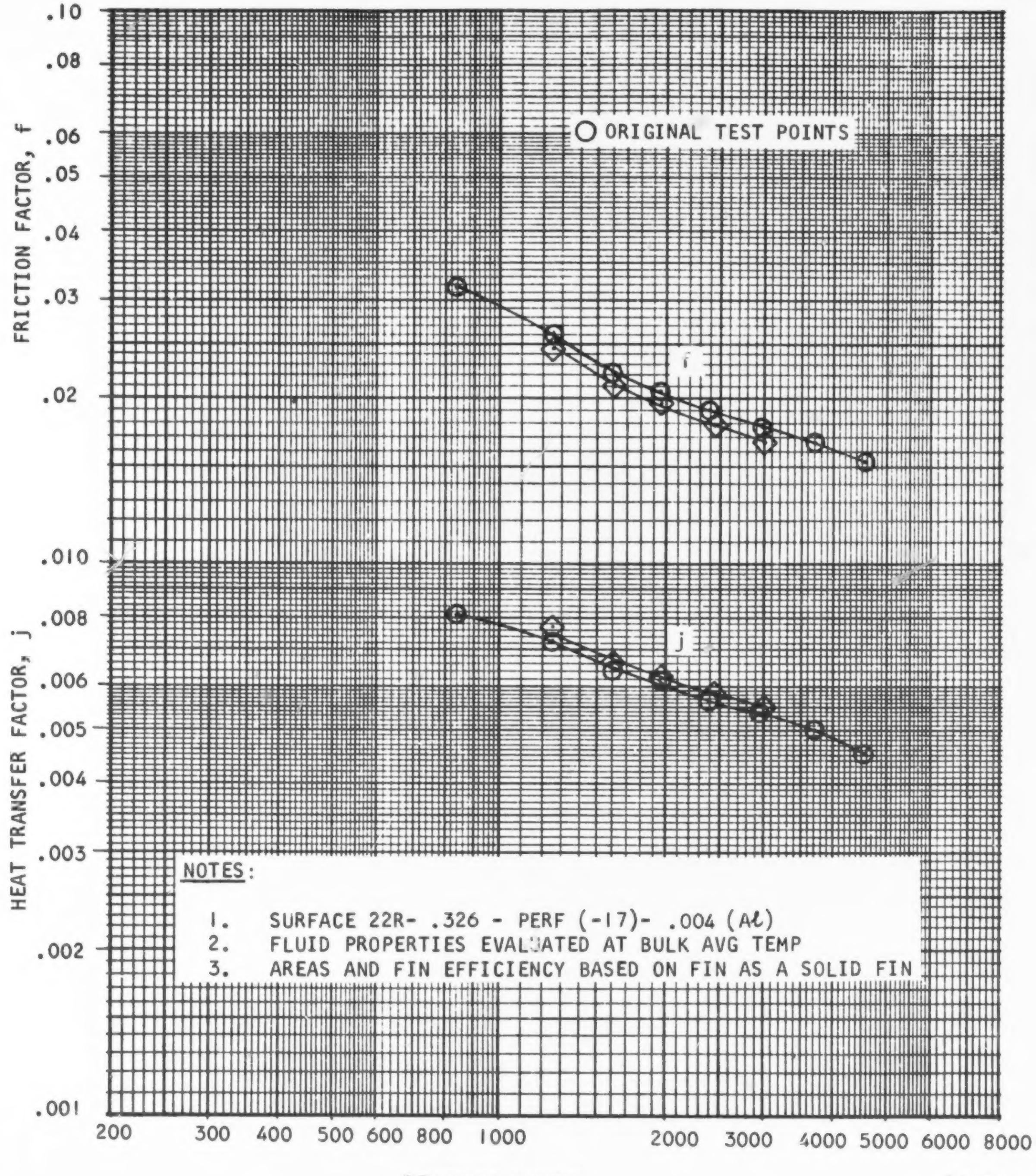

Figure 5-28. Performance Parameters for the -17 Perforated Fin

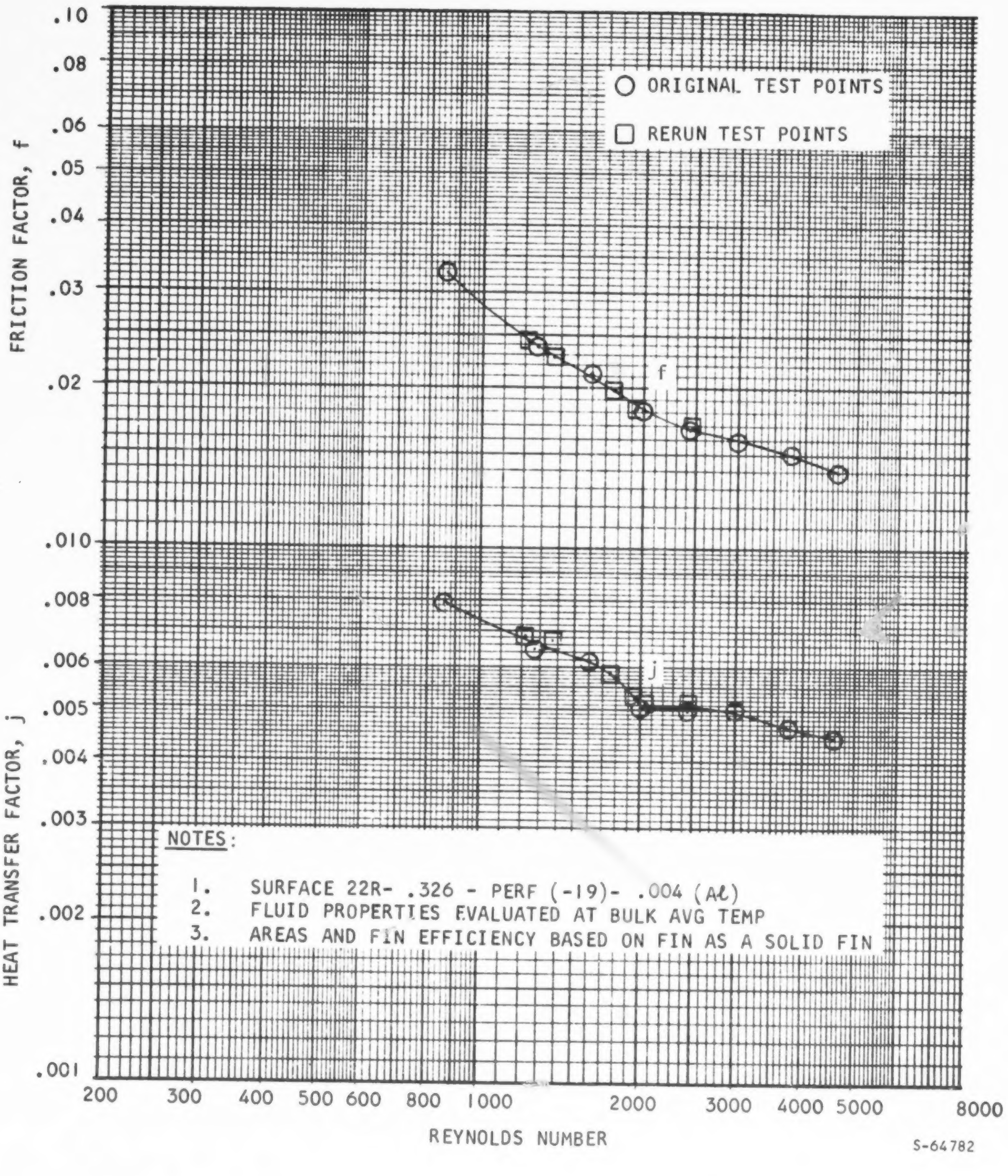

Figure 5-29. Performance Parameters for the -19 Perforated Fin

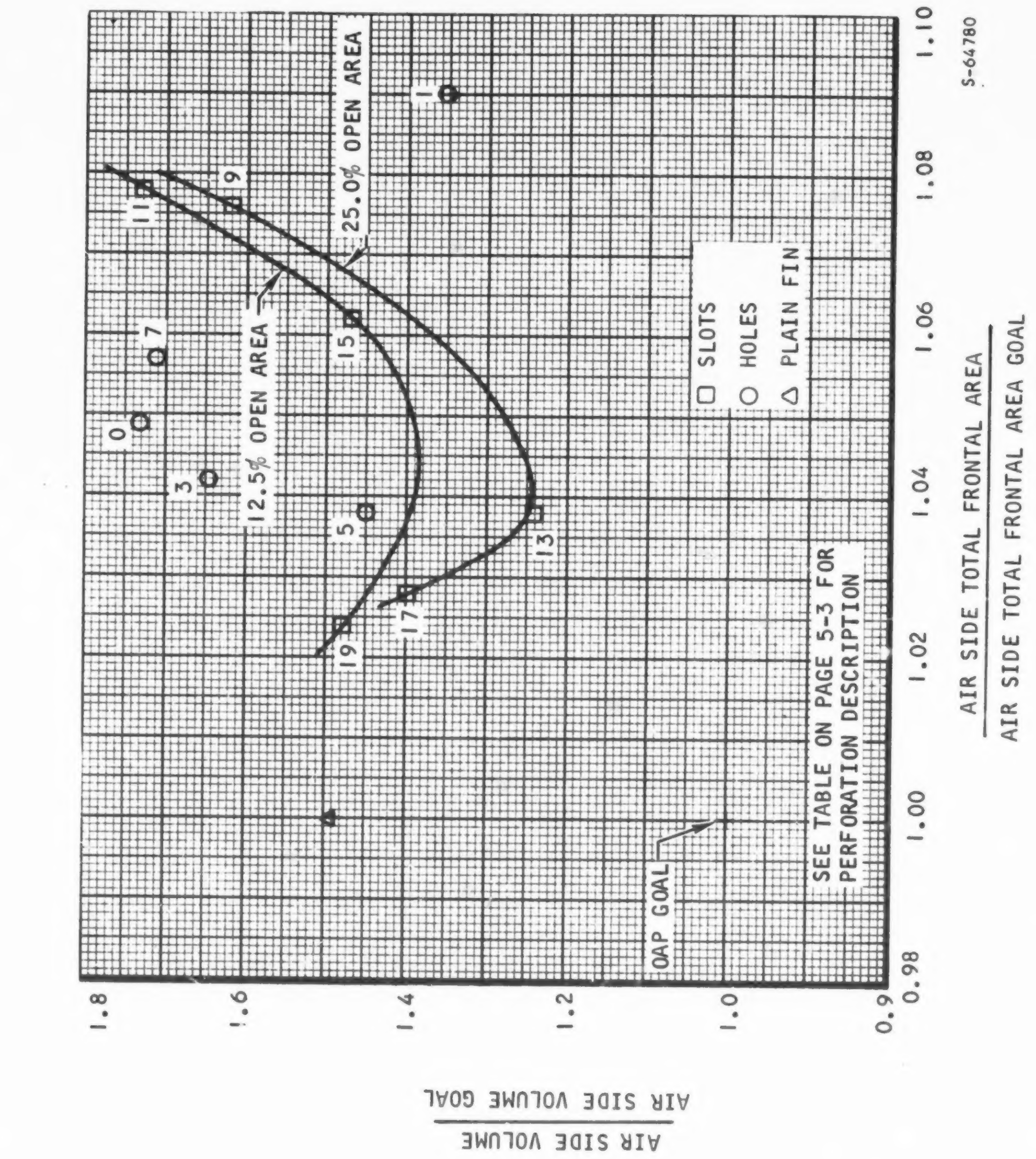

Figure 5-30. Summary of Minimum Frontal Area Solutions for Perforated Fins

Selection of the best fin for the condenser cannot be made on the basis of Figure 5-30 unless it is established that frontal area is the overriding criterion. If frontal area is the only consideration, the best perforated fin is 19; however, the plain fin which meets the area goal would be selected over all the perforated fins. It is more likely, however, that selection of a condenser will involve a tradeoff between frontal area and volume, in which case additional information not shown on Figure 5-30 is required. This information, the manner in which the volume and area vary for each fin while still providing solutions, is presented below.

The effect on the condenser size of inducing turbulence upstream of the test cores is shown in Figure 5-31. The f and j data obtained with upstream turbulence yielded smaller condensers for all four of the fins tested. The reduction in condenser volume and area is shown in the figure for the minimum frontal area solutions. Again the best plain fin (without upstream turbulence) is shown for comparison. The effect of upstream turbulence is significant since it reduces both the volume and the area. The points shown on Figures 5-30 and 5-31 are the minimum frontal area condenser configurations. As was shown in Section 3, there are actually many combinations of frontal area and volume which will yield condensers for the given heat load and air horsepower requirement. Figure 5-32 shows the locus of points which represents these condenser sizes for several fins and turbulence conditions. The point of inflection in each of these curves corresponds to the minimum area solutions given in Figures 5-30 and 5-31. The difference in the scales of the volume and area coordinates should be noted. Because of the fact that the condenser solutions are more sensitive to volume than to area, it is possible to achieve significant decreases in volume with small increases in frontal area by moving "down the curve" for a given fin. For instance, with the -13 fin and upstream turbulence, the minimum frontal area solution occurs at a volume of 18 percent over the volume goal and an area 2 percent over the area goal. However by moving "down the curve," a solution also exists at the volume goal with an area 3.4 percent over the area goal. The volume was reduced significantly while the area increased only slightly.

The effect of turbulence is shown in Figure 5-32 by comparing equal frontal area solutions with and without upstream turbulence. The -17 core minimum frontal area solution (at an area ratio of 1.028) had a volume ratio of about 1.39; however with upstream turbulence the volume ratio decreased to 1.03 for the same frontal area.

Introduction of upstream turbulence improved the fin performance such that slightly smaller condensers are obtained. While improvements in heat transfer due to upstream turbulence have been observed by several investigators, this phenomenon, as well as the effects on the friction factor, are not well understood. Kreith (Reference 4) states that an increase in the upstream turbulence level may increase the heat transfer coefficient on a cylinder in crossflow by as much as 50 percent. Shvets et al (Reference 5) investigated the influence of the upstream turbulence level on heat transfer to air flowing inside pipes and found that for a high level of upstream turbulence, the local heat transfer coefficient at the inlet increased by 5 to 15 times and the average h for a pipe of L/D = 75 increased by 20 to 30 percent. No friction factor data was reported by these investigators. Review of the current data for upstream turbulence (Figures 5-20, 5-24, 5-26, and 5-28) shows, in all cases, an increase in the heat transfer factor j over that for no upstream turbulence, an unchanged f for the -9 and -13 fins, and a decreased f for the -1 and -17 fins. The changes in f and j were approximately 5 to 10 percent which is estimated to be the order of the experimental uncertainty. It is possible that the indicated lower pressure drop was due to the pressure tap being located in the wake of the middle turbulence generating rod so that a lower than actual upstream pressure was measured. The reasons for the decreased f and increased j are not fully understood at this time, however similar data was obtained previously. Shah and Osborn (Reference 1) presented f and j data with and without upstream turbulence for one perforated plate matrix, and obtained an increased j and a decreased f in the transition range.

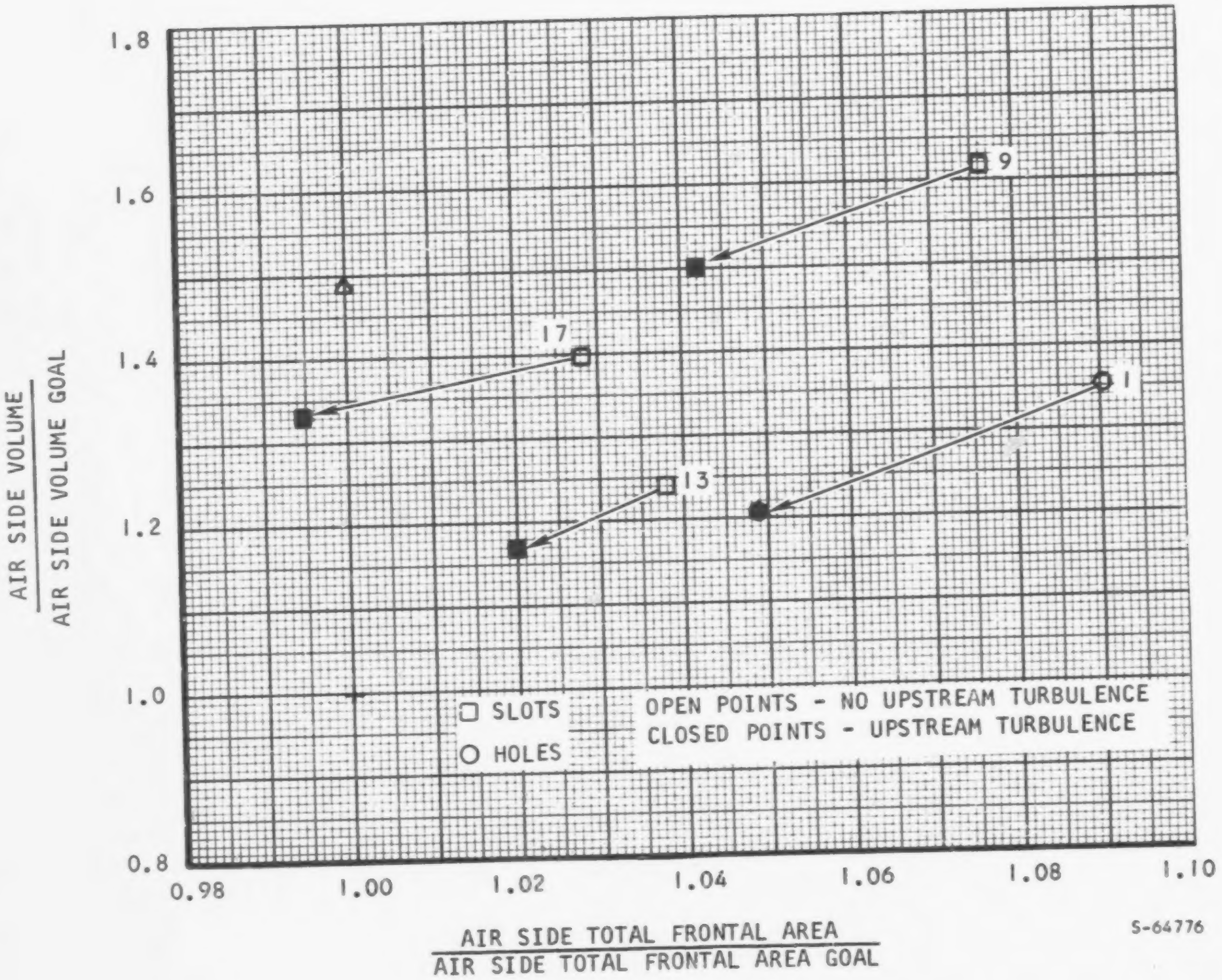

Figure 5-31. Effect of Upstream Turbulence on Condenser Minimum Frontal Area Solutions

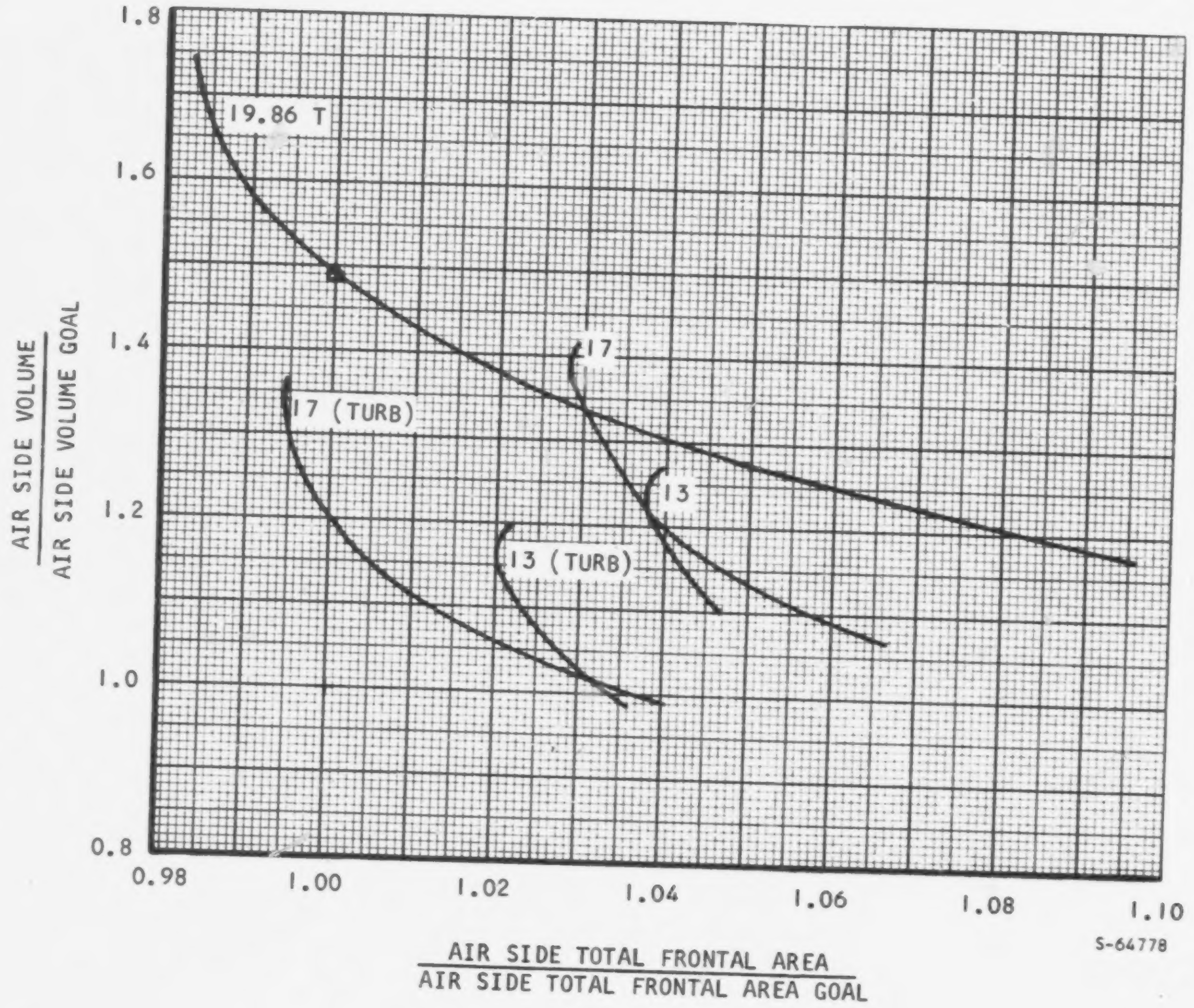

Figure 5-32. Condenser Solutions for Selected Fins

SECTION 6

APPLICATION TO FULL-SIZE CONDENSER

OPTIMIZED CONDENSERS

Optimum condensers were designed using the f and j data for the perforated fins. As can be seen from Figure 5-32, either the -13 or the -17 fin could be used, depending on the relative importance of volume and area. If area is most significant, the -17 fin would be used since smaller areas can be achieved with this fin. However, if it is desired to meet the volume goal and the unit is so designed, the -13 fin is best because it yields a smaller face area at a volume ratio of 1.0 as seen in the figure. In the current design, it was decided that a reasonable tradeoff of volume and area would be to design at an area ratio of 1.03 which yielded a volume ratio of 1.02. The data for the -13 fin with upstream turbulence was used in the design of the optimum cores. The optimum designs are shown below.

Heat Rejection Rate, Btu/hr	Goal		Results	
	Area, sq in.	Volume, cu ft	Area, sq in.	Volume, cu ft
0.5×10^6	266	0.5	274	0.51
1.0×10^6	533	1.0	549	1.02
1.5×10^6	799	1.5	823	1.54
2.0×10^6	864	2.0	1097	2.05
2.5×10^6	864	2.5	1371	2.56

At the two highest heat loads, the frontal areas exceed the design goals by 27 and 59 percent, while the volume remains 2 percent above the design goal.

The condenser designs using heat transfer data which existed before this study and presented at the end of Section 4 are compared with the perforated fin condensers below. The areas and volumes are shown relative to the area and volume goals.

Heat Rejection Rate, Btu/hr	Based on Previous Data (Plain Fin)		Based on Current Data (Perforated Fin)	
	$\frac{\text{Area}}{\text{Area Goal}}$	$\frac{\text{Volume}}{\text{Volume Goal}}$	$\frac{\text{Area}}{\text{Area Goal}}$	$\frac{\text{Volume}}{\text{Volume Goal}}$
0.5×10^6	1.0	1.48	1.03	1.02
1.0×10^6	1.0	1.48	1.03	1.02
1.5×10^6	1.0	1.48	1.03	1.02
2.0×10^6	1.21	1.92	1.27	1.02
2.5×10^6	1.51	2.40	1.59	1.02

COST ANALYSIS

An analysis was conducted to determine the cost for the condenser over a range of heat loads. The particular condenser configurations used in the analysis corresponded to the optimized designs presented above, and covered a range of heat loads between 0.5 million and 2.5 million Btu/hr.

To provide a realistic basis for a cost analysis, a layout drawing (SK51843) of a prototype condenser suitable for high volume production was prepared and is shown following this page. In this design the tube plates and the working fluid manifold sections are formed as an integral part. This construction technique is especially adaptable to high volume production because it eliminates using separate header bars and closure strips which results in a significant savings in core stacking time. The unit is fabricated using aluminum alloy and is designed to be brazed in a vacuum without using a flux.

Dimensions of the prototype condenser shown on the following page are representative of a unit that just meets the OAP face area (799 in.^{2}) and air-side volume (1.50 ft^3) design goals for a heat rejection of 1.5 million Btu/hr. It was presumed that the air-side perforated fin performance would yield the required size.

The vapor and condensate manifold dimensions are based on using water as the working fluid. A larger manifold with multiple inlet connections could possibly be required if an organic working fluid were specified. The condensate passages are 0.050-in. high which is considered to be reasonable with regard to pressure drop if steam is condensing. A rectangular offset or strip fin is utilized on the vapor side. A detailed analysis of the condensing-side heat transfer and pressure drop characteristics could possibly change this selection, but a revised fin selection would not significantly affect the cost analysis.

Perforated fins are used on the air side. Basic fin geometry is as follows: 22 fins per in., 0.326 in. high, and 0.004 in. thick. Details of the perforation geometry are not specified because further optimization studies are required and the perforating operation is not considered to affect cost. It is believed that the cost for perforating can be recovered by selling the scrap resulting from the operation especially when the surface open area exceeds 25 percent.

The air fins are flush with the sides of the tube plates to facilitate automatic core stacking. The leading and trailing edges of the air fins are not fully active because they are not in full contact with the vapor passage. Therefore, an allowance of 0.15 in. has been added to the calculated air fin length to account for the partially active fin.

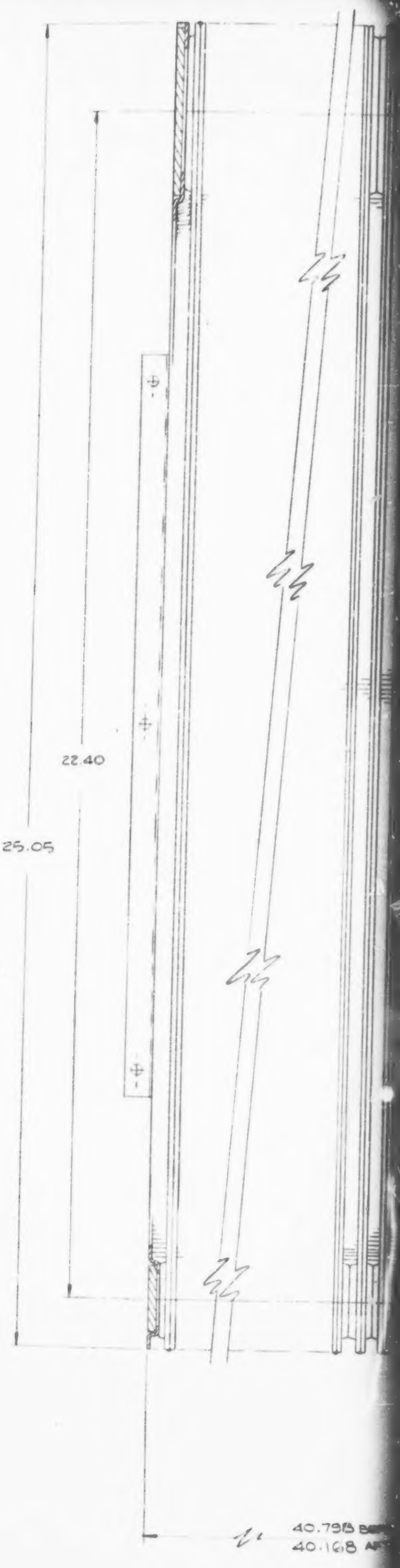
22.40
25.05
40.793
40.168

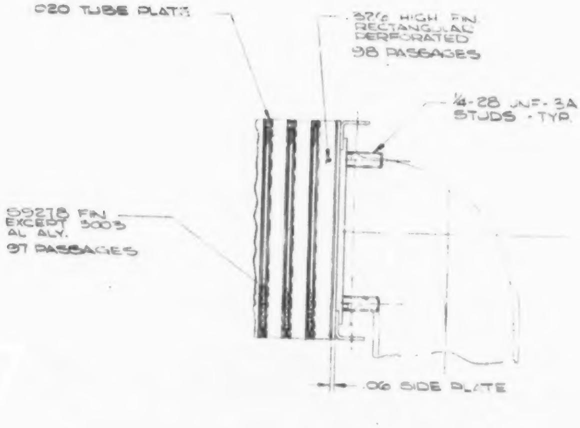
.020 TUBE PLATE
37½ HIGH FIN RECTANGULAR PERFORATED
98 PASSAGES
¼-28 UNF-3A × 5/8 LG STUDS - TYP.
59278 FIN EXCEPT 3003 AL ALY.
97 PASSAGES
.06 SIDE PLATE

SECTION A-A

DESIGN SPECIFICATION

HEAT REJECTION	1.5 MILLION Btu PER HR
FAN POWER (IDEAL)	9.0 HORSE POWER
INLET COOLING AIR TEMP.	95° F
VAPOR CONDENSING TEMP.	220°F
CONDENSING SIDE HEAT TRANSFER COEFFICIENT	2000 Btu PER HR FT² °F

FURNACE BRAZE PER

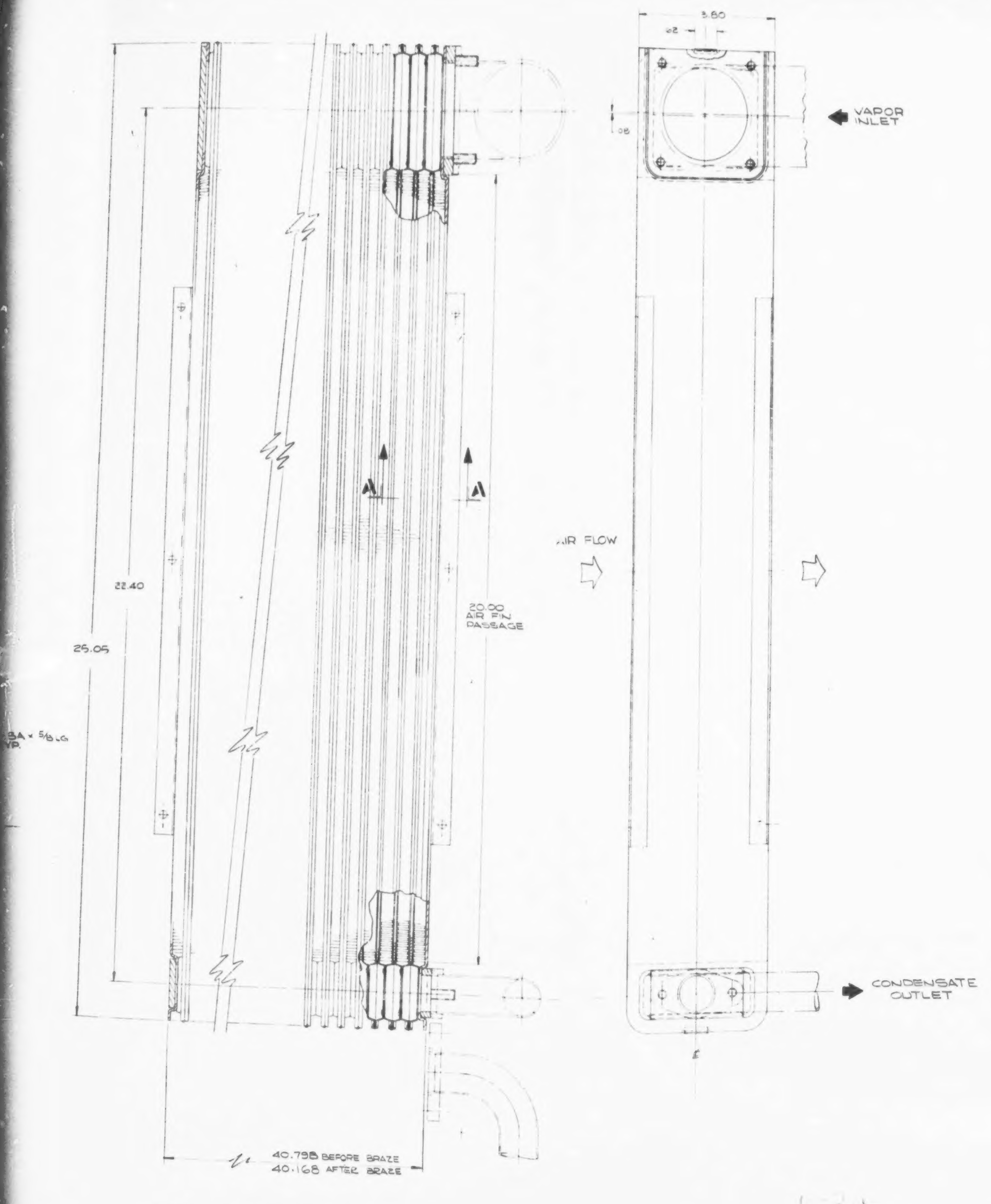
3.80
62
08
VAPOR INLET
22.40
25.05
8A × 5/8 LG
YP.
A
A
AIR FLOW
20.00 AIR FIN PASSAGE
CONDENSATE OUTLET
40.798 BEFORE BRAZE
40.168 AFTER BRAZE

FURNACE BRAZE PER WBS-27

Metal gauges for the reference design specified on Drawing SK51843 are as follows:

Tube plates	0.020 in.
Air fin	0.004 in.
Vapor fin	0.004 in.
Top and Bottom Sideplates	0.063 in.

A detailed review of the condenser environment including structural loads and working fluid corrosion rates could lead to a reduction in tube plate thickness with a corresponding cost reduction (tube plates account for about 65 percent of **total** materials cost).

Results of the cost analysis are summarized in Table 6-1 and are presented graphically on Figure 6-1.

The costs are considered to be typical for a commercial facility which is set up primarily to build heat exchangers. A production rate of 100,000 units per year was assumed. To meet this production rate at a reasonable cost the following types of manufacturing operations were assumed:

(a) Tube plates - automatic production on a multiple station press. Unattended operation except to manually load coils of raw material.

(b) Air and vapor fins - automatic production. One man required to monitor press operation and to load material.

(c) Core stacking - manual operation. Tube plates and fins are stacked directly into a suitable brazing fixture.

(d) Brazing - batch process in a vacuum-type furnace using a 30 minute cycle time.

Automation of the core stacking and cleaning operations and the use of a continuous type of braze furnance could reduce the direct labor cost.

Material costs are based on lot sizes of at least 30,000 lb. to obtain minimum cost. No significant dollar savings in material costs could be realized by buying in larger lot sizes. As noted above, a savings in material costs could be achieved by reducing the tube plate metal gage, but this would require operating experience to verify satisfactory performance. Material costs include a 15 percent allowance for scrappage.

Direct labor costs are subject to change depending on the degree of plant automation. A savings of about 50 percent in direct labor costs could be achieved by automating the core stacking and brazing operations.

Factory burden was assumed to be equal to 50 percent of the total direct labor plus material costs. This figure could vary depending on the degree of automation and the heat exchanger production rate.

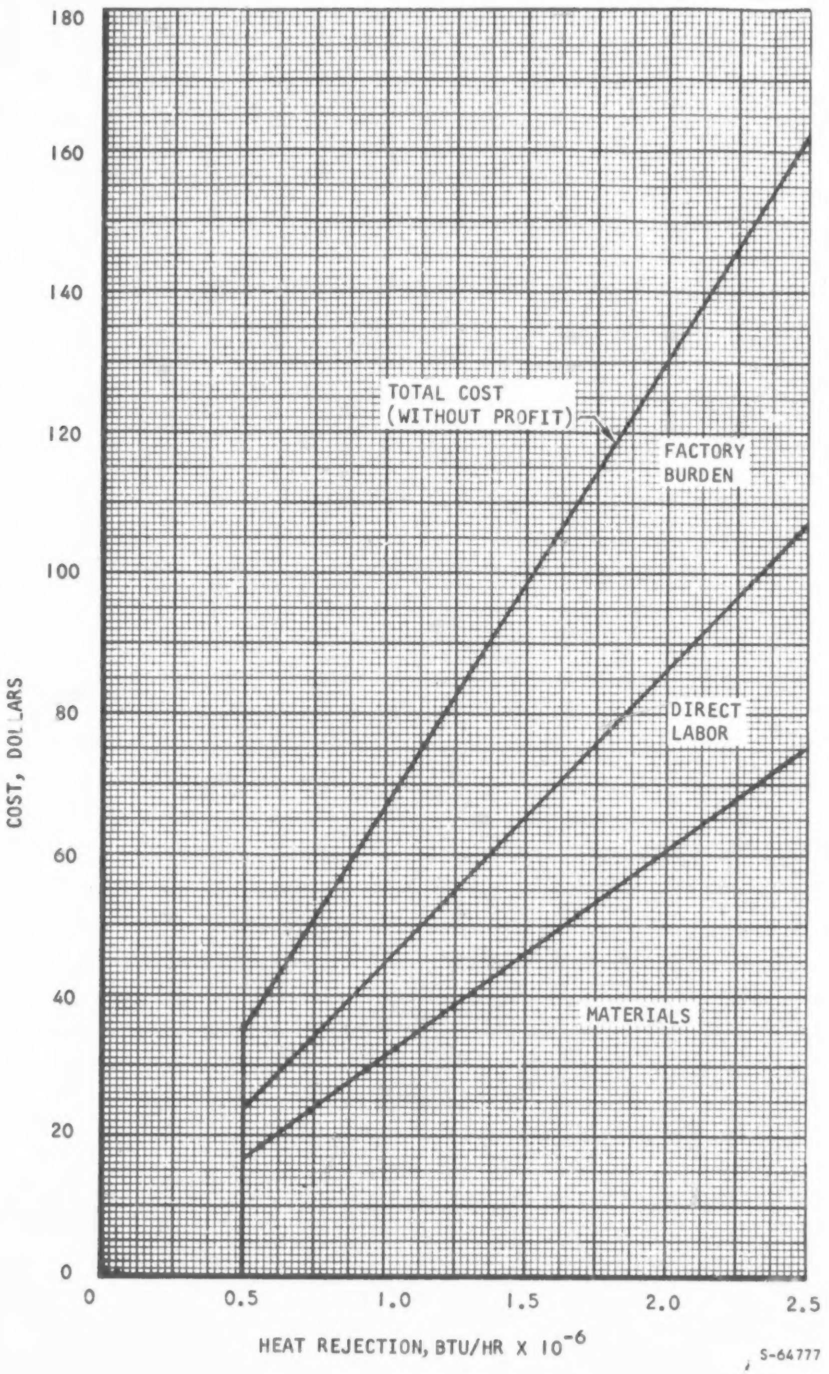

Figure 6-1. Summary of Cost Analysis

TABLE 6-1
CONDENSER COST ANALYSIS

Heat Rejection Rate, But/hr	Goal		Results					
	Frontal Area, in.^{2}	Volume, ft^3	Frontal Area, in.^{2}	Volume, ft^3	Stack Height,* in.	Air Fin Length, in.	Air Flow Width, in.	Cost,** $
0.5×10^6	266	0.5	274	0.51	14.37	3.96	20.0	35
1.0×10^6	533	1.0	549	1.02	28.70	3.96	20.0	67
1.5×10^6	799	1.5	823	1.54	42.55	3.96	20.0	97
2.0×10^6	864	2.0	1097	2.05	56.97	3.96	20.0	129
2.5×10^6	864	2.5	1371	2.56	70.89	3.96	20.0	161

* Over sideplates, after braze

** Total cost including materials, direct labor and factory burden but without profit

SECTION 7

REFERENCES

1. Shah, R. H., and H. H. Osborn, "Final Report - Advanced Heat Exchanger Designs of Compact Heat Exchangers When Operating in a Marine Environment," Air Preheater Company, Wellesville, New York, May, 1967.

2. Kays, W. M., "The Heat Transfer and Flow Friction Characteristics of a Wavy Fin, A Strip Fin, and A Perforated Fin Heat Transfer Surface," Technical Report No. 39, Stanford University, Stanford, California, October 31, 1958.

3. Kays, W. M., and A. L. London, Compact Heat Exchangers, Second Edition, McGraw-Hill Book Company, New York, New York, 1964.

4. Kreith, F., Principles of Heat Transfer, Second Edition, International Textbook Company, Scranton, Pennsylvania, 1965

5. Shvets, I. T., Ye. P. Dyban, M. V. Stradomskiy, and E. Ya. Epik, "Experimental Investigation of Influence of Turbulence of Flow on Heat Exchange During Motion of Air in Pipes," Teplo-i Massoperenos (Heat- and Mass Transfer) 1963, Vol. 3 pp. 370-381. (AFSC FTD-MT-65-367 Translation).